SATELLITE PLASMA SHEATH ANOMALIES

DR. S. FRED SINGER, et al
PROFESSOR OF PHYSICS
UNIVERSITY OF MARYLAND

REPRINTED FROM ELECTRO-JET CORPORATION
FINAL REPORT UNDER CONTRACT NObsr 84714

BUREAU OF SHIPS · NAVY DEPARTMENT · WASHINGTON 25, D.C.

The views expressed herein are the personal opinions of the authors and are not necessarily the official views of the Department of Defense or of the Navy Department.

TABLE OF CONTENTS

INTRODUCTION

by CDR Keith N. Sargent, USN

From the standpoint of National Defense the most vexing problem facing the Surveillance and Detection Planners is the combination of physical limitations imposed by line of sight propagation from a tangent point on a sphere and the requirement to detect in the total volume surrounding the sphere. With the advent of higher velocity vehicles together with the resultant shortening of available reaction time and the exponential increase in aero-space volume to be searched as orbital dimensions grow, the need for a breakthrough in surveillance capability became more and more urgent.

As a result, when Dr. S. Fred Singer and his University of Maryland group approached the Bureau of Ships with his hypothesis regarding plasma sheath anomalies in space, the Detection and Countermeasures Branch of the Warfare Systems Research and Development Division was receptive to his thinking. If his hypothesis proved out, it was recognized that target enhancement could be achieved that would permit tracking of satellites at ranges where skin-tracking was impracticable, if not indeed impossible. It was further recognized that plasma sheath detachments due to coulomb drag could provide track signatures to detectors before the vehicle itself rose above the radar horizon.

Therefore, a modest effort was financed through the Electro-Jet Corporation to permit Dr. Singer and his group to pursue his hypothesis. This report is the result of their efforts. While experimental proof has not yet been obtained, an experiment has been designed and will be performed to this end.

Because of the promise for a unique satellite and missile early warning capability through the Kraus-Singer effect, it is considered that this technical report should be shared with the scientific military community in advance of the experimental proof. It is anticipated that a subsequent technical report will be issued upon completion and evaluation of the experiment which is planned for the near future.

Experimental Studies of the Kraus Effect

by Richard T. Bettinger

The following is based on my trip to the Ohio State Observatory on June 21, 1961, Dr. Kraus' paper (Ref. 1) and Dr. Villard's paper (Ref. 2).

Critical Resume of Observations

The Ohio State work has included both radar and C.W. type observations, the former extending from early 1959 through late 1960. The radar equipment utilized for the most part consisted of a 25 KW peak power transmitter operating at a pulse repetition rate of 30 pulses per sec., a pulse width of one millisecond, and a frequency range from 17-19 mc. The antennas utilized included everything from 1/2 wave dipole to a fixed 20 DB parabolic reflector. The most commonly used receiver band width was 4 kc with values varying from 1 - 8 kc.

The Croft-Villard experiments at Stanford used two systems. The first consisted of a 50 kw radar transmitter operating with 1 millisecond pulses at a repetition rate of 10 pulses per sec. Frequencies of from 10-30 mc were utilized and moderately high gain antennas (fixed rhombics) were in general employed. The Stanford group also included a phase coherence measurement, i.e. phase of the returning signal was compared to that of the generating system and the phase difference recorded. No statement concerning receiver band width is made; however, it is presumed to be of the order of 2 kc.

Except for the additional phase measurement at Stanford, there seems to be no fundamental difference in the experimental techniques employed by the two groups. The Stanford group had available a considerably wider frequency range, however, they state that the system was adjusted for maximum return dependent upon the particular ionospheric conditions that exist at the time. This would imply that frequencies of the order of 15 mc dominated, and the average frequency used should not differ significantly from that of Ohio State.

The data taking techniques and interpretation of the data of the two groups differed significantly however. The Stanford group considered two satellites and set up to make measurements only on those occasions when these two satellites would pass through the beams of one of their available antennas. The Ohio State group, however, tended to set up their equipment and allow it to run continuously, and then observe the data obtained for "interesting or unusual events". When one of these was detected they attempted to the best of their ability to relate it to a satellite pass. This is a difficult process because of the relatively large number of satellites in orbit and the dearth of readily available accurate data on all of these. This process of locating all satellites at the time of this event was obviously time consuming and has prevented a large number of events from being examined. The Stanford group, on the other hand, defined their interval of interest as the period in which the satellite was between the half power points and counted all anomalies in that time as possible events. The events were classified to the best of the reader's ability in terms of the probability that it was a satellite-induced or satellite-related event. The details of the rating system will not be gone into here, however the techniques employed seem reasonable and under the circumstances as good as can be done with this type of approach.

The Ohio State group employed still another technique for the measurement of these reflection anomalies which very simply consisted of a receiving antenna and receiver set to WWV at 10, 15 or 20 mc. The antennas again varied considerably but in general were relatively low gain. The most important aspect of this experiment was that the receiver had relatively poor long term stability so that the center frequency over a period of time tended to drift up to 5 kc from its prior setting. Receiver band widths were of the order of 2 or 3 kc. Although originally set directly on WWV, after running overnight they were very often plus or minus 5 kc from the original setting. In this off-tune position a number of events

which Kraus has described as satellite related, have been detected. A high velocity plasma cloud, (or reflecting surface of some type) will Doppler shift the signal (depending upon orientation), and place the reflected signal outside of the receiver capabilities of either of the radar experiments previously described. However because of the accidental drift in the Kraus CW experiment they would presumably measure these Doppler shifted signals with a considerable enhancement of signal to noise ratio. Widening the receiver band width sufficiently to include a widely shifted Doppler signal would have degraded the signal to noise ratio badly, possibly making the signals undetectable. The evaluation techniques again are similar. An event is noted and an attempt is made to correlate it to a satellite passage. If some reasonable correlation exists then other factors are introduced as possible variables. A large number of these events have been reported in detail by Kraus.

Discussion

The following observations seem germane:

1. Little or no attention has been ascribed to the ability or inability of the antenna systems used to localize the source of the reflection; we are simply trading off reflecting area versus antenna orientation, i.e. the same response is obtained from a side lobe which is 10 db down and looking at a tenfold larger reflecting surface. In general the techniques employed to date provide no localization in space beyond a very rough indication.

2. When considering the reflection caused by the local ionization in the vicinity of a satellite, one in general would expect little or no results. If the satellite is charged negatively then the charge sheath consists of a positive ion sheath whose thickness is in general only a few debye lengths and whose projected area will scarcely exceed that of the physical area of satellites. In any case, radio propagation is relatively insensitive to the

ion charge sheath, which merely represents a small hole in the electron distribution which will tend to scatter but not reflect. The immediate wake of the satellite does represent an electron enhanced area, more precisely an ion evaluated area, but one would not expect considerably enhanced electron densities. In short, one would not, except under exceptional circumstances, expect any excessive ionization to be present in the immediate vicinity of the satellite. There will be a trail of ionization turbulence in the wake of the satellites which I would off hand assume to be relatively small. In no case has anyone reported, that I know of, direct reflections from ionization trails related to satellite passages. In general, Kraus' work which has been the motivation of these general studies has indicated reflections from anomalies which tend to originate at or in the general vicinity of a satellite orbit, but are in general moving in directions not associated with the orbit and in general at very high velocities. We would conclude, therefore, that an experiment (such as the Stanford one) which strictly localizes the immediate vicinity of the satellites would probably not be fruitful.

3. The events reported by Kraus' are sufficiently few that the effects, if in fact satellite related, are relatively rare and presumably related to fairly specialized conditions. Hence, any statistical study must have a relatively large source in order to establish the presence of correlation.

At this stage of the game all the work that has gone into this area still seems highly inconclusive. Kraus' measurements may in fact indicate satellite correlated local areas of ionization, however, this is certainly not conclusive based on his evidence. This work is in no way prejudiced by the Stanford report since they allowed themselves almost no possibilities of detecting the type of phenomenon reported by Kraus. If in fact these high velocity areas of enhanced ionization do exist, then the relatively narrow

band widths of the receivers used in the radar studies almost preclude the possibility of detection. (The exception of course is a cloud moving with zero radial velocity.)

The Stanford work, on the other hand, seems to establish that there are no directly associated ion clouds with reflective areas larger than 1 or 2 orders of magnitude greater than the satellite physical area directly associated with the satellite while moving in orbit. The numbers are still sufficiently small so that the statistical conclusion is subject to reasonably large errors, however no large scale systematic effect is present. The result is of course not surprising.

The nature of the phenomenon with which we are dealing is best described by Kraus; "Most of our observations indicate a transient or sporadic phenomenon in which detectable ionization appears in the general vicinity of the satellite, but not necessarily very close to it. In fact, fast moving echoes, with velocities of from 30 to 150 kilometers per sec which appear to originate in the satellite seem to be frequently involved". Kraus' data seems to indicate that these clouds do not propagate parallel or perpendicular to the magnetic field, but in general at some skew angle. We might summarize the germane characteristics of such a phenomenon in terms of the experimental parameters of prime interest.

1. Effective area as a function of frequency.
2. Space-time localization with the highest possible accuracy.
3. Effective cloud velocity.
4. Trail reflectivity and persistence, if it exists.

The experimental problems associated with obtaining definitive information on these parameters are obviously tremendous, however if a serious attempt to describe this type of phenomenon is to be made, these parameters must be attacked simultaneously. The velocity of the clouds is a very important

point; a cloud moving with a radial velocity of 100 kilometers per sec will have a Doppler shift of 12 kc, hence it will in general be outside the response band of the radars currently in use, hence undetectable. The motion relative to the earth's magnetic field is presumably not random so that the motion relative to the observing station will probably show preferential relative angles and a limited range of radial velocities.

References

1. J. D. Kraus, "The Satellite Ionization Phenomena as Studied by CW-Reflection and Pulse Radar Technique," Am. Astronautical Soc. Symposium on Interactions of Space Vehicles with an Ionized Atmosphere, Washington D.C., March 17, 1961.
2. T. A. Croft, and O. G. Villard, "An HF Radar Search for the Effects of Earth Satellites Upon the Ionosphere,"Radio Science Laboratory, Stanford University Technical Report No. 24, March 10, 1961.

PLASMA SHEATH AND SCREENING AROUND A RAPIDLY MOVING BODY

E. H. Walker

ABSTRACT

The distribution of the potential and the charge density is derived quite generally for a stationary charged sphere and for a charged body moving rapidly through a plasma. Previous treatments were restricted to the cases where either the body's potential was small, being limited to less than five times the plasma temperature (i.e. $\emptyset \lesssim 5kT/e$), or the body was small compared to the Debye length (i.e. $a < (kT/4\pi n_e e^2)^{1/2}$), or the body was moving slowly compared to the ion velocity.

PLASMA SHEATH AND SCREENING AROUND A RAPIDLY MOVING BODY

1. INTRODUCTION

Several workers[1,2,3,4,5,6] have investigated the nature of screening of bodies of various geometries that are embedded in a plasma. This question is particularly important in considering such problems as the significance of electron and ion density measurements in the laboratory and in space, the charging of probes and satellites, and the production of a wake by such bodies.

The limitations that beset the existing calculations are:

(a) The assumption of local thermodynamic equilibrium is very often unsatisfactory. In many practical screening problems, under laboratory or space conditions, the mean free path of particles is found to be large compared with the Debye screening length.

(b) The use of a barometric type of formula for the density of screening particles is generally not valid. Although this is equivalent to the previous assumption, it is sometimes used even though calculations are performed that take account of the motions of the particles. This is done either because calculations are limited to small bodies or because of a failure to distinguish between nonaccreting and accreting orbits.

(c) The assumption that the ions do not respond quickly enough to the potential field and thus maintain their ambient density is a simplifying assumption that is not satisfactory. (1) In the case of the screening of a stationary body, there is no distinction to be made between the screening of a positively charged body and a negatively charged body. (2) It must be noted that as a particle with energy kT moves into a region where the potential is greater than kT, it must be subjected to considerable acceleration. It will be found that for satellite velocities, considerable deflections do occur.

(d) The calculations generally apply only to either small potentials or to small bodies. However, since potentials on satellites probably reach values of 50 kT, and since the bodies' dimensions are usually many times the Debye screening distance, these limitations are unsatisfactory for most problems.

We wish to obtain solutions of the screening of a body which will not be subject to these limitations. In particular, we will obtain exact solutions to the problem of screening for the case of a stationary sphere embedded in a plasma and also we will obtain the screening for a rapidly moving body.

2. SELF-CONSISTENT CALCULATION OF THE SCREENING OF A STATIONARY CHARGED SPHERE.

We wish to obtain solutions for the problem of the screening of a stationary charged sphere that is embedded in a plasma with a mean free path for its constituents that is long compared to the Debye length h. The general equations that will be used here have been derived by Opik[7]. A brief resume of the essential details is presented below.

In the neighborhood of any point in a spherically symmetric potential field we may express the potential in the form

$$\emptyset = Kr^{-n} \tag{1}$$

where K and n must be evaluated in that neighborhood. It will be convenient for the calculations to use this type of expression.

The conservation of angular momentum and energy may be written in terms of the particle velocity, v, at r, the impact parameter, q, and the velocity of the particle at infinity, u (See Fig. 1).

$$rv \sin\alpha = qu \tag{2}$$

and

$$\tfrac{1}{2}mv^2 = \emptyset + \tfrac{1}{2}mu^2 \tag{3}$$

where α is the angle between $\underline{v}$ and $\underline{r}$, and $\emptyset$ is the potential energy of the particle relative to infinity and is positive for an attractive force and

negative for a repulsive force. If we write

$$U = {}^{1}/_{2}mv^2$$

we have on combining the angular momentum and energy equations

$$\sin^2\alpha = \frac{q^2}{r^2(1+\phi/U)} \tag{4}$$

This expression can be used to distinguish between two types of particle motions. The first type is called periastron motion. For this type as r decreases from infinity, there always exists a value of r for which

$$q^2 = r^2\,(1+\phi/U) \tag{5}$$

so that

$$\sin^2\alpha = 1$$

Under this condition the space inside this value of r is not accessible to the particle. For a repulsive potential this condition can always be satisfied.

If we now substitute Eq. (1) into Eq. (5) we have

$$\sin^2\alpha = \frac{q^2}{r^2 + Kr^{2-n}/U} \leq q^2/F \tag{6}$$

When $n<2$, the denominator, F, always approaches zero as r goes to zero.

However, if $n>2$ there is a point r_c for which $\sin^2\alpha$ reaches a maximum value. This value of r is obtained by setting the derivative of F equal to zero

$$\frac{\partial F}{\partial r} = 0 \tag{7}$$

giving

$$2 + 2\phi/U + r\phi'/U = 0 \tag{8}$$

which gives for the potential at r_c

$$\phi_c = \frac{2U}{(n_c-2)} \tag{9}$$

The value of r is

$$r_c = \left[\frac{(n_c-2)K_c}{2U}\right]^{\frac{1}{n_c}} \tag{10}$$

where the subscripts refer to the values of the quantities at corresponding value of r_c. Thus, inside r_c the particle spirals toward the origin. Here the orbit is described as pericritical. For a given value of q, the maximum value of α is obtained from Eq. (4)

$$(\sin^2\alpha)_{max} = q^2 \frac{(n_c-2)}{n_c}^{(n_c-2)/n_c} \left(\frac{2U}{K_c}\right)^{2/n_c} \tag{11}$$

We note that n_c and K_c depend on U but on nothing else. Hence $(\sin^2)_{max}$ varies directly as q^2. Evidently, the limiting condition for entry into the periastron region is

$$(\sin^2\alpha)_{max} \geq 1 \tag{12}$$

Thus Eq. (11) sets a lower limit on q_p for the target radius of periastron type orbits for the case $n > 2$

$$q \geq q_p = \frac{n_c^{1/2}}{(n_c-2)^{\frac{n_c-2}{2n_c}}} \left(\frac{K_c}{2U}\right)^{1/n_c} \tag{13}$$

or

$$q_p = r_c \sqrt{n_c/(n_c-2)} \tag{14}$$

Particles satisfying Eq. (13) will enter a periastron and emerge from it in a pseudo-hyperbolic trajectory. Those with $q < q_p$, however, will always make an angle of less than 90^0 with the radius and spiral inwards indefinitely. These orbits are of the pericritical type.

We are now in a position to calculate the accretion of particles through a spherical surface. The number of particles passing through a target ring q to q + dq is

$$dA_q = 2\pi q\, dq\, uN_o$$

where N_o is the ambient density. Now from Eq. (4) we have

$$q\, dq = r^2 (1 + \emptyset/U) \sin\alpha \cos\alpha\, d\alpha \tag{16}$$

Thus

$$dA_\alpha = 2\pi r^2 uN_o(1 + \emptyset/U) \sin\alpha \cos\alpha\, d\alpha \tag{17}$$

The integral of this for the periastron case for which all values of α are allowed is

$$A_{pa} = 2\pi r^2 uN_o(1 + \emptyset/U) \int_0^{\pi/2} \sin\alpha \cos\alpha\, d\alpha$$

$$= \pi r^2 u\, N_o(1 + \emptyset/U) \tag{18}$$

Now for pericritical interaction, when $\emptyset > 0$, $n > 2$ and $r < r_c$, the accretion is constant, involving all the particles that have reached the pericritical surface, r_c. Thus, the accretion has the same value for all $r < r_c$

$$A_{pc} = \pi r_c^2\, uN_c(1 + \emptyset_c/U) \tag{19}$$

This result is also obtained by using the limits 0 to α_{max} in the integration of Eq. (18).

The particle density can now be obtained in terms of the potential energy from the above accretion formula. Thus, we have the density contributed by particles moving at an angle between α and $\alpha + d\alpha$

$$dN = dA/4\pi r^2 v \cos\alpha = {}^1/_2\, N_o(1+\emptyset U)^{1/2} \sin\alpha\, d\alpha \tag{20}$$

For periastron orbits an integration of this yields

$$N_{pa} = {}^1/_2 QN_o(1 + \emptyset/U)^{1/2} \int_0^{\pi/2} \sin\alpha\, d\alpha = {}^1/_2 QN_o(1 + \emptyset/U)^{1/2} \tag{21}$$

The factor Q is the return factor. If a particle that passes through the spherical surface at r is elastically reflected by the body so as to return and again pass through the surface at r, the particle orbit must be counted

twice and, thus, the return factor will have a value 2 for this particle. If the particle is absorbed and does not return, the value is 1 for this orbit. The return factor in Eq. (21) is an average value of the return factor taken over all particles. If the collision is inelastic, a more involved calculation may become necessary. It will be found, however, that inelastic collisions are not important since the reflection coefficient for both ions and electrons is small[8,9,10,11]. Furthermore, although secondary electrons are produced, they ordinarily can be neglected; a calculation that includes their effect will be made in Section 4.

The expression for the density in the case of pericritical interaction is obtained by an integration of Eq. (20) over the limits 0 to α_{max}, where α_{max} is given by Eq. (11):

$$N_{pc} = {}^1/_2 QN_0(1 + \emptyset/U)^{1/2} \left\{1 - \left[1 - \frac{q_p^2}{r^2(1 + \emptyset/U)}\right]\right\}^{1/2} \tag{22}$$

To obtain the screened potential and the particle densities as functions of r, Eq. (22) is now used in conjunction with Poisson's equation which in spherical coordinates is

$$\frac{d^2\emptyset}{dr^2} = 4\pi e^2(N_- - N_+) - \frac{2}{r}\frac{d\emptyset}{dr} \tag{23}$$

where N_- and N_+ for a negatively charged sphere are respectively, the density of electrons and the density of the ions times Z_i, the number of charges per ion. For a positively charged sphere, N_+ is the density of electrons while N_- is the density of the ions times Z_i.

Equation (23) can be written in non-dimensional form by defining

$$\psi = \emptyset/kT; \quad \rho = r/h \tag{24}$$

where k is the Boltzmann constant, T is the temperature of the plasma and h is the Debye screening distance as given by

$$h = \sqrt{\frac{kT}{4\pi e^2 N_0}} \tag{25}$$

where e is the electronic charge and N_0 is the ambient density. Thus Eq. (23) becomes

$$\psi'' = \frac{N_-}{N_0} - \frac{N_+}{N_0} - \frac{2\psi'}{\rho} \tag{26}$$

and for a negatively charged body embedded in a plasma of singly charged ions the densities are

$$N_-/N_0 = {}^1/_2 Q(1 - {}^2/_3|\psi|)^{1/2} \tag{27}$$

$$N_+/N_0 = {}^1/_2 Q(1 + {}^2/_3|\psi|)^{1/2} \quad w \tag{28}$$

where

$$w = \begin{cases} 1, \text{ when } n < 2 \text{ or } (|n-2|\psi/3)^{1/n} < 1 \\ 1 - \left[1 + \dfrac{n(|n-2|\psi/3)^{2/n}}{|n-2|(1 + 2\psi/3)}\right]^{1/2} \quad \text{in all other cases} \end{cases} \tag{29}$$

The value of n must be evaluated at each point in the integration since the potential does not follow a simple power law over a wide range of r.

It will be noticed that a Maxwellian velocity distribution has not been included in the derivation of these equations. Expressions have been obtained which take account of the Maxwellian velocity distribution[7], but because of the added difficulty of the calculations, these equations have not yet been employed.

3. RESULTS OF THE SCREENING CALCULATIONS

The integration of Eq. (26) using Eqs. (27), (28) and (29) for densities of the screening particles was obtained by numerical methods. The self-consistent field calculation proceeded from a position ρ_0, for which a small value of the potential ψ_0 was specified, toward the origin (rather than starting from the surface of the charged body). The formula derived for the screening under local thermodynamic equilibrium provided an approximate value for ψ_0' :

$$\psi' = -(1 + \rho)\psi/\rho \tag{30}$$

any error in the initial conditions will be automatically damped out with a proper choice for the integration interval $\Delta\rho$. This procedure produced curves that are independent of the radius of the charged sphere provided either that few electrons reach the surface of the body or that the value of Q is 2. We have set the return factor for the electrons and for the ions to be equal in this calculation. It can be included as an additional parameter in ψ by setting

$$\psi = \frac{\phi}{Q\,kT} \tag{31}$$

It is this function which is plotted in the curves.

In Fig. 2 we have plotted log ψ against log ρ, to obtain a family of curves. A curve connecting the pericritical surfaces is also shown. It will be found from these curves that the potential falls off much more slowly than in the case of local thermodynamic equilibrium. In Fig. 3a, b we plot the ratio h^*/h against ρ, where h^* is the value of the Debye length necessary in the Debye type screening formula ϕ_D to make $\phi_D(h^*,r) = \phi(h,r)$ and $\phi_D'(h^*,r) = \phi'(h,r)$ in our calculation for a given point. A set of curves are given which correspond to the set of curves in Fig. 2. Thus the Debye type formulation gives a much stronger screening than that presented here. The most interesting curves, however, are those for N_+/N_0, N_-/N_0 plotted against ρ, as shown in Figs. 4a, b, c, d, e, f, g. In these curves, the density of the electrons (assuming the body to be negatively charged) falls rapidly to zero, whereas the density of the ions first rises slightly, then falls rapidly to quite low values and finally rises rapidly as the screening particles converge toward the origin.

4. THE SCREENING OF A CHARGED BODY WHEN Q_+ IS VARIABLE

In experiments performed by Fowler and Farnsworth[11] it has been found that the reflection coefficient for low energy electrons striking a metallic surface is, for our purposes, small; its value is of the order of 5%. Hagstrum[8,9,10] has found that ions striking a metal surface will be neutralized by Auger charge exchange with an efficiency of nearly 100%. It would therefore seem that it is not satisfactory to set Q equal to 2 for particles which strike the surface of the body. We will derive an expression for the return factor for the ions, Q_+, and we will assume a sufficiently large negative potential for the body to allow us to use a value of 2 for the electron return factor, Q_-. The value of Q_+ can be obtained from the expression for the accretion. If A_ρ represents the accretion through a surface of radius ρ and A_c represents the accretion through the pericritical surface, the value of the ionic return factor outside of the pericritical surface is

$$Q_+ = 2 - \frac{A_c}{A_\rho} = 2 - \frac{\rho_c^2(1 + {}^2/_3\,\psi_c)}{\rho^2(1 + {}^2/_3\,\psi)} \tag{32}$$

where the subscripts refer to the values of the quantities on the pericritical surface.

The use of two different expressions for the ionic and electronic return factors modifies the screening most strongly for small values of ψ. If we assume ψ to be small, the Poisson equation can be written as

$$\begin{aligned}\psi'' + \frac{2}{\rho}\psi' &= {}^1/_2 Q_-\,(1 - {}^2/_3|\psi|)^{1/2} - {}^1/_2 Q_+\,(1 + {}^2/_3|\psi|)^{1/2} \\ &= \frac{Q_- - Q_+}{2} - \frac{Q_- + Q_+}{6}\,|\psi|\end{aligned} \tag{33}$$

If we take ρ to be large enough then on the pericritical surface ψ_c, as obtained from our previous calculations, will be less than 1. Thus the first derivative

term in Eq. (33) will be small (these conditions are met if ρ is about 10 or more) and we can neglect it. We will then have the condition

$$\frac{Q_- - Q_+}{2} < \frac{Q_- + Q_+}{6} |\psi| \tag{34}$$

which must be satisfied in order for the screening equation to be valid. Substituting for Q_+ on the left side of the inequality we obtain

$$|\psi| > \frac{3\rho_c^2}{(Q_- + Q_+)\rho^2} \frac{(1 + {}^2/_3 |\psi_c|)}{(1 + {}^2/_3 |\psi|)} \tag{35}$$

If we further reduce this using

$$|\psi| << 1 \tag{36}$$

$$Q_+ \approx 2$$

$$|\psi_c| \leq {}^3/_2$$

we obtain, approximately:

$$|\psi| > {}^3/_2 \left(\frac{\rho_c}{\rho}\right)^2 \tag{37}$$

We also have the condition that if no screening at all occurs

$$|\psi| = |\psi_c| \frac{\rho_c}{\rho} \tag{38}$$

this shows that ψ must vary as

$$\psi = Kr^{-n} \; ; \quad 1 < n < 2 \tag{39}$$

for small values of $|\psi|$. Furthermore, this result will hold in a modified form for the case of local thermodynamic equilibrium.

The pericritical surface as indicated by Eqs. (37) and (38) must be given by

$$\rho_c \leq \sqrt{{}^2/_3 |\psi|}\ \rho \tag{40}$$

If $Q_+ = 2$, then Eq. (34) is always satisfied, and for the region of small ψ an integral of the equation can be obtained of the form

$$|\psi| \approx k\rho^{-1} e^{-\rho} \tag{41}$$

It might appear that if one chooses ρ to be large enough, then the difference

between Q_+ and Q_- could be neglected. By the substitution of Eq. (32) into the Poisson equation we can show what prevents this. We have

$$\psi'' + \frac{2}{\rho}\psi' \approx \frac{\rho_c^2}{2\rho^2} - {}^2/_3 |\psi| \tag{42}$$

for small ψ. Thus, if we choose

$$\rho_c^2/2\rho^2 \ll {}^2/_3 |\psi| \tag{43}$$

we would obtain a potential of the form given in Eq. (43). However, ρ_c, ρ, and ψ cannot be chosen independently. Furthermore, if

$$\rho_c^2/2\rho^2 \not\ll {}^2/_3 |\psi| \tag{44}$$

then since ψ varies as ρ^{-2}, the condition in Eq. (43) cannot be satisfied for any other choice of ψ and ρ. It appears that the potential does not vary according to Eq. (41) over any portion of the curve for which ψ is small and Q_+ is given by Eq. (32).

Experiments performed by Hagstrum[8,9,10] have shown that as the result of the neutralization of ions striking a metal surface, secondary electrons will be produced with an efficiency of about 25%. These electrons have not been included in the above considerations. Their effect may be easily included into the calculations by introducing into the Poisson equation the term N_s/N_0 where

$$N_s/N_0 = \frac{\gamma\rho_c^2 (1 + {}^2/_3 \psi_c)}{4\rho^2 \sqrt{{}^2/_3(\psi_0 - \psi)}} \tag{45}$$

where γ is the efficiency of secondary electron production, and ψ_0 is the potential at the surface of the charged body (or alternatively at the surface for which the secondary electron energy is zero).

In Fig. 2, we have plotted a curve to show the effect of this term on the screening. Nevertheless, the effects of the secondary electron term upon the previous results will be small if the surface of the body has a high potential.

5. SELF-CONSISTENT FIELD CALCULATION FOR A MOVING CHARGED BODY.

The calculation of the screening of a moving charged body, except for cases of extremely low velocities, is much more complicated than the calculations for a stationary body. The accretion and density formulae obtained in the second section depend heavily upon the spherical symmetry of the problem. This symmetry allows us to integrate over α and q without consideration of variations of the integrand over an equipotential surface and without consideration of individual particle orbits.

For the calculation of the screening of a moving body, it will be necessary to follow individual particle orbits in order to calculate density contributions. These density contributions will then be used to calculate the protential in the neighborhood of the particle position, and then the potential is used to continue the orbit calculations, etc.

In order to avoid the necessity of iterations in the calculations we assume Q_+ to be unity for all particles. Thus a particle will be artificially removed from the calculation when its orbit becomes parallel to the local equipotential surface. It should be noted from the solution of the screening of a stationary sphere that if μ_0, the initial position for the calculation is chosen to be large, then the pericritical surface occurs almost immediately. Thus, very few particles will be excluded in an artificial way. The actual computations will proceed as follows.

First, the position of a new equipotential surface, $\emptyset_n$, is found, making use of the orbit density as obtained for the $\emptyset_n$ position of the particle from a calculation of orbits from the $\emptyset_{n-1}$ to the $\emptyset_n$ surface. The calculation of the potential follows lines which we will call $\emptyset$ lines, perpendicular to the equipotential surfaces (actually, these are the electric field lines). Calculations are made from the $\emptyset_{n-1}$ to the $\emptyset_n$ surface by making use of the appropriate

value of ΔS, the line element perpendicular to the $\emptyset$ surface. For this calculation, the position, the direction of the surface normal and the value of $\emptyset'_n$ must be obtained.

Secondly, the orbit density is found. Since the new potential surface has been obtained, the orbits can be calculated starting from the last $\emptyset$ surface and proceeding to the new $\emptyset$ surface. In order to obtain densities from these orbits, however, it is necessary to also obtain the position of another particle orbit that is nearby. We will obtain later an expression for the separation of the nearby particle. A weight factor is carried in the calculations for each particle orbit which represents the spacing of the particles at infinity. This weight factor will be used in making averages over several orbit densities. Thus, if we initially start with one region on the $\emptyset$ surface (actually the quantity we are considering is the initial impact parameters rather than the initial angle) thickly sown with test particles, whereas, another region is sparsely sown, the densities contributed by the particles in the sparse region must count more than the other particles. Each orbit, along with its companion, contains enough information to give a value of the density at the position of the particle, not just a density contribution. However, it is necessary to average over several densities when several orbits pass near a $\emptyset$ line position.

6. DENSITY OF COLD SCREENING PARTICLES IN AN AXIALLY SYMMETRIC POTENTIAL FIELD WITH VELOCITY U.

Assume that we have an axially symmetric charged body moving in a cold plasma. In the center of mass, we can view the body as stationary while ions move parallel to the axis of symmetry with a velocity u and impact parameters represented by q. The accretion of particles between q and $q + \Delta q$ (see Fig. 5) is

$$\Delta A = 2\pi q \Delta q \, N_\infty u \tag{46}$$

The density N can be related to the flux J and the velocity of the particles at some point v by

$$N = J/v \tag{47}$$

Now the flux is given in terms of the component of the axial surface element perpendicular to v, $\Delta S_\perp$, by

$$J = \Delta A/\Delta S_\perp \tag{48}$$

Since

$$\Delta S_\perp = 2\pi r^2 \sin\theta\Delta\theta \cos\alpha \tag{49}$$

where α is the angle between the velocity vector $\underline{v}$ and the radius vector, we have for the density

$$N = \frac{\Delta A}{v\,\Delta S_\perp} = \frac{q\,\Delta q\, N_0 u}{v\, r^2 \sin\theta\Delta\theta\cos\alpha} = \frac{N_0\, q\Delta q}{r^2(1+\phi/U)^{1/2}\sin\theta\Delta\theta\cos\alpha} \tag{50}$$

Now, in terms of the angle subtended by Δq we can write

$$\sin\theta_0 = \frac{q}{r_0} \tag{51}$$

where the subscripts refer to the initial values of these quantities on the initial potential surface as specified by the boundary conditions that we choose. The differential is

$$\cos\theta_0\,\Delta\theta_0 = \frac{\Delta q}{r_0} \tag{52}$$

so

$$N = \frac{N_0\, r_0^2 \sin\theta_0\cos\theta_0\,\Delta\theta_0}{r^2(1+\phi/U)^{1/2}\cos\alpha\sin\theta\,\Delta\theta} \tag{53}$$

It will be noticed that N goes to infinity as α approaches the value 90°. This is due to the neglect in the above derivation of the curvature of the surface element ΔS which is subtended by the angle $\Delta\theta$. We correct this by obtaining $\Delta S_\perp$ by an integration.

By axial symmetry we can write for $\Delta S_\perp$ (see Fig. 6).

$$\Delta S_\perp = 2\pi r \sin\theta\ \Delta\ell \tag{54}$$

where $\Delta\ell$ is the projection of the width of the surface ring element perpendicular

to the particle orbit. If $\Delta\ell$ is divided into elements $d\Delta\ell$ we have for these

$$d\Delta\ell = r d\Delta\theta_i \sin(90^\circ - \alpha + \Delta\theta_i) \tag{55}$$

Integration yields

$$\Delta\ell = v\left[\cos\alpha \sin\Delta\theta + \sin\alpha(1 - \cos\Delta\theta)\right] \tag{56}$$

Therefore, we can write

$$\Delta S_\perp = 2\pi r^2 \sin\theta \left[\cos\alpha \sin\Delta\theta + \sin\alpha(1 - \cos\Delta\theta)\right] \tag{57}$$

rather than

$$2\pi r^2 \sin\theta \cos\alpha \Delta\theta \tag{58}$$

We have for N

$$N = \frac{N_o r_o^2 \sin\theta_o \cos\theta_o \Delta\theta_o}{r^2(1 + \phi/U)^{1/2} \sin\theta \left[\cos\alpha \sin\Delta\theta + \sin\alpha(1 + \cos\Delta\theta)\right]} \tag{59}$$

A further correction must be made for the $\sin\theta$ factor. As θ approaches zero N approaches infinity. This effect, which is quite accurate under the assumption of a cold plasma, is, nevertheless, unsatisfactory and arises from our neglect of the thermal velocities of the screening ions. Initially the test particles in velocity space fill a sphere of radius v_T where

$$v_T \approx \sqrt{\frac{3kT}{m}} \tag{60}$$

located at a distance u from the origin. All particles with velocity vectors initially lying in the plane of the calculations will have for their minimum angular approach to the axis, θ_{min}, a value zero. All test particles with v_T lying out of this plane will pass with some larger value of θ_{min}. If ℓ is the total integrated path of the particles, then $\bar{\theta}_{min}$, the average of θ_{min} is obtained with the aid of fig. 7:

$$\ell' = \ell \frac{v_T}{u} \tag{61}$$

If we define λ and λ' to be the distances ℓ and ℓ' in terms of Debye lengths

$$\lambda = \ell/r \tag{62}$$

Then

$$\bar{\theta}_{min} \approx \frac{\lambda v_T}{\rho u} \tag{63}$$

[illegible] which includes [illegible]

$$\cos\left(|\theta - 90^{\circ}| - \bar{\theta}_{min}\right) \tag{64}$$

The expression for the density then becomes

$$N = N_0 \left| \frac{\rho_0^2 \sin\theta_0 \cos\theta_0 \ \Delta\theta_0}{\rho^2(1 + \phi/U)^{1/2} \cos\left(|\theta - 90^{\circ}| - \frac{\lambda V_T}{\rho u}\right)\left[\cos\alpha \sin\Delta\theta + \sin\alpha(1 - \cos\Delta\theta)\right]} \right| \tag{65}$$

7. CALCULATION OF $\Delta\theta$ FROM $\Delta\theta_0$

In our calculation of particle densities we wish to follow one test particle orbit and obtain by appropriate computations the value of the density at the points along this orbit. Thus far we have obtained an expression for the density involving the value of α, θ, θ_0, ρ_0, ρ, ϕ/U, λ, $\Delta\theta_0$ and $\Delta\theta$. If we know the particle orbits, all of these quantities may be obtained except for the quantities $\Delta\theta_0$ and $\Delta\theta$. These presuppose the existance of two orbits and these quantities designate the angular separation of the particle positions when they are on equipotential surfaces. The first of these, $\Delta\theta_0$, designates the initial separation of the particles.

We now wish to obtain $\Delta\theta$ by assuming the two orbits to be extremely close. Thus, we will be able to find an expression giving the change in $\Delta\theta$ as we proceed along only one orbit.

An expression[12] for $d\theta$ in terms of dr, ℓ, the angular momentum, U, the initial kenetic energy, v, the distance to the particle, and $\phi(r)$, the potential energy in a central field. Locally we can assume our potential function to be a central field. Thus, we will write

$$d\theta = \frac{dv}{mv^2 \sqrt{\frac{2}{m}(U + \phi(r)) - \frac{\ell^2}{2mr^2}}} \tag{66}$$

where

$$\ell = muq \tag{67}$$

Now $\Delta d\theta$ the change in the angular separation between the two particle positions as shown in Fig. 8 does not depend explicitly upon r, ϕ, nor dr, since these quantities on the same equipotential surface will be the same for both particles. Also, since initially the two particles had the same energy, this is not the variable that determines the variation in $d\theta$. The angular momentum, however, is not the same for the two particles. Initially it is given by

$$\ell_o = m\, uq = mur \sin\alpha_o \tag{68}$$

and ℓ'_o is

$$\ell'_o = mu\, r \sin(\alpha_o + \Delta\theta_o) = \ell_o + \Delta\ell_o \tag{69}$$

Now

$$\Delta\ell_o = mu\, r \left[\sin(\alpha_o + \Delta\theta_o) - \sin\alpha_o\right] = muq\, \Delta\theta_o \cot\alpha_o \tag{70}$$

or more generally between two surfaces

$$\Delta\ell = m\, v\, r\, \Delta\theta \cos\alpha \tag{71}$$

It should be noted that the assumption of the conservation of momentum is not necessary to this derivation since the particles are close together. Variations in the angular momentum will only contribute higher order terms to $\Delta\ell$.

Now, let us differentiate $d\theta$ with respect to ℓ. This gives

$$\Delta d\theta = d\theta\, \frac{\Delta\ell}{\ell}\left[1 + \frac{m v^2 \sin^2\alpha}{\left(U+\phi - \frac{\ell^2}{2mr^2}\right)}\right] \tag{72}$$

and upon substitution for $\Delta\ell$

$$\Delta d\theta = d\theta\, \Delta\theta \cot\alpha \left[1 + 2\tan^2\alpha\right] \tag{73}$$

Where $d\theta$ is the angular movement of the particles in moving from one potential surface to the next and $\Delta\theta$ is the separation of the particles.

These formulae along with those used to follow individual particles from surface to surface and to follow the ϕ lines give the equipment for a self-consistent field calculation of both the screened electric field and the density of screening ions.

8. RESULTS OF THE SCREENING CALCULATION FOR A TYPICAL PROBLEM

The results of one set of calculations are shown in Fig. 9 and 11. The calculations are made for a body moving at a velocity $u = 7$ km/sec through a plasma of O^+ ions and electrons, corresponding to the altitude range of 300 to 1500 km in the earth's atmosphere. The temperature of the plasma is taken as $T = 1500^oC$. The radial distance from the center of the body to the edge of the screening sheath is set at 180 Debye lengths. Of course, the shape and size of the body itself will be taken to be that of the appropriate equipotential surface (to be determined from the solution of this problem). The values of ψ are given in terms of the kinetic energy of the ambient ions as measured in the coordinate system moving with the satellite, i.e. $^1/_2\, m_i u^2$ and not in terms of kT; the relation between the two is:

$$\psi(\emptyset/kT) = .0318 \quad .$$

The electrons have been included in this calculation by merely setting

$$N_- = N_o e^{-\emptyset/kT} \tag{74}$$

where N_- is the density at a potential $\emptyset$ in terms of the ambient density N_o. This expression is satisfactory for our purpose and can be shown to be exact under all conditions involving an exclusively repulsive field, even where the magnetic field is important.

It will be noticed that Fig. 9 includes results only on the front side of the body. This is due to the fact that, as yet, satisfactory initial conditions have not been calculated for the back side of the body. The calculations given actually involved following 51 electric field lines and 75 particle pairs.

In Fig. 9 we give a plot of the equipotential surfaces, the equidensity surfaces of the ions and six simple trajectories of particles moving in the field. These values are displayed using a plot with the radius as the ordinate

(in units of Debye lengths) and the angle θ (in radians) plotted along the abscissa (the corresponding distance is also provided). Figure 10 indicates the mapping involved in this type of plot. It should be noticed that the scale of the ordinate is smaller by a factor of 100 as compared to the abscissa. Thus the trajectories of the ions shown in Fig. 9 are actually quite curved. On the other hand, the equipotential and equidensity surfaces are only slightly aspherical.

In Fig. 11 we show plots of the density of ions and potential as a function of the radial distance for three different angles to the direction of motion.

Acknowledgment. The author would like to express his appreciation to Dr. S. F. Singer for suggesting the problem as well as his helpful discussions and to Dr. E. J. Öpik for his fundamental derivations. A portion of the numerical calculations were performed by Y. Laohavanich to whom I am deeply indebted.

REFERENCES

1. S. Rand, "The electrostatic field about an ion moving slowly through a highly ionized gas", Convair Report ZPH-023, September 1958.
2. S. Rand, "Structure of the satellite wake", Convair Report, ZPH-028, Jan. 1959.
3. R. Jastrow, and C. A. Pearse, "Atmospheric drag on the satellite", J. Geophys. Res., 62, 3 (1957).
4. J. Holdsworth and S. Rand, "Further studies on the structure of the satellite wake", Convair Report ZPH-032, April, 1959.
5. I. B. Bernstein and I. N. Rabinowitz, "Theory of electrostatic probes in a low density plasma," Project Matterhorn Report PM-S-38, October 1958.
6. A. Guthrie and R. K. Wakerling, editors, The Characteristics of Electrical Discharges in Magnetic Fields (McGraw-Hill, New York, 1949).
7. E. J. Öpik, Interactions of Space Vehicles with an Ionized Atmosphere (Am. Astronaut. Soc. Symp. March 1961) editor, S. F. Singer, MacMillan, New York, 1962.
8. H. Hagstrum, "Auger ejection of electrons from tungsten", Phys. Rev. 96, 325 (1954).
9. H. Hagstrum, "Theory of Auger ejection of electrons from metals by ions," Phys. Rev. 96, 336 (1954).
10. H. Hagstrum, "Auger ejection of electrons from molybdenium by noble gas ions", Phys. Rev. 104, 672 (1956).
11. H. A. Fowler and H. E. Farnsworth, "Reflection of very slow electrons", Phys. Rev. 111, 103 (1958).
12. H. Goldstein, Classical Mechanics, (Addison-Wesley, New York, 1959).

FIGURE CAPTIONS

Fig. 1. Diagram showing the parameters involved in the motion of a screening particle.

Fig. 2. ψ plotted again ρ, with pericritical surface indicated and one curve with secondary electrons. The curves a, b, c, d, e, f, and g represent the family of curves that give the potential as a function of the radius vector. For example, assume a body with radius of 23 Debye lengths has a potential of 15 kT volts. This would be point **A** and thus the potential would fall off according to curve e. The pericritical surface would occur at a distance of 35 h and potential at 0.105 kT. If we include the effects of secondary electrons and charge this sphere to a potential 20 kT then this will put us at point c so that the curve e' represents the variation of ψ vs. ρ.

Fig. 3. A plot of h*/h, the ratio of the effective Debye length to the actual value, vs. the nondimensional distance ρ. These curves correspond to those of Fig. 2 as indicated by the letter labels.

Fig. 4a. Plot of N_+/N_0 and N_-/N_0 against ρ for the potential curve a.

4b. Plot of N_+/N_0 and N_-/N_0 against ρ for the potential curve b.

4c. Plot of N_+/N_0 and N_-/N_0 against ρ for the potential curve c.

4d. Plot of N_+/N_0 and N_-/N_0 against ρ for the potential curve d.

4e. Plot of N_+/N_0 and N_-/N_0 against ρ for the potential curve e.

4f. Plot of N_+/N_0 and N_-/N_0 against ρ for the potential curve f.

4g. Plot of N_+/N_0 and N_-/N_0 against ρ for the potential curve g.

Fig. 5. The initial parameters involved in the self-consistent calculation of screening for a moving sphere.

Fig. 6. Illustration of the parameters used to calculate the correction to $\Delta S_\perp$ for small α.

Fig. 7. Illustration of the parameters used to calculate θ_{min} for the correction of $\sin\theta$.

Fig. 8. Illustration of the change $\Delta d\theta$ in the angular separation of the companion particle.

Fig. 9. A plot of the equipotential surfaces, equidensity surfaces and six sample particle trajectories for the front side of a satellite. The body is assumed to be moving at 7 km/sec through a plasma of O^+ ions and electrons. The temperature of the plasma is taken to be 1500°C. The ordinate is the radial distance in Debye lengths and the abcissa gives the angle in radians.

Fig. 10. Figure to show the mapping employed in Fig. 8. A portion of a polar plot has been mapped into a cartesian coordinate system.

Fig. 11. The variation in the nondimensional potential ϕ/kT and the normalized density n along the radius vector for several representative angles: θ = 0, 1.005, 1.445 radians.

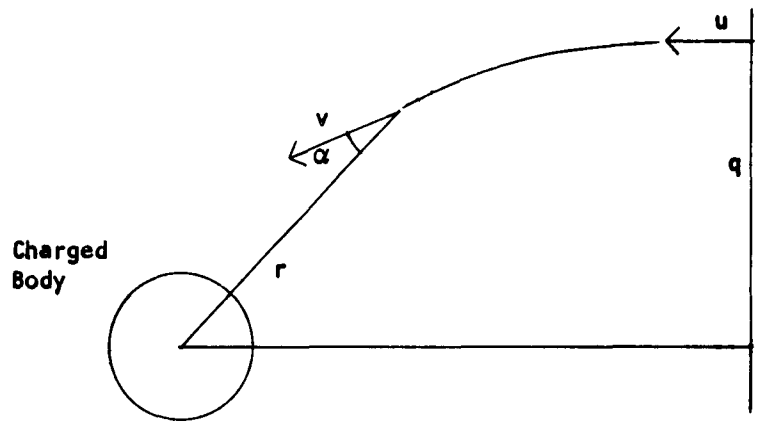

Figure 1.

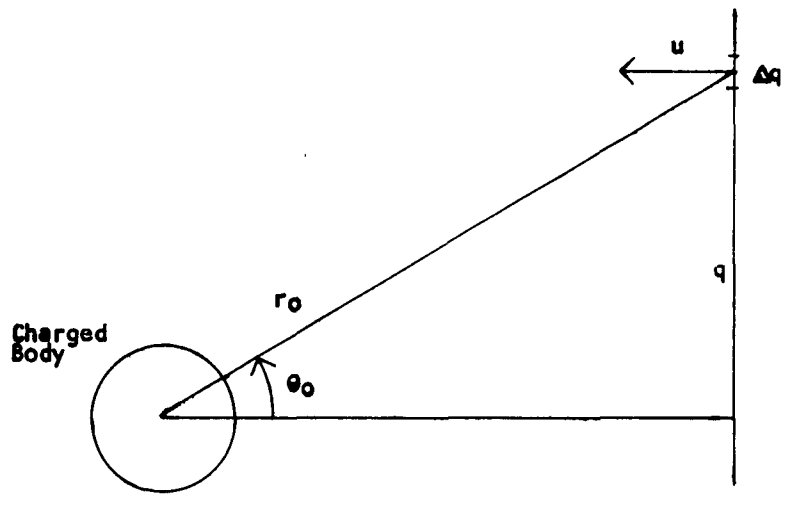

Figure 5.

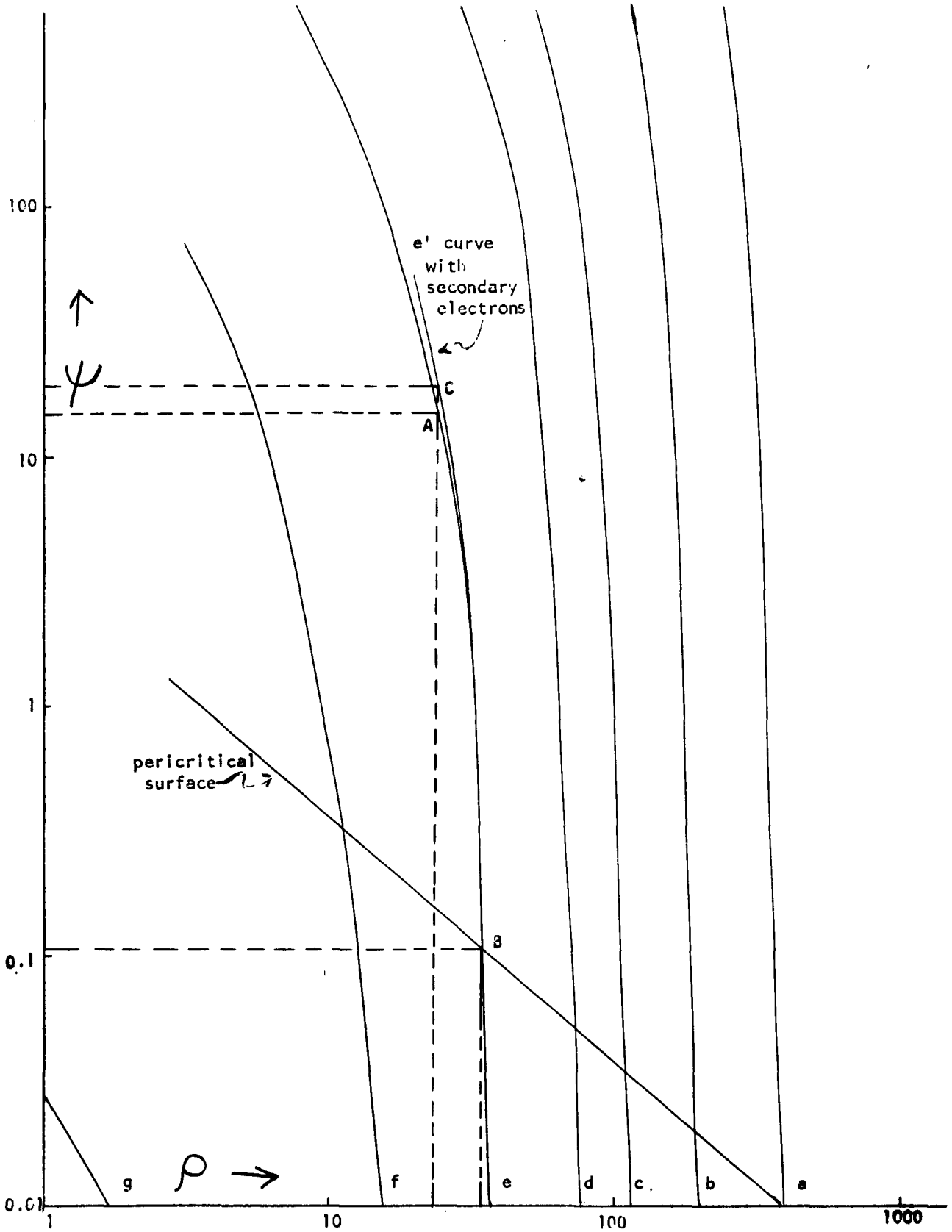
100
10
1
0.1
0.01
1
10
100
1000
ψ
ρ
e' curve with secondary electrons
C
A
B
pericritical surface
a
b
c
d
e
f
g

Fig. 2.

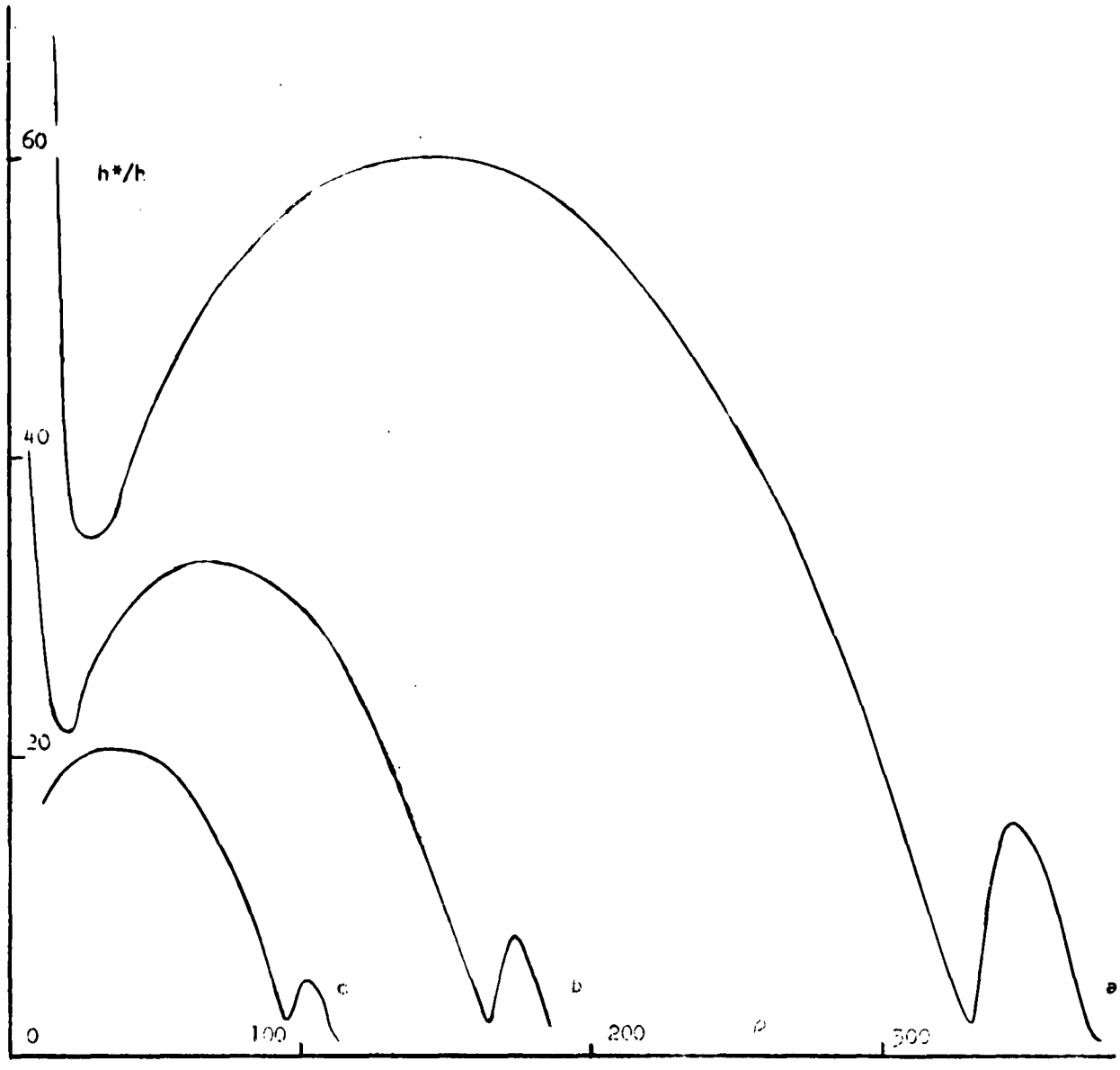

Fig. 3 a

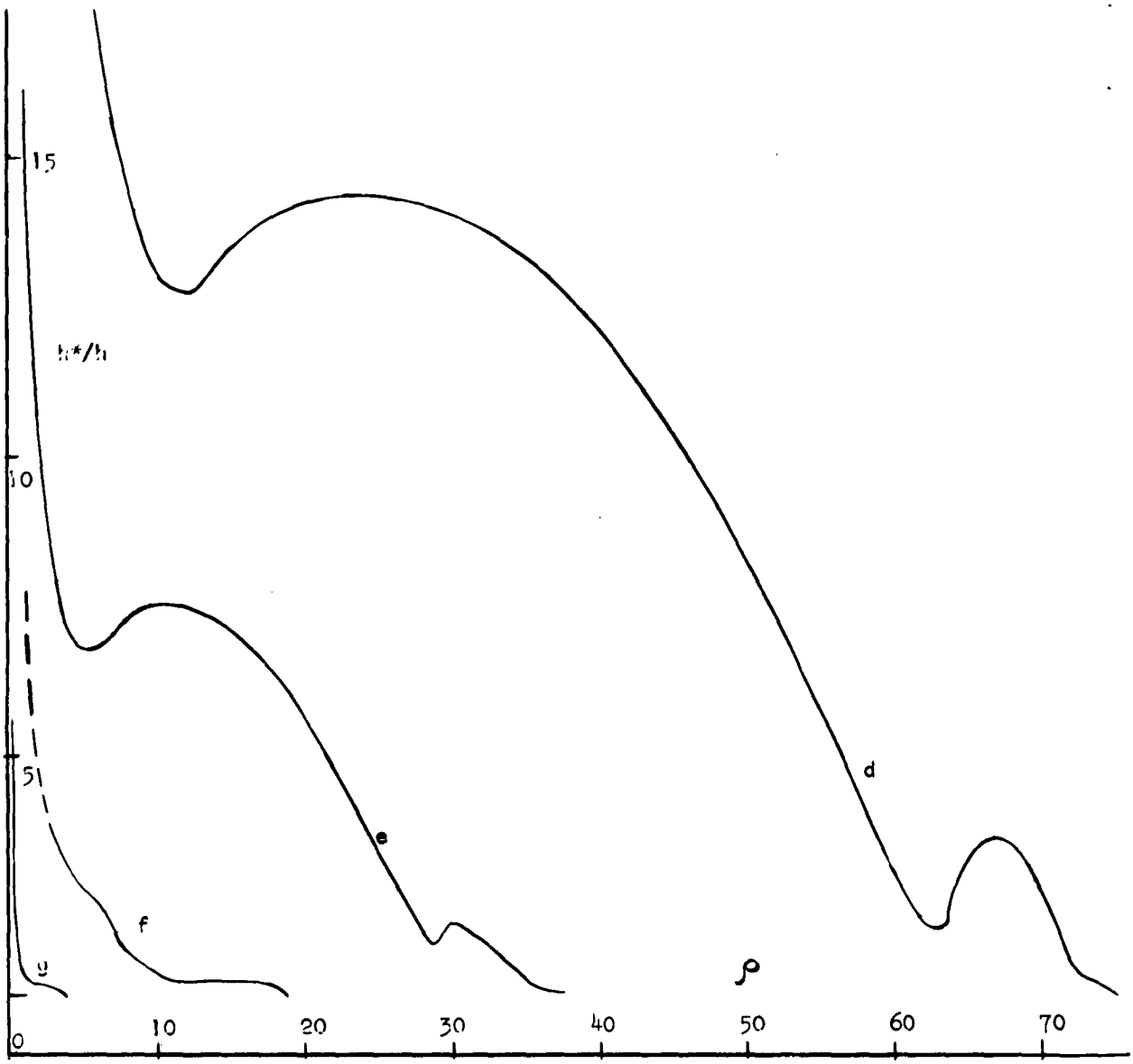

Fig. 3 b

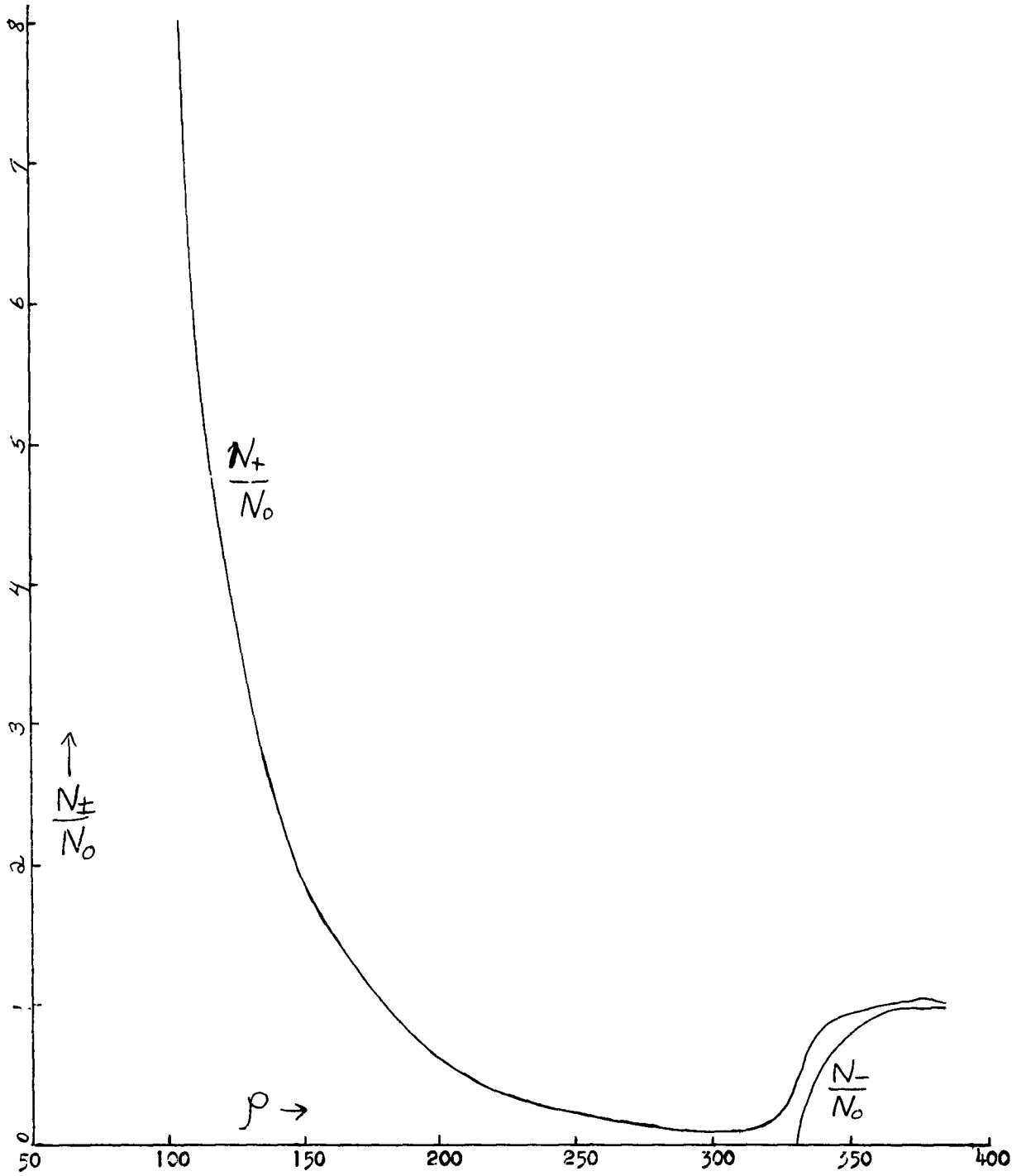
8
7
6
5
4
3
2
1
0
50
100
150
200
250
300
350
400
$\frac{N_+}{N_0}$
$\frac{N_\pm}{N_0}$
$\rho \rightarrow$
$\frac{N_-}{N_0}$

Figure 4.a.

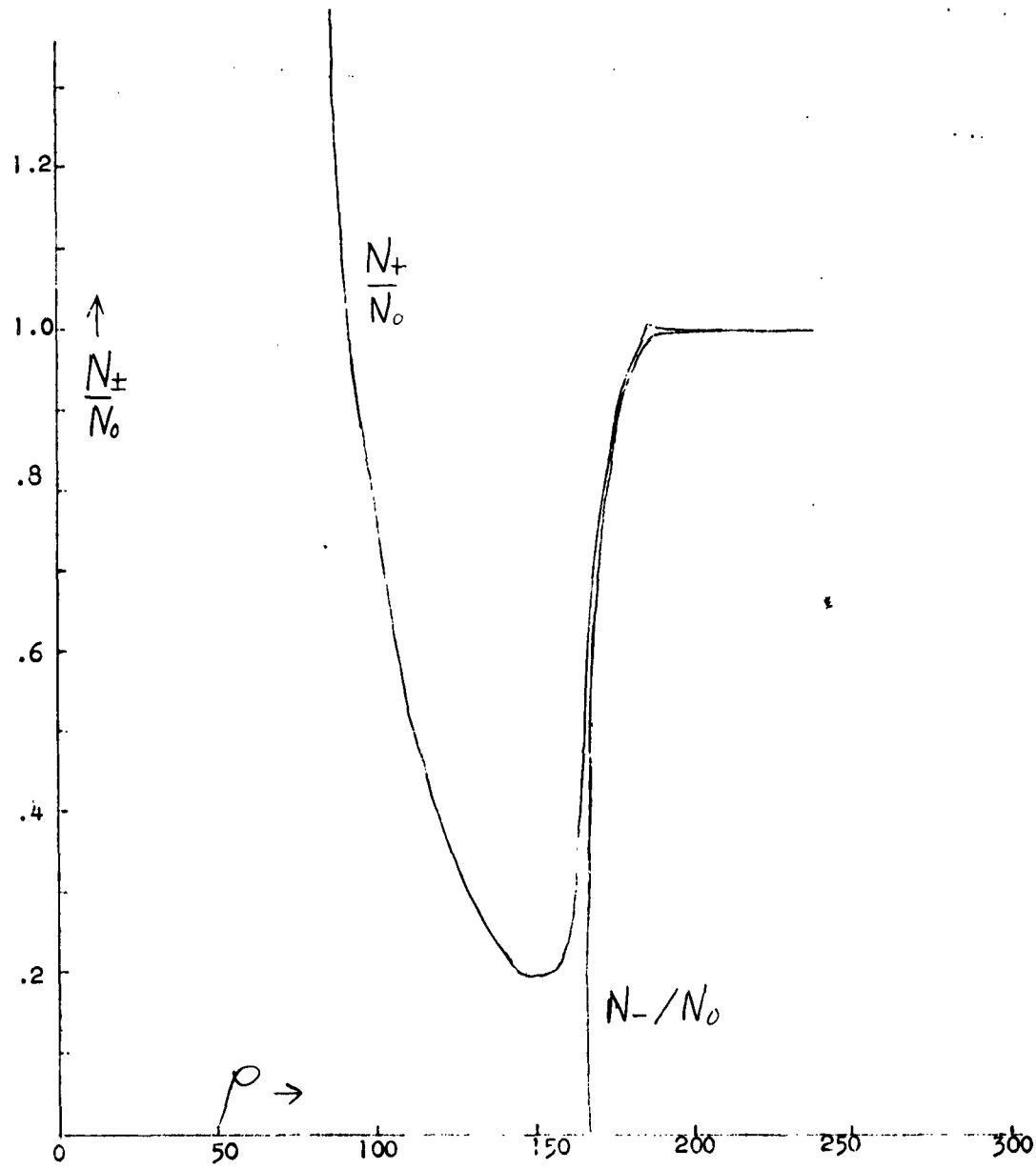

Figure 4 b.

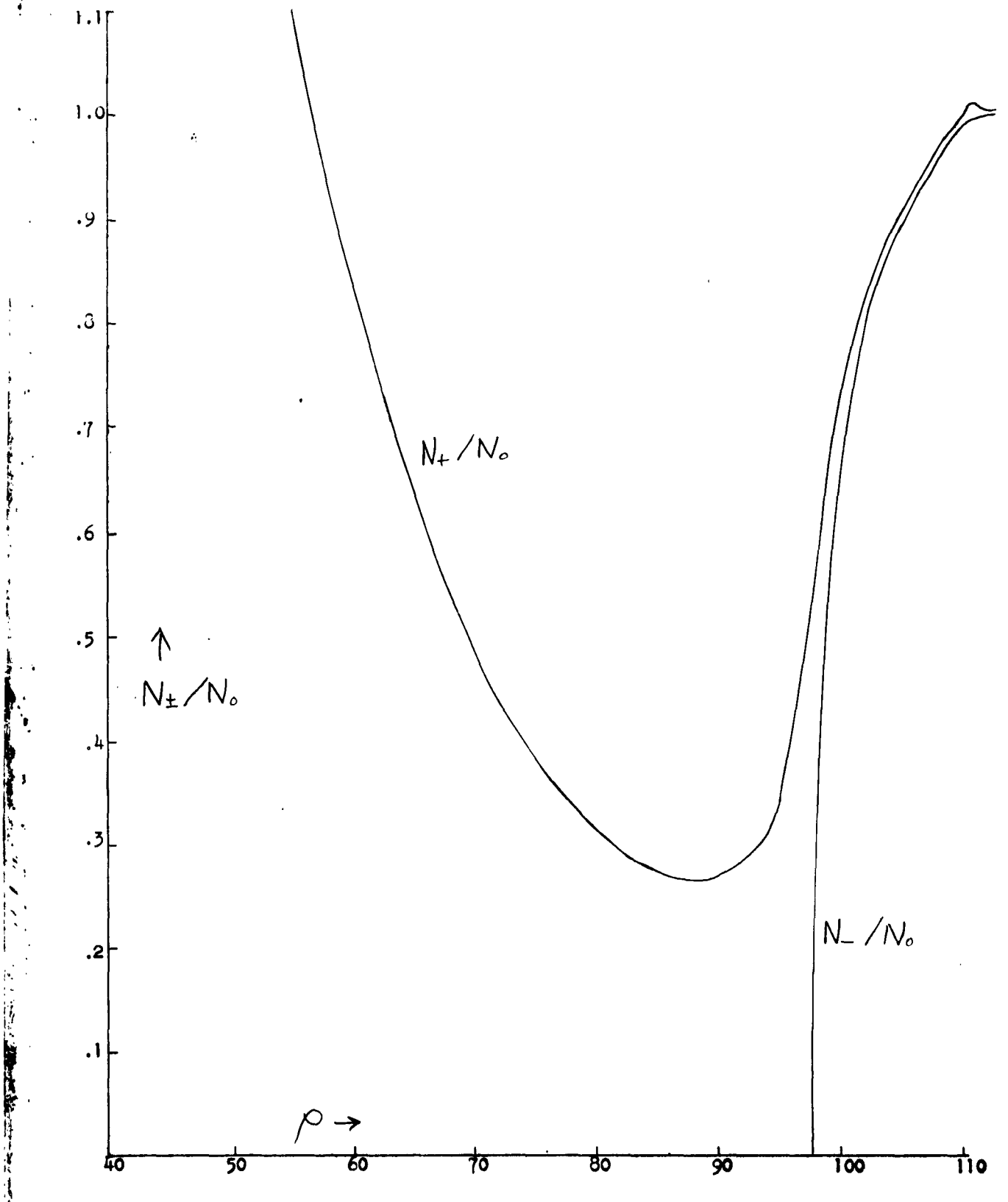
1.1
1.0
.9
.8
.7
.6
.5
.4
.3
.2
.1
$N_\pm / N_o$
N_+ / N_o
N_- / N_o
$\rho \rightarrow$
40
50
60
70
80
90
100
110

Figure 4 c.

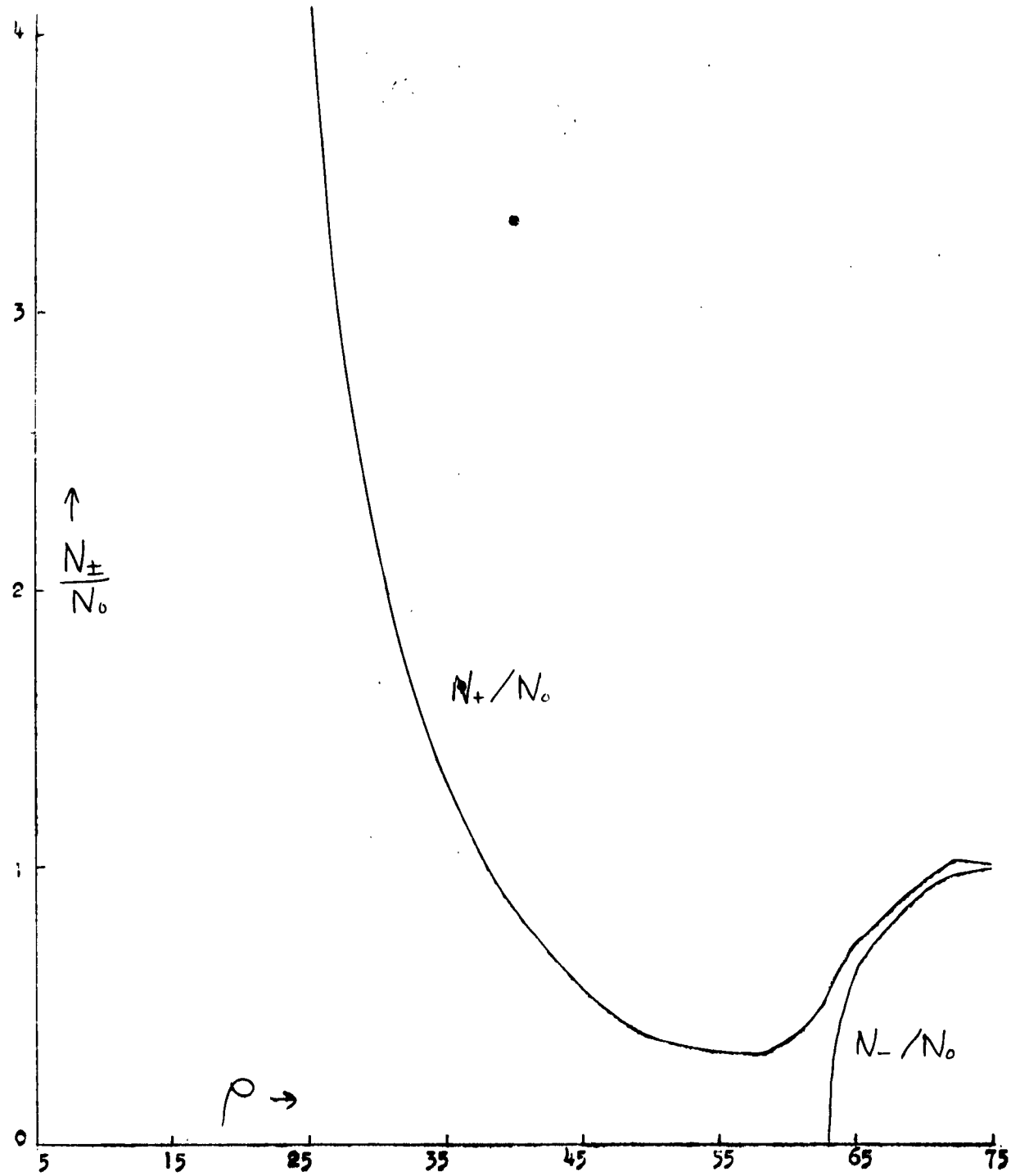

Figure 4d.

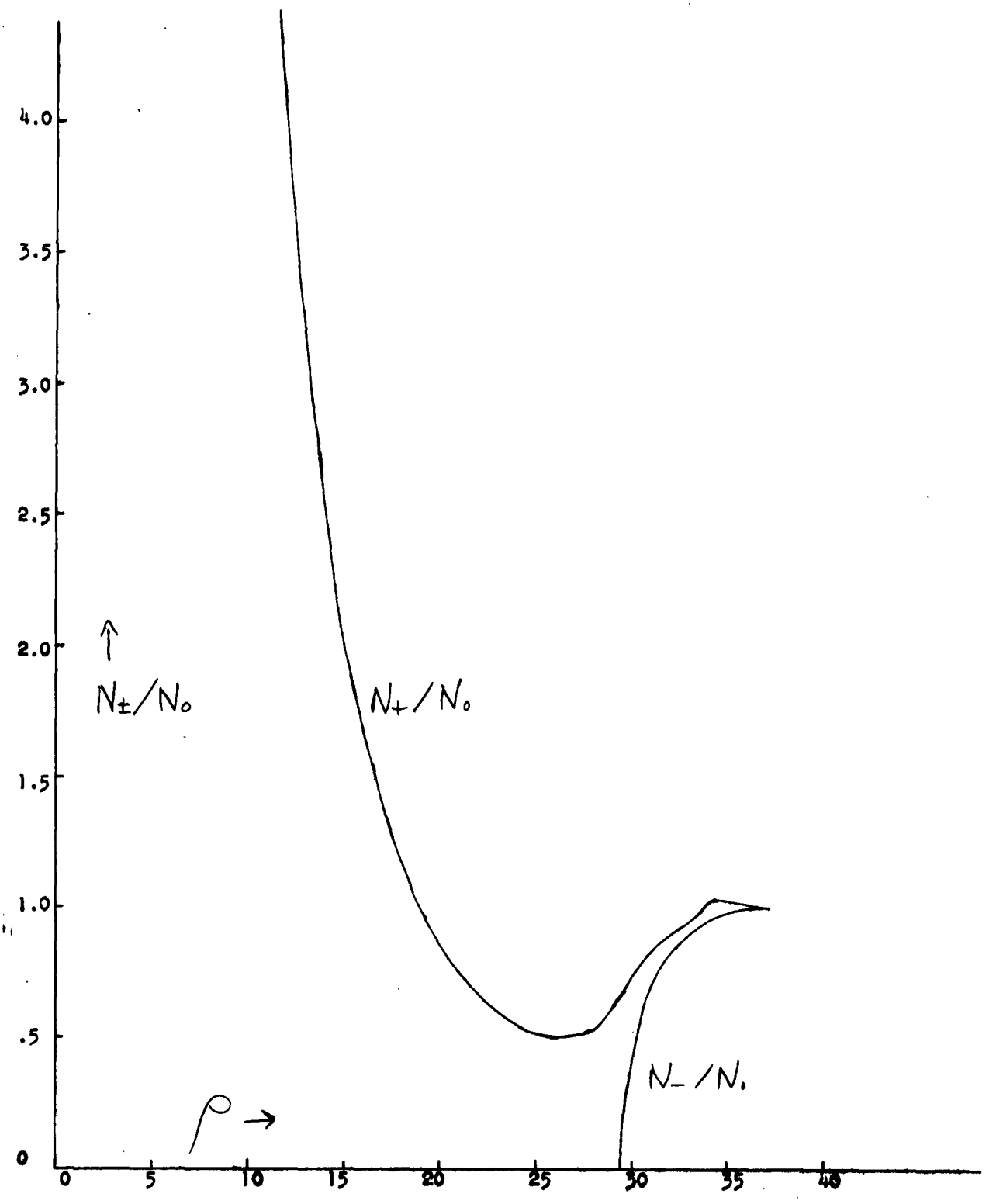

Figure4 e.

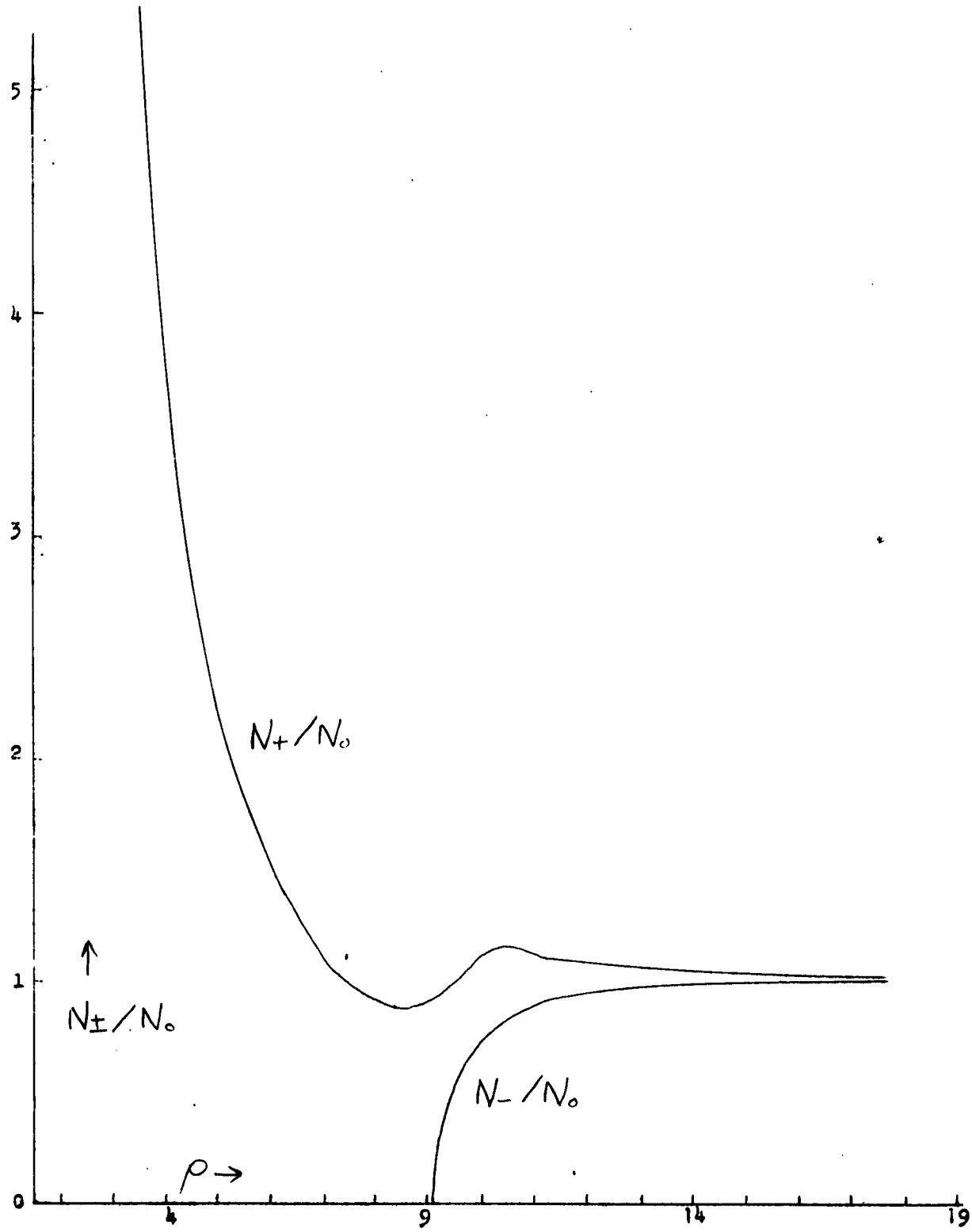

Figure 4 f. Pl[illegible] f.

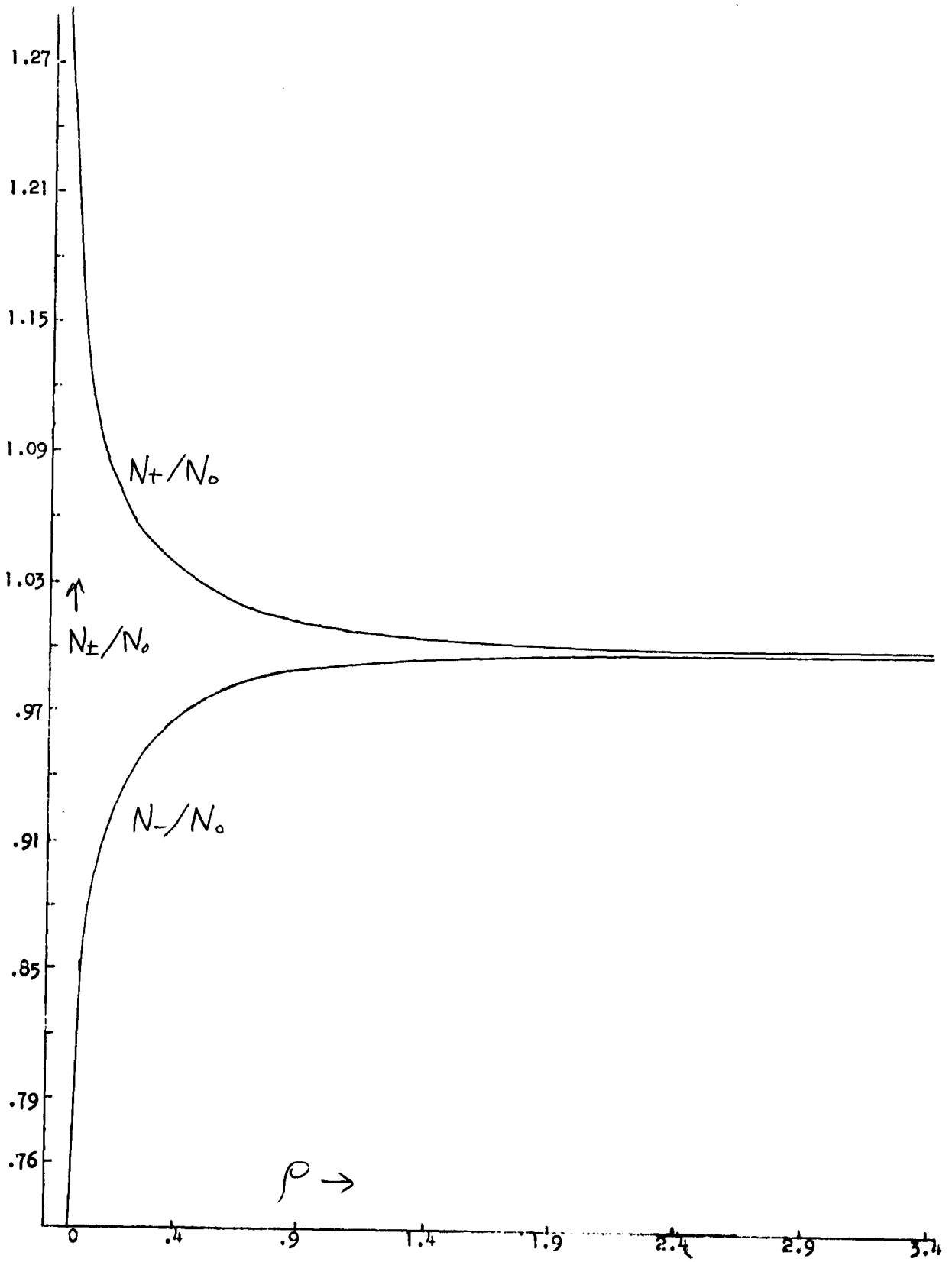

Figure 4 g. Plo

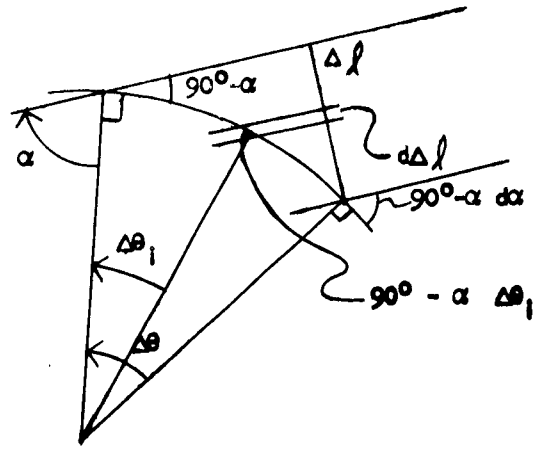

Figure 6.

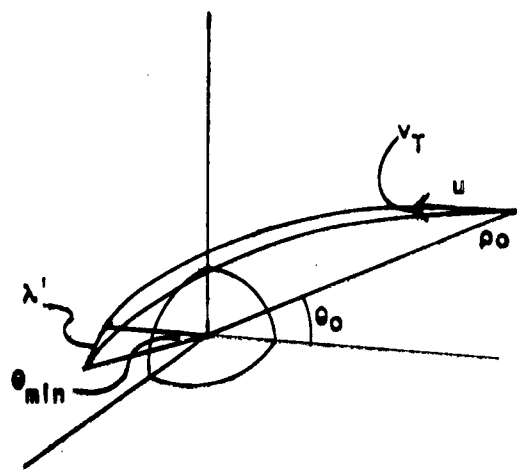

Figure 7.

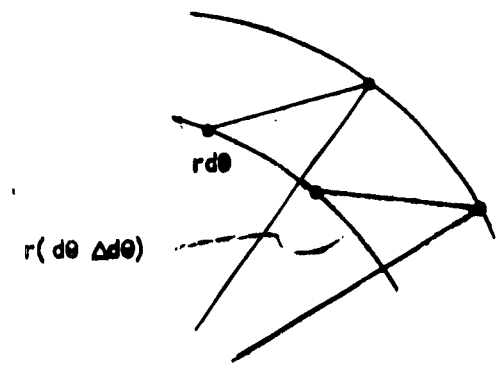

Figure 8.

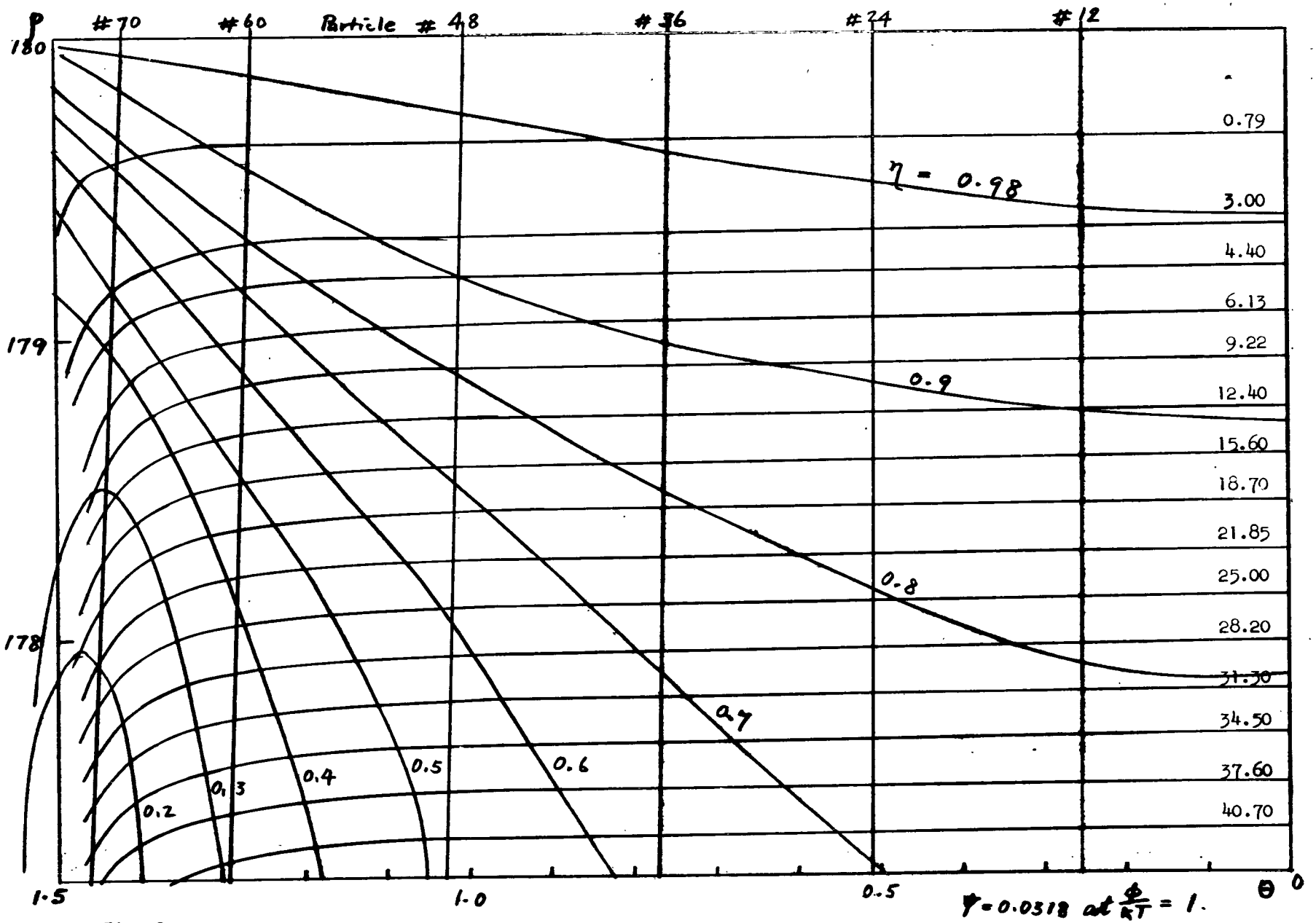
P
#70
#60
Particle #48
#36
#24
#12
180
179
178
0.79
3.00
4.40
6.13
9.22
12.40
15.60
18.70
21.85
25.00
28.20
31.30
34.50
37.60
40.70
η = 0.98
0.9
0.8
0.7
0.6
0.5
0.4
0.3
0.2
1.5
1.0
0.5
0
θ
ψ = 0.0318 at ε/kT = 1.

Fig. 9

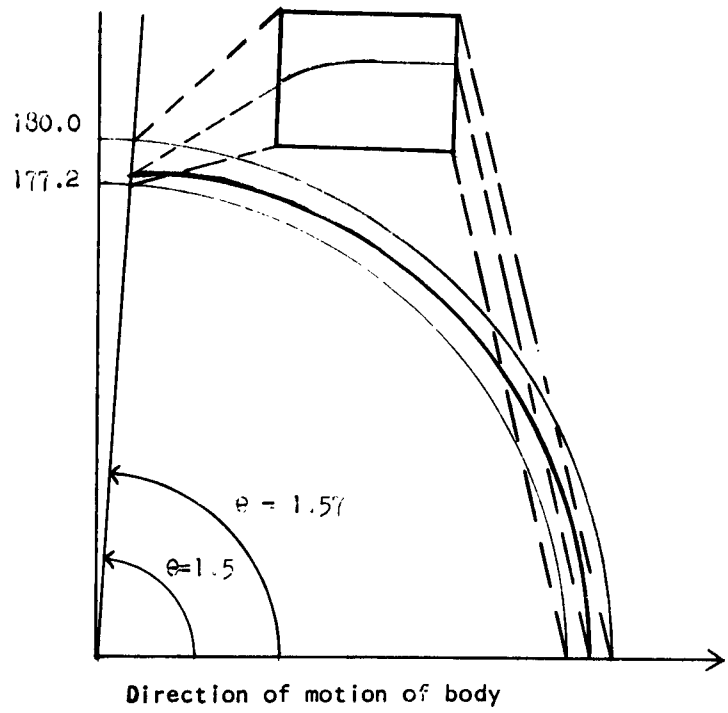

Fig. 10

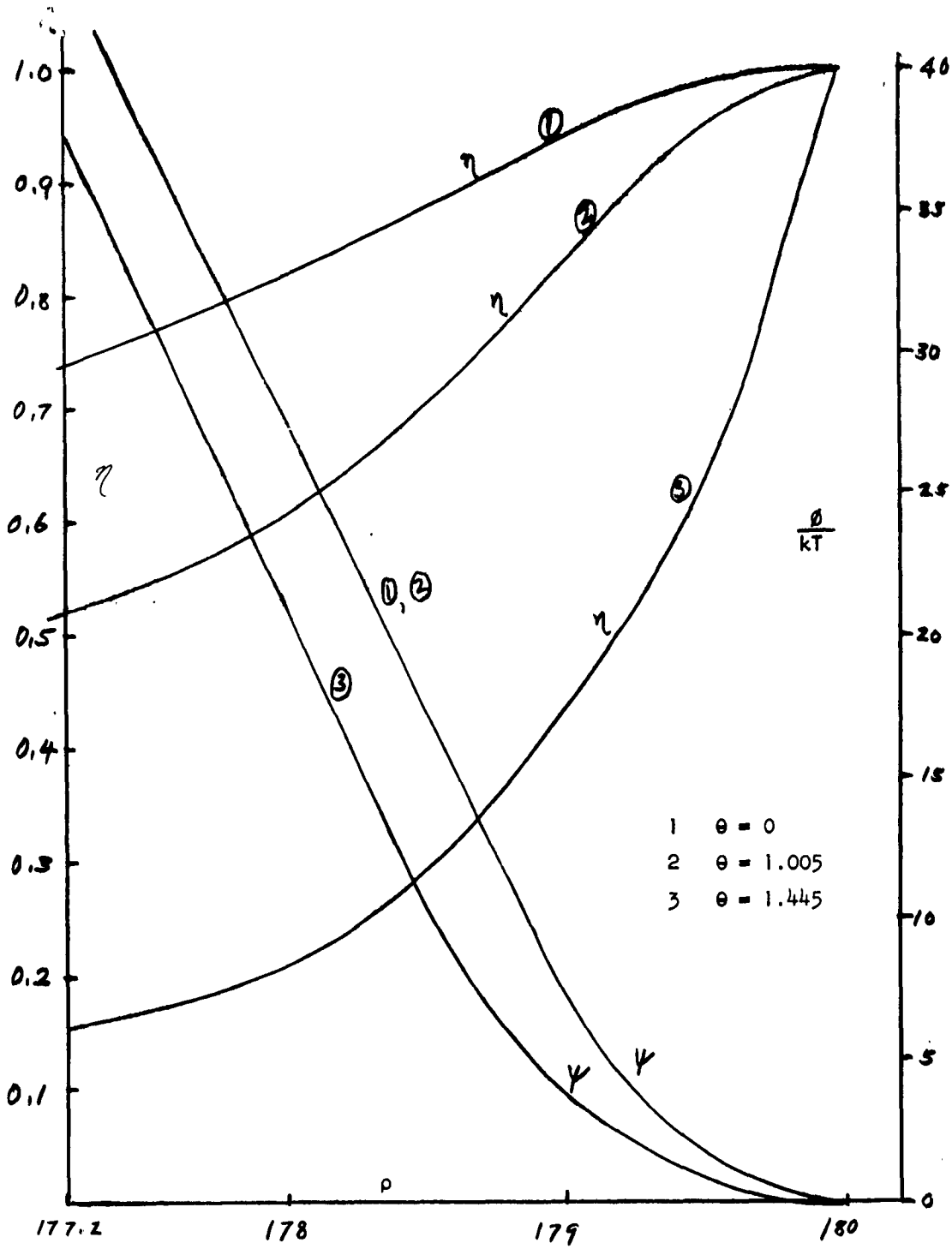

$\psi = 0.0318, \frac{\phi}{kT} = 1.$

Fig. 11

PLASMA COMPRESSION EFFECTS PRODUCED BY SPACE VEHICLES IN A MAGNETO IONIC MEDIUM

S.F. Singer and E. H. Walker

ABSTRACT

A novel phenomenon is discussed which leads to the creation of large clouds of compressed plasma[1]. It is based on a theoretically predicted mechanism which is caused by the interaction of an electrically charged body with the surrounding ambient plasma, in the presence of a magnetic field. The cloud consists of ions which have been scattered into quasi-trapped orbits. Their injection and removal are studied in detail. Under non-steady state conditions the cloud may detach itself from the body and give rise to "ghosts". It is quite possible that this phenomenon is the cause of the unusual "bursts" and radar echoes observed to be associated with passes of earth satellites.

1. Statement of the Problem

If a body carrying an electric charge moves rapidly through an ionized gas pervaded by a magnetic field, ions will be deflected by the electrostatic field of the body and will remain quasi-trapped by the magnetic field until removed by scattering. We wish to consider the extent to which a charged body can produce a buildup of the ion density along or near its path.

If we consider the ion velocities to be much less than the velocity of the charged body, i.e. if the plasma is cool, then in a coordinate system moving with the charged body the incident ions (field particles) all move with a velocity v until they are deflected through an angle θ (which depends on the impact parameter p), and then either move ahead of or behind the charged body (Fig. 1). Because of the presence of the magnetic field (assumed for the moment to be parallel to v) those ions (or test particles) that are deflected through an angle close to 90° will continue to move with the deflecting body and will remain in the neighborhood of the body until scattered.

The buildup of the density distribution of the test particles is countered by four possible removal mechanisms:

1. Collision with ambient ions (field particles),
2. Collision with neutral atoms,
3. Collision with other test particles,
4. Collision with the charged body.

The collisions with the neutral atoms, because of the low cross section, will not be as important as collisions with the ambient ions at altitudes above 300 km. Collisions with other test particles will only be important when the compression of the test particles becomes large; furthermore, their scattering will not be qualitatively different from that of the field particles, and therefore they can be included by an appropriate choice of the mean free path λ of

the test particles.

If the potential of the body is positive and greater than kT/Ze, collisions with the charged body will not be important. However, special attention must be given to the case of a negative sphere. This will be considered along with the effects of screening in Section 9. For an initial approach, we will consider the case of a low density plasma so that we may neglect the effects of screening.

2. Calculations of Important Parameters for the Deflection of Ions by Charged Bodies

It is important to consider the orders of magnitude of several lengths which enter into our problem. The following equations are in MKS units.

We have the following relation between the impact parameter, p, and the scattering angle θ

$$p = \frac{Zeq}{8\pi\epsilon_0 E} \cot\frac{\theta}{2} = p_0 \cot\frac{\theta}{2} = 9.57 \times 10^7 \frac{ZaV}{AV^2} \cot\frac{\theta}{2} \qquad (1)$$

where E is the energy of the ions, q the charge on the body, V is the potential on a body of radius a, Ze is the charge of the ion, A is the atomic weight of the ion and p_0 is the 90^0 impact parameter.

The radius of gyration, ρ , of a particle in a magnetic field is given by

$$\rho = \frac{mv}{ZeB} \sin\theta = \rho_0 \sin\theta = 1.045 \times 10^{-8} \frac{Av}{ZB} \sin\theta \qquad (2)$$

where m is the mass of the particle, B is the magnetic induction and ρ_0 is the radius of gyration for a test particle moving at right angles to the field.

The Debye screening length h is

$$h = \sqrt{\frac{\epsilon_0 k T}{e^2 n_e}} = 69.0 \left(\frac{T}{n_e}\right)^{1/2} \qquad (3)$$

where k is Boltzmann's constant, T is the temperature of the plasma, and n_e is the ambient electron density.

Table I contains numerical values of these important quantities.

The mean free path for energy loss and for angular scattering for an ion moving somewhat faster than the thermal ions but more slowly than the thermal electrons is important in determining our approach to the problem of the build-up of an ion cloud near a satellite.

For an ion which is moving at a velocity of 7 km/sec through a plasma of ionized oxygen at a temperature of 1500°K (for which the root mean square thermal velocity for the ions is 1.53 km/sec and for the electrons 261 km/sec), the coefficient of dynamical friction produced by the electrons $\langle \Delta w_{i\perp} \rangle_e$ divided by $\langle \Delta w_{i\perp} \rangle_i$ for the ions is, according to Spitzer[2]

$$\frac{\langle \Delta w_{i\parallel} \rangle_e}{\langle \Delta w_{i\parallel} \rangle_i} = \frac{(m_i+m_e)\ G(w/w_e)}{2z_i^2\ m_i\ G(w/w_i)} = \frac{G(.035)}{2G(6.0)} = 0.46 \qquad (4)$$

and for hydrogen ions the values is 0.031. For this reason we need not be concerned with energy loss to the electrons. The ratios of the deflection time t_D to the energy exchange time t_E and also to the slowing-down time t_s, again according to Spitzer[2], are

$$t_D/t_E = \frac{4G(w/w_i)}{\Phi(w/w_i) - G(w/w_i)} = 0.057 \qquad (5)$$

for oxygen and 1.12 for hydrogen while

$$t_D/t_s = \frac{2G(w/w_i)}{\Phi(w/w_i) - G(w/w_i)} \left(\frac{w}{w_i}\right)^2 = 1.00 \qquad (6)$$

for oxygen and 0.74 for hydrogen. This shows that change in the velocity of the test particles will occur approximately as fast as the change in angle. In the derivation of an expression for the density and extension of a buildup of test particles into a cloud moving with the charged body, we will first consider the angular deflection of the test particles, assuming the velocity to be constant and then consider the effect of their slowing down.

The effective cross section σ for the deflection of a test particle by the field particles can be obtained from Spitzer[2]:

$$\sigma = \frac{8\pi e^4}{v^4 m^2} \left[\phi\left(\frac{w}{w_1}\right) - G\left(\frac{w}{w_1}\right) \right] \ln \Lambda \qquad \text{(cgs units)} \qquad (7)$$

For v = 7 km/sec, T = 1500°K, n = 10^5 cm^{-3} the mean free path λ for a 90° deflection of an O^+ test particle is 900 km; for H^+ the mean free path is 5 km.

3. Approximate Density of the Deflected Ions

An approximate expression for the number density or concentration of the deflected test particles, n, is obtained by dividing $(\pi p^2 vT) n_e$, the volume swept out by the charged body in a time T times the ambient ion (or electron) density, by $\pi(2\rho)^2 \ell$, the volume containing the helical paths of the ions for a time interval T. Since we have for ℓ

$$\ell = vT \cos\theta \qquad (8)$$

we get for n

$$n = \frac{p^2}{4\rho^2 \cos\theta} n_e \qquad (9)$$

Let us take as an example a spherical satellite of radius 1 meter charged to a potential of 10 volts moving with a velocity of 7 km/sec in a magnetic field of 3×10^{-5} webers/m^2. If we take an intermediate value for θ of 60° then n/n_e has a value of 10.9 for H^+ ions but is completely negligible for O^+ ions since they would be moving too rapidly to be affected appreciably by the magnetic field.

A more refined expression than Eq. (9) can be obtained. Let us assume that in an equilibrium situation the rate of injection of test particles into helical paths corresponding to a deflection angle θ is I_0. If these test particles are removed by collisions, what will be their number I_θ at any time t after the injection? We have

$$\frac{dI_\theta}{dt} = I_\theta n_e \sigma v_r \qquad (10)$$

where the relative velocity between the test particles and the field particles, v_r, is given by

$$v_r = 2v \sin \frac{\theta}{2} \tag{11}$$

Therefore, we have

$$I_\theta = I_o \, e^{-n_e \sigma v_r t} \tag{12}$$

The rate of injection of test particles between the angles θ and $\theta + d\theta$ can be expressed in terms of $\Sigma(\theta)$, the scattering cross section for ions deflected by the charged sphere:

$$I_o \, d\theta = J \, \Sigma(\theta) \, 2\pi \sin\theta \, d\theta \tag{13}$$

where J is the flux of incident field particles given by

$$J = n_e v \tag{14}$$

$\Sigma(\theta)$ is given by

$$\Sigma(\theta) = p_o^2 \frac{\cos \theta/2}{2 \sin\theta \sin^3 \theta/2} \tag{15}$$

so that

$$I_\theta = n_e v \, \pi p_o^2 \frac{\cos \theta/2}{\sin^3 \theta/2} \, e^{-n_e \sigma v_r t} \tag{16}$$

The time can be expressed in terms of the distance from the center of the charged sphere, x, by the substitution for t of

$$t = - x/(v \cos \theta) \tag{17}$$

If we substitute Eq. (16) into (14) and integrate over x we obtain

$$n_\theta \Big|_o^x = \frac{\pi p_o^2}{2\sigma} \cdot \frac{\cos \theta/2}{\sin^4 \theta/2} \left[1 - e^{-\frac{2\sigma n_e \sin \theta/2}{\cos \theta} x} \right] \tag{18}$$

We can drop the exponent if we take x to be large. Integrating over all angles from θ_o to 180^o gives v for the total number of ions N

$$N = \frac{\pi p_o^2}{3\sigma} \left[\sin^{-3} \frac{\theta_o}{2} - 1 \right] \tag{19}$$

If n_x is defined as the linear density of ions, its average value $\bar{n}_x$

can be expressed in terms of x_o where

$$x_o = \frac{\cos\theta}{2\sigma n_e \sin\theta/2} = \lambda \frac{\cos\theta}{2\sin\theta/2} \tag{22}$$

which is the range of a test particle initially deflected through an angle θ. We have for $\bar{n}_x$:

$$\bar{n}_x = \frac{N}{x_o} = \frac{2\pi}{3} \rho_o^2 n_e \frac{\sin\bar{\theta}/2}{\cos\bar{\theta}} \left[\sin^{-3}\frac{\theta_0}{2} - 1\right] \tag{23}$$

where $\bar{\theta}$ represents an average angle of deflection. To obtain the average volume density, $\bar{n}$, in the case where the test particle's radius of gyration $\rho_o >> \rho_o$ we divide $\bar{n}_x$ by the area covered by the helical paths which is $4\pi\rho^2$. However, we must use the average value of ρ

$$\rho = \rho_o \sin\bar{\theta} \tag{24}$$

Therefore we have

$$\bar{n} = \frac{n_e \rho_o^2}{6\rho_o^2} \cdot \frac{1}{\sin\bar{\theta}/2 \cos\bar{\theta}} \left[\sin^{-3}\frac{\theta_0}{2} - 1\right] \tag{25}$$

The density expression where $\rho_o >> \rho_o$ is

$$\bar{n} = \frac{\bar{n}_x}{\pi\rho^2} = \frac{2\pi}{3} n_e \frac{\sin^3\bar{\theta}/2}{\cos^2\bar{\theta}/2 \cos\bar{\theta}} \left[\sin^{-3}\frac{\theta_0}{2} - 1\right] \tag{26}$$

Eqs. (25) and (26) describe the density more accurately then Eq. (9) which was based on dimensional considerations.

Equations (25) and (26) give us the equilibrium density of test particles along the path of the charged body. We will use these expressions to determine the compression produced by satellites moving parallel to a magnetic field.

In Eq. (6) we showed that the mean time for the slowing down of the test particles is almost the same as the mean time for the deflection of the test particles for both H^+ and O^+. This will mean that the forward velocity of the test particles will fall off as an exponential function (or even faster) about as rapidly as the particles are removed by deflections. Since the

density varies inversely with the velocity of the ions, this effect results in a sustained or in some cases a growing density. The sweep back of these ions is also important. This gives rise to a folding back of the ion cloud onto itself. For large clouds such that $\rho_o >> \rho_o$ the sweep back ions will contribute as greatly as the main stream of ions but where $\rho_o >> \rho_o$ this would not be the case except for the fact that the ions are slowing down and reducing ρ_o. We should therefore add, in either case, a factor of 2 to Eqs. (25) and (26) to account for the sweep back effects.

4. The Diffusion Equation

Let $f(x,\theta)\ dx\ d\Omega$ represent the number of ions in a plane perpendicular to x, located in an interval dx at x and within an angular interval $d\theta$ at θ. If we assume that the test particles suffer energy loss more slowly than angular deflection, we can derive a differential equation for $f(x,\theta)$. If v is the same for all particles then we can write a continuity equation. The divergence of $f(x, \theta)\ v\cos\theta$ in an interval $dx\ d\Omega$ is equal to the total number of particles scattered from all other dx' and $d\Omega'$ minus those scattered from $dx\ d\Omega$ into all dx' and $d\Omega'$. This gives

$$\begin{aligned} &\frac{d}{dx}\left[f(x,\theta)\ v\cos\theta\ 2\pi\sin\theta\ d\theta\right] \\ &= 2v\, n_e \int_{\phi=0}^{2\pi}\int_{\Omega'} f(x,\Psi)\ \sin\frac{\Psi}{2}\sigma(\Psi)\ \sin\theta\ d\theta\ d\phi\ d\Omega' \\ &- \int_{\Omega'} f(x,\theta)\ 2v\sin\frac{\theta}{2}\ n_e\sigma(\theta')\ d\Omega'\ 2\pi\sin\theta\ d\theta \end{aligned} \tag{27}$$

where Ω' is the solid angle of integration which includes all scattering directions, which is expressed in terms of Ψ. Since the first integration is to be carried out over all possible pairs of $d\Omega$ and $d\Omega'$, it is possible to define a new set of coordinates in which cylindrical symmetry exists. Thus a factor of 2π can be integrated out of the first integral. The second depends

only on Ω' and thus can be expressed in terms of σ, the total cross section. We obtain:

$$\frac{d}{dx} f(x,\theta) + \frac{2n_e \sigma \sin \theta/2}{\cos \theta} f(x,\theta) = \frac{4\pi m_e}{\cos\theta} \int_0^{\pi} f(x,\psi)\sigma(\psi) \sin \frac{\psi}{2} \sin \psi \, d\psi \qquad (28)$$

The integral term represents the back scatter; for if we set the integral term equal to zero, then we obtain the "first scatter" solution $f_1(x,\theta)$

$$f_1(x,\theta) = f_{1o} \exp \left[- \frac{2\sin \theta/2}{\cos \theta} x \right] \qquad (29)$$

Here f_{1o} is the number of ions deflected into an element of length dx at an angle θ; i.e.

$$f_{1o} = I_o / v \cos\theta \qquad (30)$$

which gives

$$f_1(x,\theta) = \pi m_e p_o^2 \frac{\cos \theta/2}{\cos\theta \sin^3 \theta/2} \exp \left[- \frac{2n_e \sigma \sin \theta/2}{\cos \theta} x \right] \qquad (31)$$

which agrees with our previous result Eq. (16) but includes the substitutions of Eqs. (17) and (30).

Equation (29) can be used to show the buildup in density near the body by those test particles which are deflected through an angle near 90°. Since $f(x,\theta) = dn_x/d\theta$, and in the "first scatter" approximation

$$dn_x = f_1(x,\theta)\, dx \qquad (32)$$

If we substitute $\theta = 90^\circ + \delta$ then we can write the integral from 0 to $\Delta\theta$ as

$$n_x \Big|_0^{\Delta\theta} = 2\pi m_e p_o^2 \int_0^{\Delta\theta} e^{-\sqrt{2}\sigma n_e x/\delta} \frac{d\delta}{\delta} \qquad (33)$$

where $\Delta\theta$ is small. The choice of x depends on the value of $\Delta\theta$; for x we must choose the minimum distance that includes all the deflected particles in the range $\Delta\theta > \delta > 0$ that have not yet been deflected. Therefore we

must take for x

$$x = \Delta\theta/\sqrt{2}\sigma n_e \tag{34}$$

If we make the change of variable $z = \Delta\theta/\delta$ we obtain

$$n_x \Big|_0^{\Delta\theta} = 2\pi n_e p_o^2 \int_1^\infty e^{-z} \frac{dz}{z} \tag{35}$$

Using the Tables of Functions by Jahnke and Emde we find

$$\lim_{\Delta\theta \to 0} n_x \Big|_0^{\Delta\theta} = 2\pi n_e p_o^2 \, (0.2194) \tag{36}$$

To obtain a more general solution for the diffusion equation we write $f(x,\theta)$ as

$$f(x,\theta) = X(x) \, \Theta(\theta) \tag{37}$$

where this is justified by the fact that Eq. (28) then becomes separable

$$\frac{1}{X(x)} \frac{dX(x)}{dx} = k = -\frac{2n_e \sigma \sin \theta/2}{\cos \theta} + \frac{4\pi n_e}{\Theta(\theta)\cos\theta} \int_0^\pi \Theta(\psi)\sigma(\psi) \sin\frac{\psi}{2} \sin\psi \, d\psi \tag{38}$$

The integration of the left side of this expression yields

$$X(x) = X_o \, e^{kx} \tag{39}$$

This shows that $f(x,\theta)$ retains the same dependence on x that was found in Eq. (29). It should be noted that it is possible for the coefficient of x in the exponential factor to be positive. Thus, test particles, initially deflected forward by the charged body may later be scatter back so as to contribute to the density of a certain region a second time. The effect of this on the density, n, will be considerable if $p_o \gg \rho_o$. If $\rho_o \gg p_\theta$ successive scatters will remove the test particles from the region of compression. Since the ions also slow down, thereby, reducing the value of ρ_o, the back scatter is important for $\rho_o \gg p_o$ also.

The function $\Phi(\theta)$ can be expressed in terms of q_o, the 90^o impact parameter for encounters between field particles and test particles, by the expression:

$$\Phi(\theta) = \Phi_0 \exp \int \left[\frac{2\pi n_e q_o^2 \cos\theta/2 + k \sin^2\theta/2 \sin\theta - 4n_e \sigma \sin^2\theta/2 \cos\theta/2}{\sin^2\theta/2 (k\cos\theta + 2n_e \sigma \sin\theta/2)} \right] d\theta \tag{40}$$

5. The Calculation of the Density as a Function of Position in Cylindrical Coordinates

Let us divide $f_1(x,\theta)$ by the area into which the particles at x with a deflection θ will move. Since an ion with impact parameter p will describe a circle of radius ρ that has its center at $r = \ell$ where ℓ is given by (see Fig. 3).

$$\ell = \sqrt{p^2 + \rho^2} \tag{41}$$

we have for $dn(r,x,\theta)/d\theta$

$$\frac{dn}{d\theta} = \frac{f_1(x,\theta)}{\pi[(\ell + \rho)^2 - (\ell - \rho)^2]} = \frac{f_1(x,\theta)}{4\pi\rho\sqrt{p^2 + \rho^2}} \tag{42}$$

where we have assumed that the ions deflected into an angle θ distribute uniformly over the ring $\ell - \rho < r < \ell + \rho$.

To obtain the density at r, x we integrate over all θ contributing to the density at r:

$$n(r,x) = \int_{\theta_a}^{\theta_b} n_\theta(x, r, \theta)\, d\theta \tag{43}$$

Since those ions scattered at $p(\theta_a)$ will distribute out as far as $\ell(\theta_a) - \rho(\theta_a)$ and since this must equal r if θ_a is to be the minimum angle to contribute to the density at r (along the positive x axis: i.e. for forward deflections) and since for the largest angle to contribute θ_b must be such that $\ell(\theta_b) + \rho(\theta_b)$ is equal to r. Therefore, the conditions for θ_a and θ_b are:

$$\theta_a;\ r = \ell(\theta_a) + \rho(\theta_a) \tag{44}$$

$$\theta_b;\ r = \ell(\theta_b) - \rho(\theta_b) \tag{45}$$

Substituting for $f_1(x,\theta)$ we get

$$n(x,r) = \int_{\theta_a}^{\theta_b} \frac{n_e \rho_o^2 \cos\theta/2 \exp\left[\frac{2\sin\theta/2\, n_e \sigma}{\cos\theta} x\right]}{4\rho_o \sin\theta\cos\theta\sin^3\frac{\theta}{2}\left[\rho_o^2\cot^2\frac{\theta}{2} + \rho_o^2\sin^2\theta\right]^{1/2}} d\theta \tag{46}$$

$$\theta_a;\ r = \left[\rho_o^2\cot^2\theta_a/2 + \rho_o^2\sin^2\theta_a\right]^{1/2} + \rho_o\sin\theta_a \tag{47}$$

$$\theta_b;\ r = \left[\rho_o^2\cot^2\theta_b/2 + \rho_o^2\sin^2\theta_b\right]^{1/2} - \rho_o\sin\theta_b \tag{48}$$

Now let us consider the distribution that results if we include the fact that the ions do not distribute uniformly over the ring at x, r. Let us first assume that all the particles $f_1(x,\theta)$ are deflected into one orbital circle, the projection of the helix onto a plane perpendicular to x. The line density of particles is $f_1(x,\theta)/2\pi\rho$. Figure 4 shows that we can write the number of ions in a ring of thickness dr at r as

$$2\,\frac{f_1(x,\theta)}{2\pi\rho} \times \frac{dr}{|\cos\alpha|}$$

where the factor of 2 comes from the two limbs of the circle crossed by the ring. Now these particles will actually be distributed randomly over this element of the ring (i.e. the ring of width dr at r). Therefore, the density is given by $f_1(x,\theta)/2\pi^2\rho r\,|\cos\alpha|$ between the points $\ell-\rho$ and $\ell+\rho$ for angle θ.

To obtain $|\cos\alpha|$ we write the equation for a circle of radius ρ that is displaced from the origin by a distance ℓ in polar coordinates:

$$r^2 - 2\ell r\cos\phi + \ell^2 = \rho^2 \tag{49}$$

Now

$$\tan\alpha = r\,\frac{d\phi}{dr} \tag{50}$$

therefore

$$\tan\alpha = \frac{\ell\cos\phi - r}{\ell\sin\phi} \tag{51}$$

or

$$\alpha = \arctan\left[\cos\phi - \frac{r}{\ell \sin\phi}\right] \tag{52}$$

Substituting for ϕ from Eq. (49) and ℓ^2 from Eq. (41) we obtain an expression for α which can be used in the density equation.

$$\frac{dn(x,r,\theta)}{d\theta} \quad \frac{f_1(x,\theta)}{2\pi^2 \rho\, r|\cos\alpha|} \tag{53}$$

If this is integrated over θ from θ_a to θ_b, where these values are given by Eqs. (47) and (48) we obtain:

$$n(x,r) = \int_{\theta_a}^{\theta_b} \frac{n_e p_o^2 \cos\theta/2 \exp\left[-\frac{2\sin\theta/2\, n_e \sigma}{\cos\theta} x\right] d\theta}{2\pi\rho_o \sin\theta\cos\theta\sin^3\frac{\theta}{2}\, r\left|\cos\arctan\sqrt{\frac{2(p_o^2\cot^2\theta/2 - r^2}{\left[2r^2(p_o^2\cot^2\frac{\theta}{2}+2p_o^2\sin^2\theta) - p_o^4\cot^4\frac{\theta}{2} - r_o^4\right]^{1/4}}}\right|} \tag{54}$$

where θ_a and θ_b are obtained from the solutions of expressions for r:

$$\theta_a;\ r = \left[p_o^2 \cot^2\frac{\theta_b}{2} + \rho_o^2 \sin^2\theta_a\right]^{1/2} + \rho_o \sin\theta_a \tag{55}$$

$$\theta_b;\ r = \left[p_o^2 \cot^2\frac{\theta_b}{2} + \rho_o^2 \sin^2\theta_b\right]^{1/2} - \rho_o \sin\theta_b \tag{56}$$

The density given by Eq. (54) assumes that the plasma is cold, that the velocity of the test particles is constant and that the test particles are removed by deflections. The expression gives a minimum value for the density for the case of motion parallel to the magnetic field.

6. Application of the Results to the Calculation of the Compression of Ions by a Satellite

Using Eqs. (25) and (26) we can obtain the value of the average density of the deflected ions. Using $\theta = 90^\circ$ and $\bar{\theta} = 120^\circ$ in Eq. (26) and setting n_e equal to 10^5 ions/cm^3, then we get, including the factor 2 for back scatter, a value of $\bar{n} = 4.0 \times 10^6$ ions/cm^3 for H^+ ions. For O^+ ions the value is, however, small. The value of $\bar{n}$ must be reduced somewhat since ρ is not

sufficiently small. If this is taken into account and if we include the back scatter, then we obtain for n for H^+ ions in ions/cm^3

	V = 1 volt	V = 10 volts	V = 100 volts
a = .1 m	8×10^3	8×10^5	3.2×10^6
a = 1 m	8×10^5	3.2×10^6	4.0×10^6

Since the compression effect is negligible for O^+ ions but large for H^+ ions, satellite compression effects will be masked below altitudes of about 600 km. Since below this altitude the density of O^+ ions is 10 times as great as the density of H^+. The density of the O^+ drops off much more rapidly than the H^+ so that their densities are equal at an altitude of 1500 km and H^+ dominates above that altitude. Therefore, large satellite wakes would be masked below about 600 km.

The scale length of the density distribution will be x_o which is the mean free path λ times the factor $\frac{\cos\theta}{2\sin\theta/2}$. Using an average value of $\theta = 120^o$, this factor becomes 0.318. From Table I we see that for H^+, $x_o = 1.6$ km and for O^+, $x_o = 290$ km.

7. Deflection by a Charged Sphere Passing Through an Ionized Gas Cloud

So far we have assumed the charged body to be moving through an ionized gas of uniform density and infinite extension. With these assumptions we obtained a solution for f_1.

Let us now assume that the charged body moves relative to a distribution of ionized gas of density $n_e(t + x/v)$ where $x = 0$ is the position of the body at $t = 0$, and we are in the system of coordinates moving with the charged body. Therefore we obtain from Eq. (28), neglecting the integral term,

$$f_1(x,\theta,t) = f_{1o} \exp\left[-\frac{2\sin\frac{\theta}{2}}{\cos\theta}\int_0^x n_e(t + x/v)\,dx\right] \qquad (57)$$

The function f_{1o} is exactly the same as before except that we must substitute

for n_e the function $n_e(t - x/v\cos\theta)$. The resulting equation is, therefore

$$f_1(x,\theta,t) = \pi p_o^2 \frac{\cos\theta/2}{\cos\theta \sin^3\theta/2} n_e\left(t - \frac{x}{v\cos\theta}\right) \cdot \exp\left[-\frac{2\sin\theta/2}{\cos\theta} \int_0^x n_e(t + x/v)\,dx\right] \tag{58}$$

8. Derivation of the Density of Ions for the Motion of a Satellite Through a Cold Plasma at an Angle to the Magnetic Field.

We consider the case where the velocity vector of the satellite makes an angle β to the magnetic field. We have already obtained an expression for $f(x,\theta)$ for the first scatter approximation. We will drop the exponential factor in the present derivation thus neglecting the scatter of test particles by the field particles and consider only $f_{1o}(x,\theta')$ where

$$f_{1o}(x,\theta') = \pi n_e p_o^2 \frac{\cos\theta'/2}{|\cos\theta| \sin^3\theta'/2} \tag{59}$$

This also neglects back scatter, however, since λ is large, back scatter will be unimportant when the satellite moves at an angle to the magnetic field.

For the present problem, we must take x parallel to B. Thus, the $\cos\theta$ term will remain unchanged in the presence of a magnetic field since it arises from the value of the component of motion of the test particle parallel to the magnetic field. However, the angle θ' is the deflection angle. In order to transform $f_{1o}(x,\theta')$ into a form appropriate to the new orientation of the magnetic field, we will introduce the azmuthal angle ϕ'. Define

$$G_{1o}(x,\theta',\phi') = \frac{d f_{1o}(x,\theta')}{d\phi'} = \frac{n_e p_o^2}{2|\cos\theta|} \cdot \frac{\cos\theta'/2}{\sin^3\theta'/2} \tag{60}$$

We now need to transform $G_{1o}(x,\theta',\phi')$ into $G_{1o}(x,\theta'',\phi'')$ where θ'' and ϕ'' are the coordinates in the lab system (see Fig. 5). Since the velocity of the coordinate system is the same as that of the deflected test particles we have

that

$$\theta'' = 90^0 + {}^1/_2\,\theta' \tag{61}$$

Thus

$$G_{10}(x,\theta'',\phi'') = \frac{n_e p_o^2}{2\,|\cos\theta|}\,\frac{\sin\,\theta''}{\cos^3\theta''} \tag{62}$$

Here again the $|\cos\theta|$ term remains unaltered.

We will now transform from the coordinates x,θ'',ϕ'' measured relative to the axis of motion to z,θ,ϕ measured relative to the direction of the magnetic field vector (see Fig. 6). The factor $\sin\theta''\cos^{-3}\theta''$ must now be transferred into the coordinate system θ,ϕ as measured about Z. Using the law of cosins for a spherical triangle we obtain

$$\frac{\sin\,\theta''}{\cos^3\theta''} = \frac{\left[1 - (\cos\theta\cos\beta + \sin\theta\sin\beta\cos\phi)^2\right]^{1/2}}{\left[\cos\theta\cos\beta + \sin\theta\sin\beta\cos\phi\right]^3} \tag{63}$$

We obtain for G_{10}:

$$G_{10}(z,\theta,\phi) = \frac{n_e p_o^2}{2\,|\cos\theta|}\cdot\frac{\left[1 - (\cos\theta\cos\beta + \sin\theta\sin\beta\cos\phi)^2\right]^{1/2}}{\left[\cos\theta\cos\beta + \sin\theta\sin\beta\cos\phi\right]^3} \tag{64}$$

The velocity of the test particle in the lab system, v', is

$$v' = 2v(\cos\theta\cos\beta + \sin\theta\sin\beta\cos\phi) \tag{65}$$

Consider now the distance st over which the charge distribution will be distributed in a time interval t. From Fig. 7 we have

$$s^2 = v^2\left[1 + 4\cos^2\theta(\cos\theta\cos\beta + \sin\theta\sin\beta\cos\phi)^2 - 4|\cos\theta|\cos\beta\,(\cos\theta\cos\beta + \sin\theta\sin\beta\cos\phi)\right]^{1/2} \tag{66}$$

Now the test particles that move parallel to B with a forward velocity $v'|\cos\theta|$ will be spread out along the line st. Therefore, the function $G_{10}(z,\theta,\phi)$ must be multiplied by the factor $v'\,|\cos\theta|/s$. Thus

$$G'_{10}(x,\theta,\phi) = 2(\cos\theta\cos\beta+\sin\theta\sin\beta\cos\phi/\left[1+4(\cos\theta\cos\beta+\sin\theta\sin\beta\cos\phi)^2\cos^2\theta - 4(\cos\theta\cos\beta+\sin\theta\sin\beta\cos\phi)\,|\cos\theta|\cos\beta\right]^{1/2} \tag{67}$$

Now to obtain the density we divide $f'_{1o}(z,\theta)$ by $v(\cos\theta_1 - \cos\theta_o)t$ and integrate over $\Delta\theta$ (i.e. we divide by vt $\sin\theta$) and also divide by the width of the distribution which is

$$4\rho(\theta) = 4\rho_o \sin\theta \tag{68}$$

where $\rho >> p$ or by

$$2p(\theta') = 2p_o \cot\theta'/2 \tag{69}$$

for $p >> \rho$. Thus we get

$$f'_{1o}(z,\theta) = \int_0^{2\pi} G'_{1o}(z,\theta,\phi)\, d\phi \tag{70}$$

so

$$n(z,\theta,t) = \frac{f'_{1o}(z,\theta)}{4\rho(\theta)\ vt\ \sin\theta} \tag{71}$$

for $\rho >> p$ and

$$n(z,\theta,t) = \frac{f'_{1o}(z,\theta)}{2p(\theta')\ vt\ \sin\theta} \tag{72}$$

for $p >> \rho$. If we transform $p(\theta')$ we get

$$p(\theta) = p_o \frac{\left[1 - (\cos\theta\cos\beta + \sin\theta\sin\beta\cos\phi)^2\right]^{1/2}}{(\cos\theta\cos\beta + \sin\theta\sin\beta\cos\phi)} \tag{73}$$

The results of the substitutions of Eq. (67), (68), (70), and (73) into Eq. (71) and (72) give for $\rho >> p$

$$n(x,\theta,t) = \frac{f'_{1o}(x,\theta)}{4\rho_o \sin^2\theta\ vt} \tag{74}$$

and for $p >> \rho$

$$n(x,\theta,t) = \frac{f'_{1o}(x,\theta)(\cos\theta\cos\beta + \sin\theta\sin\beta\cos\phi)}{2p_o\ vt\left[1-(\cos\theta\cos\beta + \sin\theta\sin\beta\cos\phi)^2\right]^{1/2}} \tag{75}$$

where

$$f'_{1o}(z,\theta) = \int_0^{\pi 2} \frac{n e p_o^2}{|\cos\theta|} \cdot \left[1-(\cos\theta\cos\beta + \sin\theta\sin\beta\cos\phi)^2\right]^{1/2} \Big/ \Big\{(\cos\theta\cos\beta + \sin\theta\sin\beta\cos\phi)^2 \left[1+4(\cos\theta\cos\beta + \sin\theta\sin\beta\cos\phi)^2\cos^2\theta - 4(\cos\theta\cos\beta + \sin\theta\sin\beta\cos\phi)\,|\cos\theta|\cos\beta\right]^{1/2}\Big\}\, d\phi \tag{76}$$

The distribution that is produced gives rise to a "shock front". If the angles between these fronts and the velocity vector of the charged body are η_1 and η_2, (see Fig. 2), then these angles are given by the expression

$$\eta_{\frac{1}{2}} = \arcsin \frac{\sin\beta(1 \pm \cos\beta)}{(1 + \sin^2\beta)^{1/2}} \tag{77}$$

where β is the angle between the velocity vector and the magnetic field vector. It is assumed here, as before, that the ions are cold. If we include the thermal velocity v_T of the ions, then

$$\eta_{\frac{1}{2}} = \arcsin \frac{\sin\beta(r \pm \cos\beta)}{R^2 + \sin^2\beta} \tag{78}$$

where

$$R \approx 1 + \frac{v_T}{v} \tag{79}$$

Let us now determine the angle for which $n(Z,\theta,t)$ will be the largest, and then determine how far the high density region extends away from the body before the density of test particles plus the density of field particles becomes $2n_e$. For $p >> \rho$, Eq. (75), there is an infinity produced for

$$1 - (\cos\theta\cos\beta + \sin\theta\sin\beta\cos\phi)^2 = 0 \tag{80}$$

However, this is spurious since it arises from the breakdown of the approximation $p >> \rho$. Likewise, the infinity produced by $\theta = 90^\circ$ is spurious, arising from the neglect of the exponential decay function.

The integration over ϕ presents considerable difficulty when compared with the physical value of such an integral. It is sufficient to note that the integration will produce a slight smoothing out of the shock front. We should note, also, that the factor $f_{10}(Z,\theta)/2p$ may be replaced by $n_e\gamma p_0$ where γn_e is the density of test particles. Since, for a positive sphere, values for γ of about 10 can be obtained, we have

$$n \approx \frac{n_e\gamma p_0}{vt} = n_e \frac{10p_0}{vt} \tag{81}$$

Thus the density of test particles will equal the density of field particles when $vt \approx 10 p_o$. If p_o is 3 meters, then this gives a wake that extends 30 meters before the density has dropped to twice the ambient. If $v \parallel B$ then for H^+ ions and an impact parameter of 3 meters, the cross section of the wake would be about 5×10^4 m^2. Because of the geometry of the wake, a long rod shaped region, the effective radio cross section would be larger.

The reflection of a radio signal can be either coherent or non-coherent. If non-coherent, then we would need an impossibly large number of electrons, more than 10^{30}.[3] If the reflection is coherent then it can be either metallic or non-metallic. Since the index of refraction for a wave, n^*, of frequency f, is

$$n^* = \sqrt{1 - \frac{n_e^2}{4 \pi f^2}} \tag{82}$$

(in cgs units) we obtain metallic reflections when

$$n \geq \frac{4\pi m f^2}{e^2} = f^2 \, 10^{-8} \tag{83}$$

Thus, when f is 2×10^7 sec^{-1} we require $n = 4 \times 10^8$. Thus we should be able to obtain large radar cross sections. For the above example the cross section is about 180 m^2, including both halves of the shock front.

9. Deflection of Ions and Electrons by a Screened Electric Field.

Thus far we have considered the charged body to be unscreened. This is accurate either for charged bodies in a low density plasma or for very small bodies. For satellites such approximations are not satisfactory. The screening for probes an for satellites has been extensively considered by Walker[4]. The potential falls off very rapidly down to a value of about kT; however, the drop is several times slower than that given by the assumption of local thermodynamic equilibrium. Below kT the field falls off more slowly than r^{-2}. Even for larger values of the impact parameter for which the

potential will be only about .1 kT significant compression of the test particles can occur.

There will also exist in this screened electric field a pericritical surface for which particle orbits become critical and the particle spirals into the charged body. We must also consider the fact that most all of the particles that strike the surface of the satellite will be neutralized. Since, for a negative sphere all of those ions that reach the pericritical surface will be accreted to the surface of the charged body, the ions with small impact parameters cannot be important in the production of large wakes. For a positively charged body, the ions will be important in the production of large wakes but the electrons that reach the pericritical surface will be accreted and, for the most part neutralized at the surface of the body. For small charged bodies, such as antennae moving at satellite velocities the pericritical surface may become distorted due to the relative motion of the ions. Thus the focal point of the spiral orbits will be shifted, and many of the ions will not be accreted. It must be noted, however, that in the presence of a magnetic field, the screening process may be sufficiently altered to allow a greater number of particles to be compressed without their being accreted to the body.

Thus, in most cases, it will be the particles with the same sign as the satellite which will be compressed. The result will be that a cloud of charge will be produced in the neighborhood of the body, and will move away along the magnetic field lines. If the body moves parallel to the magnetic field an extensive cloud of charge will be produced that moves ahead of and behind the satellite.

Using these facts, we can obtain descriptions for the form of the wake under various circumstances. If a negatively charged sphere moves with

satellite velocities parallel to the magnetic field, the ions will be accreted to the surface of the body and will not be compressed. The electrons, because of their velocity, will be reflected on both the front and rear sides of the body. However, since the electrons that are reflected merely take the place of those that normally would come from the opposite side of the body, there will arise only a slight compression due to the displacement of the particles. If the body were moving with a velocity comparable to the electron thermal velocity, the compression of the electrons would be significant. If the negatively charged sphere is moving at an angle to the magnetic field, essentially the same thing will occur. The ions are accreted to the surface of the body and neutralized while the electrons are reflected and produce only a slight compression.

For a positively charged body moving parallel or at an angle to the magnetic field, the electrons will be accreted to the surface of the body while the ions are deflected and produce a wake with a density several times the ambient density.

Still other factors may be important: If the body is equipped with ion collectors or other apparatus that is driven positive with respect to the rest of the body, then this portion of the vehicle will produce plasma compressions in the manner described.

REFERENCES

1. E. H. Walker and S. F. Singer, Bull. Am. Phys. Soc., 5, 47, (1960)

2. L. Spitzer, "Physics of Fully Ionized Gases", Interscience Publishers, New York, pp. 68-81, 1956.

3. L. Lerner, R. Baron, and H. Spector, "Detection of Ballistic Missiles by Low-Frequency Radio Reflection", Wright Air Development Division, TR 59-516.

4. E. H. Walker, "Plasma Sheath and Screening Around a Rapidly Moving Body" to be published, 1962.

	O^+ ions		H^+ ions	
	Thermal Velocities 1.53 km/sec	Satellite Velocities 7 km/sec	Thermal Velocities 6.1 km/sec	Satellite Velocities 7 km/sec
ρ_o	25.6	1.24	25.8	19.5
ρ_o	8.52	39.0	2.12	2.44
λ		9×10^5		5×10^3
h	8.45×10^{-3}			

Table I. Important parameters

The values of ρ_o, ρ_o, h for singly ionized oxygen and hydrogen ($Z = 1$): Satellite potential $V = 10$ volts, satellite radius $a = 1$ m, ambient electron density $n_e = 10^{11}$ m^{-3}, temperature $T = 1500^o$ K, magnetic induction $B = 3 \times 10^{-5}$ w/m^2, A is the atomic weight, v is the velocity of the ion and $v_\perp$ is the component of the velocity perpendicular to the magnetic field. The results are expressed in meters.

Figure Captions

Fig. 1. Diagram showing parameters entering into the trajectory of a cold proton moving in the electric field of a charged body as seen in the center of mass system.

Fig. 2. The form of the shock fronts formed by the passage of a charged body through a cold plasma at an angle to the magnetic field.

Fig. 3. Diagram showing the relation of to ρ, the radius of gyration and p, the impact parameter.

Fig. 4. Diagram showing parameters entering into the calculation of the density of test particles in a ring of thickness dr and radius r.

Fig. 5. Illustration of the relation between the lab coordinates and the center of mass coordinates.

Fig. 6. Transformation of the coordinates x, θ'', ϕ'' measured relative to the direction of the magnetic field vector.

Fig. 7. Illustration of the distance over which the charge cloud is distributed by the motion from the point of initial deflection to a position $v'/\cos\theta/t$.

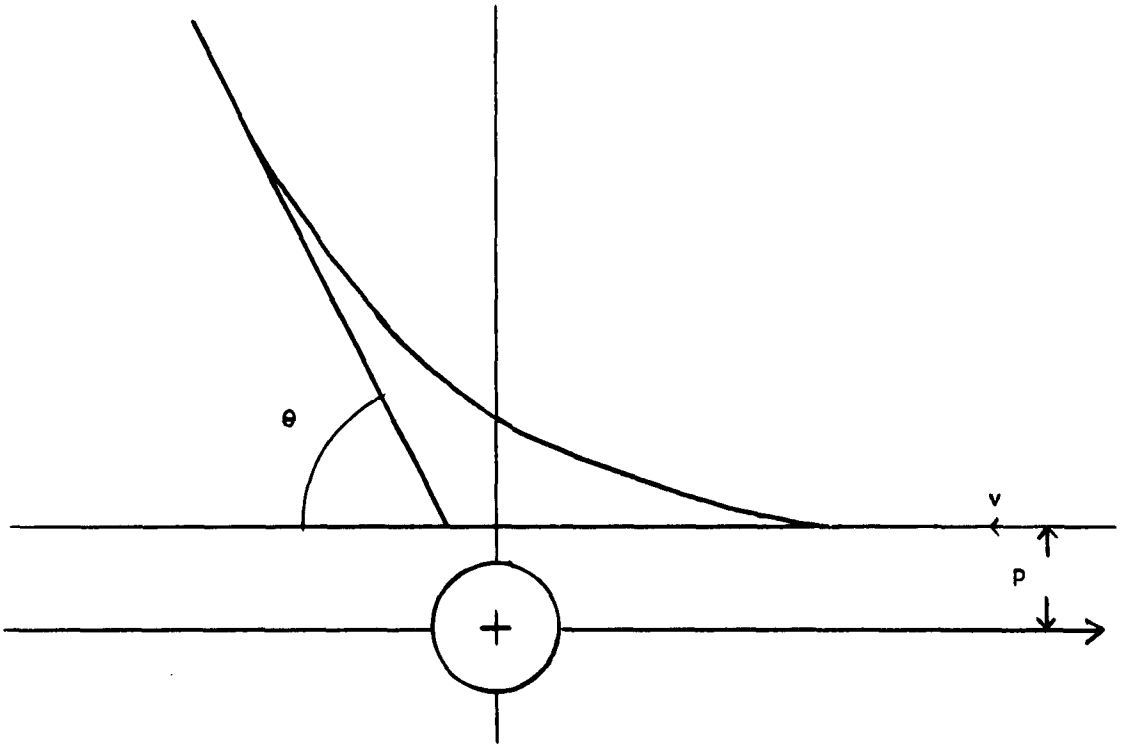
θ
v
p

Fig. 1

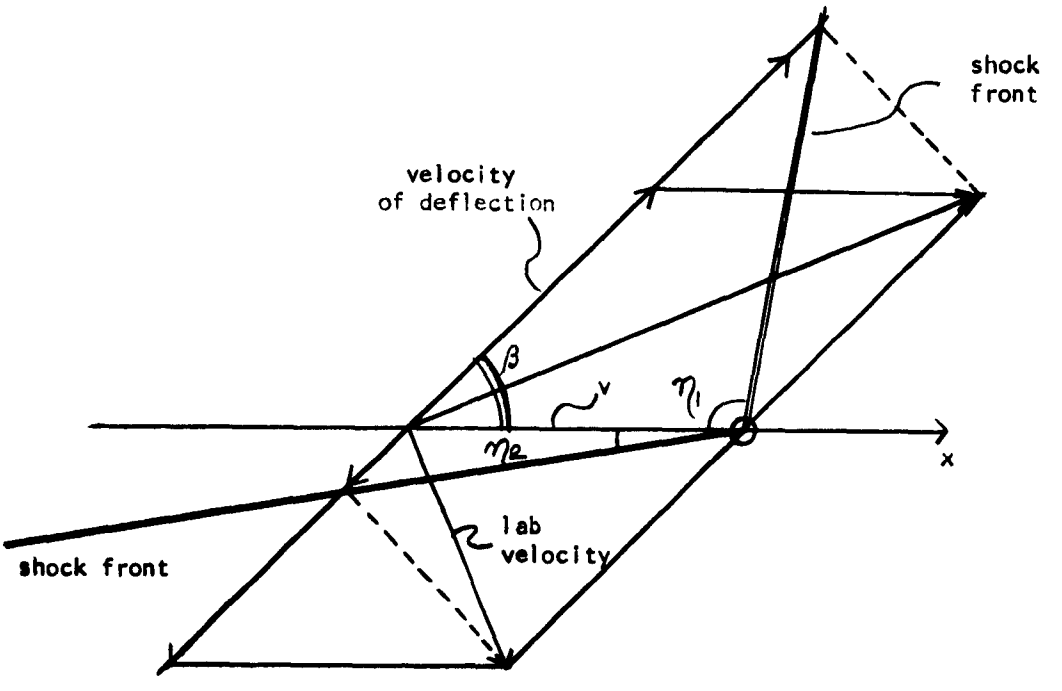
shock
front
velocity
of deflection
β
v
η1
η2
x
lab
velocity
shock front

Fig. 2

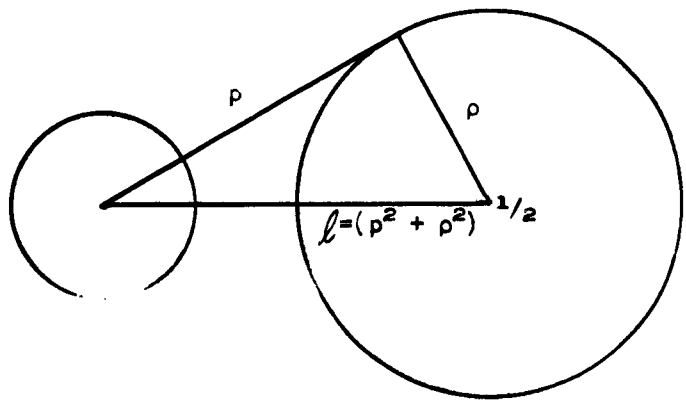

Fig. 3

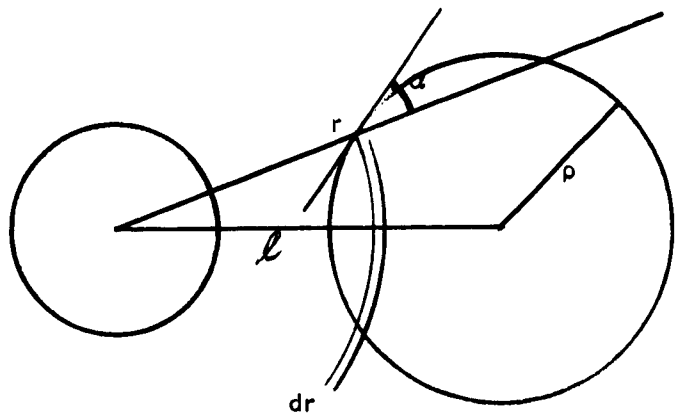

Fig. 4

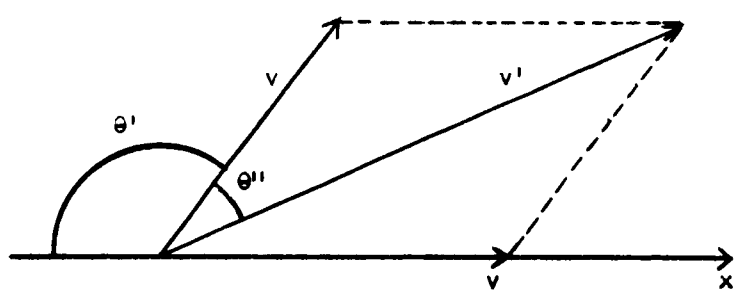

Fig. 5

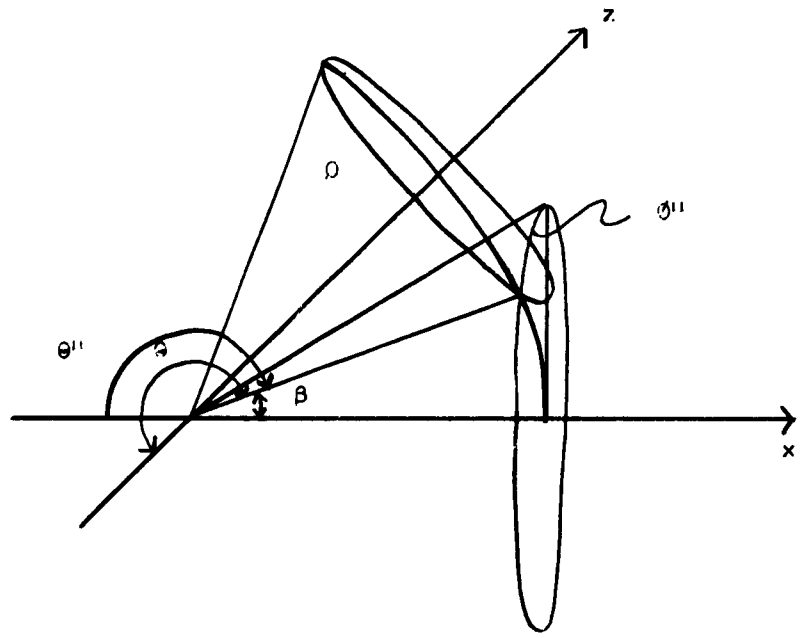

Fig. 6.

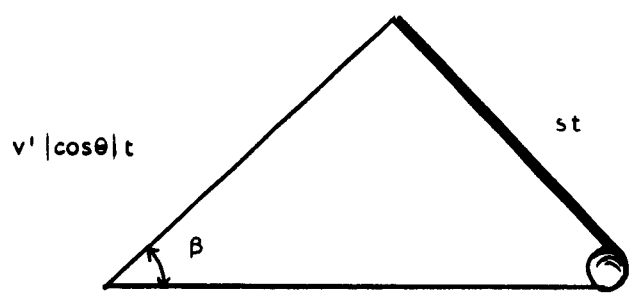

Fig. 7

REFLECTION OF RADIO WAVES INCIDENT ON BOUNDARY SURFACES WITH APPLICATION TO THE THEORY OF THE KRAUS EFFECT

E. H. Walker

Abstract

Satellite wakes present sharp boundaries to radio waves that are incident upon them. Also the wake produced by a satellite is not free to dispurse in all directions but is constrained by the earth's magnetic field so as to form a large and sharply defined boundary surface which persists long after the passage of the satellite. In order to show the relation between such satellite wakes and the Kraus effect a treatment of the reflection of radio waves off sharp boundary surfaces is presented. Although these wakes have been considered by many authors to be insufficient to account for the Kraus effect, we show that the reflection coefficient for these boundaries become significant under favorable conditions of observation. The very large size of the wakes and their geometry result in an inverse square law rather than an inverse fourth power law relating the power to signal strengths for radar observations.

REFLECTION OF RADIO WAVES INCIDENT ON BOUNDARY SURFACE WITH APPLICATION TO THE KRAUS EFFECT

1. Introduction

In a previous paper[1] we presented a mechanism involving the deflection of the ions of the plasma by a charged satellite so as to form a wake. The earth's magnetic field will produce a compression of this plasma in the immediate neighborhood and, if the satellite moves parallel to the magnetic field an extensive region of compressed plasma will result in favorable cases. Because of the constraint of the earth's magnetic field and because of the large mean free path of the ions in the upper ionosphere, these ions maintain a coherent geometry long after their density has dropped to very low values, thus presenting large sharply defined boundary surfaces.

It is most important that these surfaces are sharp and flat (or at least with only a slight curvature). Due to random fluctuations in density, regions of high or low density constantly appear throughout the ionosphere. However, these regions are of small size and occur with a random distribution and with various random shapes. Thus, even though the wake of the satellite is superimposed on a medium having fluctuations in density, the fact that the reflection from the wake is coherent whereas the reflection from the random fluctuations is incoherent causes the satellite related radio reflections to be much stronger, when they occur, than in background reflections from the random density fluctuations.

This distinction between coherent and incoherent reflections is obvious from a consideration of the expression for radiation from an accelerated charge. If a point charge q undergoes an acceleration $\dot{u}$, then the rate at which this body radiates energy in the form of electromagnetic radiation, dW/dt is[2]

$$\frac{dW}{dt} = \frac{q^2 \dot{v}^2}{6\pi \epsilon_0 c^3} \tag{1}$$

The dependence upon the total amount of charge is very strong, varying as the square of the total charge that is radiating coherently. For a collection of charges that are distributed over a region of space and which radiate out of phase with one another, the total radiation will be greatly reduced, no longer depending upon the square of the total charge. The amount of radiation from such an assemblage of charges depends upon their geometry and phase relation but these might be so chosen as to produce only quadrapole or a higher multipole radiation.

When the terms "coherent" and "incoherent" are applied to the reflection and scattering of electromagnetic waves from a region, they indicate whether the wave was reflected by charges that are reradiating in phase, or by charges that are out of phase.

The following sections give a treatment of the reflection of radio waves off of sharp boundary surfaces that separate regions of plasma that are at different densities. We will first consider the problem quite generally and then apply this to the Kraus effect.

2. Derivation of the General Reflection Equations.

Let us first consider the motion of an electron in a plasma when it is subjected to an electric field E.

The drift velocity V_D of an electron with mass m and charge e that moves freely except for collisions with ions and other electrons can be related to the electric field by the equation

$$\frac{eE}{m} = \frac{dV_D}{dt} + \frac{1}{\tau} V_D \tag{2}$$

where τ is the average time between collissions. Since the current density j is

$$j = ne\, V_D \tag{3}$$

where n is the density of electrons, we have the relation between E and j:

$$\frac{ne^2 E}{m} = \frac{dj}{dt} + \frac{1}{\tau} j \tag{4}$$

The Maxwell's equations can be used to obtain the equation

$$\nabla^2 E = \mu \frac{\partial j}{\partial t} + \mu\epsilon \frac{\partial^2 E}{\partial t^2} \tag{5}$$

If we now substitute into Eqs. (4) and (5)

$$j = J_o e^{-i\omega t} \tag{6}$$

we obtain

$$\frac{ne^2 E}{m} = \frac{1 - i\omega\tau}{\tau} j \tag{7}$$

and

$$\nabla^2 E = - i\omega\mu j + \mu\epsilon \frac{\partial^2 E}{\partial t^2} \tag{8}$$

Thus, upon substituting Eq. (7) into Eq. (8) we have

$$\nabla^2 E = - \frac{i\omega\tau}{1 - i\omega\tau} \cdot \frac{\mu ne^2}{m} E + \mu\epsilon \frac{\partial^2 E}{\partial t^2} \tag{9}$$

If we substitute for E the expression

$$E(\xi) = E_o(\xi)\, e^{-i\omega t} \tag{10}$$

into Eq. (9) we have

$$\frac{\partial^2 E}{\partial \xi^2} = - \frac{i\omega\tau}{1 - i\omega\tau} \cdot \frac{\mu ne^2}{m} E - \mu\epsilon\omega^2 E \tag{11}$$

In metals $\tau\omega \ll 1$ for frequencies below the optical region. This approximation along with the relation between τ and the conductivity σ:

$$\sigma = \frac{ne^2 \tau}{m} \tag{12}$$

can be used in Eq. (11) to obtain

$$\frac{\partial^2 E}{\partial \xi^2} = - \mu\epsilon\omega^2 E - i\omega\mu\sigma E \tag{13}$$

This last equation governs the so-called metallic reflection phenomena.

If we assume $\tau\omega \gg 1$ then Eq. (11) becomes

$$\frac{\partial^2 E}{\partial \xi^2} = -\mu\epsilon\omega^2 E + \frac{4\pi ne^2}{m} E \qquad (14)$$

This expression applies in those cases where the electrons can be considered as non-interacting with other particles. We will refer to this type of reflection as non-metallic.

In the ionosphere, both metallic and non-mettalic reflections can occur. The angular frequency ω that divides the two types of reflections depends upon τ. According to Spitzer[3], the resistivity ρ is

$$\rho = 65.3 \frac{\ln \Lambda}{T^{3/2}} \quad \text{(ohm - m)} \qquad (15)$$

where T is the absolute temperature and the value of $\ln\Lambda$ can be obtained from Table 1. From Eq. (12)

T, ^{0}K	n, m^{-3}					
	10^6	10^9	10^{12}	10^{15}	10^{18}	10^{21}
10^2	16.3	12.8	9.43	5.97		
10^3	19.7	16.3	12.8	9.43	5.97	
10^4	23.2	19.7	16.3	12.8	9.43	5.97
10^5	26.7	23.2	19.7	16.3	12.8	9.43

Table 1

Values of $\ln\Lambda$ for various values of T and n according to Spitzer[3].

We obtain for τ

$$\tau = \frac{T^{3/2}}{n \ln \Lambda} \; 5.45 \cdot 10^5 \quad \text{sec.} \qquad (16)$$

where n is the number of electrons per cubic meter.

In a region of the ionosphere where the density is 10^{12} m^{-3} and the temperature is 1000 ^{o}K, we obtain for the conditions on ω for metallic reflection

$$\omega \ll 7.45 \cdot 10^{2} \text{ sec}^{-1}$$

i.e., for metallic reflection to dominate the frequency of the radio wave must be much less than 118 cycles/sec the reflections are non-metallic. The penetration depths for both metallic and non-metallic reflection from the ionosphere are small compared to the thickness of the ionosphere as will be shown in section 4.

3. Coherent and Incoherent metallic reflections.

Equation (13) can now be used along with the boundary conditions to obtain a complete description of metallic reflections. The boundary conditions that relate E of the incident ray, E'' of the reflected ray and E' of the transmitted ray are

$$\underline{n} \times (\underline{E} + \underline{E}'') = \underline{n} \times \underline{E}' \tag{17}$$

and

$$\underline{n} \times (\underline{k} \times \underline{E} + \underline{k}'' \times \underline{E}'')/\mu_1 = \underline{n} \times (\underline{k}' \times \underline{E}')/\mu_2 \quad . \tag{18}$$

where $\underline{n}$ is the unit vector normal to the surface and $\underline{k}$ is the propagation vector. Similar expressions relate the magnetic field vectors $\underline{H}$, $\underline{H}''$ and $\underline{H}'$ across a boundary.

If we express Eq. (13) as

$$\frac{\partial^2 \underline{E}}{\partial \xi^2} = - (\mu\epsilon\omega^2 + i\omega\mu\sigma)\underline{E} \equiv - K^2 \underline{E} \tag{19}$$

where

$$K = \alpha + i\beta = k \sqrt{1 + \frac{i\sigma}{\epsilon\omega}} \tag{20}$$

Then the boundary conditions will give

$$\underline{E}' = \underline{E}_0' \; e^{-\beta\xi} \; e^{i(\alpha\xi - \omega t)} \tag{21}$$

and

$$\underline{h}' = \frac{\underline{k} \times \underline{E}'}{\mu\omega} \; \frac{(\alpha + i\beta)}{k} \tag{22}$$

Furthermore, the reflection coefficient r can be shown to be

$$r \equiv \left| \frac{E''}{E} \right|^2 = \left| \frac{1 - \alpha^2 - \beta^2 - 2i\beta}{1 + 2\alpha + \alpha^2 + \beta^2} \right|^2 \tag{23}$$

in this general situation.

The condition that the reflection be coherent is equivalent to setting $\epsilon\omega \ll \sigma$, a condition that is met in metals below the optical region. In this case, Eq. (21) and (22) become

$$\underline{E}' = \underline{E}'_0 \; e^{-\sqrt{\frac{1}{2}\mu\sigma\omega}\,\xi} \; e^{i\left(\sqrt{\frac{1}{2}\mu\sigma\omega}\,\xi - \omega t\right)} \tag{24}$$

and

$$\underline{H}' = (1 + i)\sqrt{\frac{\sigma}{2\mu\omega}}\; \underline{n} \times \underline{E}' \tag{25}$$

These fields fall of to $1/e$ of their surface value in a distance δ, the skin depth

$$\delta = \sqrt{\frac{2}{\mu\sigma\omega}} \tag{26}$$

The expression for the reflection coefficient, Eq. (23), under this approximation becomes

$$r = 1 - 2\sqrt{\frac{2\epsilon\omega}{\sigma}} \tag{27}$$

4. Non-Metallic Reflections

In a low density plasma the expression for metallic reflection are no longer valid so that we must return to Eq. (14). We will express this in the form

$$\frac{\partial^2 E}{\partial \xi^2} = \left(\frac{\mu n e^2}{m} - \mu\epsilon\omega^2\right) E = -K^2 E \tag{28}$$

where

$$K = \sqrt{\mu\epsilon\omega^2 - \frac{\mu n e^2}{m}} \tag{29}$$

We thus have

$$\underline{E}' = \underline{E}'_0 \; e^{i(K\xi - \omega t)} \tag{30}$$

and

$$H' = \frac{k \times E}{\mu\omega} \left(\frac{K}{k}\right) \tag{31}$$

If $\frac{\omega^2}{n} < 3.17 \cdot 10^3$ (M.K.S. units) then this wave is damped out in a characteristic distance

$$\delta' = \frac{1}{\sqrt{\frac{\mu n e^2}{m} - \mu\epsilon_0 \omega^2}} \tag{32}$$

A calculation of the reflection coefficient yields for a wave going from a region of density n_1 to a region of denisty n_2

$$r = \left(\frac{1 - \left(\sqrt{1 - \frac{\mu n_2 e^2 c^2}{m\omega^2}} \Big/ \sqrt{1 - \frac{\mu n_1 e^2 c^2}{m\omega^2}} \right)}{1 + \left(\sqrt{1 - \frac{\mu n_2 e^2 c^2}{m\omega^2}} \Big/ \sqrt{1 - \frac{\mu n_1 e^2 c^2}{m\omega^2}} \right)} \right)^2 \tag{33}$$

It is interesting to note from Eqs. (26) and (32) that under the conditions of the ionosphere at T = 1000°K and n = 10^{12} m^{-3} and at the frequency of 118 cycles sec that divides the metallic reflections from non-metallic reflections, δ has a value of 7.55 m while δ' has a value of 5.34 m. Indeed, the ratio δ/δ' always equal $\sqrt{2}$ at the frequency where $\omega\tau = 1$ so long a $n > 2 \cdot 10^4 m^{-3}$.

5. Application to Radio Reflections in the Ionosphere

In the region of the ionosphere, reflections are non-metallic except at very low frequencies. Thus, the reflections of signals at all but the lowest frequencies will be governed by Eq. (33). Let us consider a few typical cases of reflections in the ionosphere. If a 20 Mc/sec wave travels from empty space into a region of density $10^{11} m^{-3}$ (or from one region at a density of $10^{11} m^{-3}$, n_1, into one of density $2 \cdot 10^{11}$ cm^{-3}, n_2), then Eq. (33) can be approximated as

$$r = \frac{e^4 c^4}{16 m^2 \omega^4} (n_2 - n_1)^2 \tag{34}$$

since $\frac{n}{\omega^2} \ll \frac{1}{\mu e^2 c^2}$ thereby giving a value of

$$r = 2.57 \cdot 10^{-5} \quad .$$

If the densities are 10 times as great then $r = 2.57 \cdot 10^{-3}$.

Let us now consider the case where $\frac{n}{\omega^2} \approx \frac{m}{\mu e^2 c^2}$; i.e., let us consider the case of reflections where n is nearly equal to the critical frequency. Thus we can define a quantity f such that

$$f = 1 - \frac{n_1}{n_c} << 1 \tag{35}$$

where n_c is the critical density which is equal to $3.15 \cdot 10^{-4} \omega^2$ (m^{-3}). We will assume that n_2 is just slightly greater

$$n_2 = n_1 + \delta n \tag{36}$$

so that $\delta n/n_1 << f$. We obtain:

$$r = \left(\frac{\delta n}{4f\, n_1}\right)^2 \tag{37}$$

As an example, take n to be 1% below the critical density and $\delta n/n_1 = 10^{-3}$. The reflection coefficient for this case is 1/1600.

This behavior is quite important to the understanding of radio reflections from satellite wakes. As an example, consider a satellite of radius 1 meter passing a particular position in the earth's magnetic field and producing locally a compression of the ions to twice their ambient density (one can also consider the results of a satellite sweeping out the ions with the same results). Since the ions spiral along the magnetic field lines, as shown in our previous paper[1], they are allowed to spread out only in one direction. Thus, when the ions have traveled 100 km, they will be confined within a region of about 10 km along the magnetic field lines. Thus, within this region the ion density would be enhanced by an amount $\delta n/n_1 = 10^{-4}$. In a region with a density within 1% of the critical density, $r = (1/400)^2$. This value in itself is small, but when we consider the other significant factors, such reflections become very important. Since the reflecting surface is not small compared to the wavelength of the incident radiation, but, on the contrary, is quite large with the shape of a flat

sheet (or of a series of rods, if the wake fluctuates), a reflected radar signal may fall off as R^{-2} or R^{-3} rather than R^{-4} as is usually the case. So far, however, we have not considered the dependence of r upon the thickness of the sheet.

6. Non-Metallic Reflection from a Layer of Electrons

Consider a slab of free electrons of thickness ℓ with an incident electromagnetic wave on the surface a. Reflection occurs at this surface. A second reflection occurs on the second boundary surface b with a portion being transmitted out of the slab. In Fig. 1 the various parameters are explained; E is the incident field, E'' is the total reflected field, E''' is the total field transmitted out of the slab, and E_1', E_2' are the fields inside the slab. The value of E_1' at the surface b is related to the value at the surface a by the expression

$$E_1'(b) = E_1'(a)\, e^{iK\ell} \equiv \gamma E_1' \tag{38}$$

From the boundary equations, Eqs. (17) and (18), we obtain

$$E + E'' = E_1' + \gamma E_2' \tag{39}$$

$$\gamma E_1' + E_2' = E'' \tag{40}$$

$$kE - kE'' = k' E_1' - \gamma k' E_2' \tag{41}$$

$$\gamma k' E_1' - k' E_2' = k E''' \tag{42}$$

Substitution of Eq. (39) into (41) to eliminate E_1' yields

$$kE - kE'' = k'(E + E'') - 2\gamma k' E_2' \tag{43}$$

Substitution of (39) into (40) to eliminate E_1' yields

$$\gamma(E + E'' - \gamma E_2') + E_2' = E''' \tag{44}$$

Substitution of (40) into (42) to eliminate E_1' yields

$$E''' = \frac{2k'}{(k' - k)}\, E_2' \tag{45}$$

Substitution of (44) into (45) to eliminate E'' yields

$$\gamma(E + E'') = \left[\gamma^2 - 1 + \frac{2k'}{k' - k}\right] E_2' \tag{46}$$

Substitution of (46) into (43) yields upon simplification

$$r = \left|\frac{E''}{E}\right|^2 = \left|\frac{2kk' - k^2(1 + \gamma^2) - k'^2(1 - \gamma^2)}{2kk'(1 + \gamma^2) + (k'^2 + k^2)(1 - \gamma^2)}\right|^2 \tag{47}$$

Since for our case $k' = K$ as given in Eq. (29), by defining $\alpha = K/k$ we can write Eq. (47) more simply as

$$r = \left|\frac{2\alpha - \alpha^2(1 - \gamma^2) - (1 + \gamma^2)}{2\alpha(1 + \gamma^2) + (1 + \alpha^2)(1 - \gamma^2)}\right|^2 \tag{48}$$

If we assume that $n_2 = n_1 + \delta n$ and that n_1 is sufficiently close to the value of n_c so that the inequality of Eq. (35) holds then we get, where $K\ell$ is small:

$$r = \left(\frac{\delta n}{4fn_1}\right)^2 \left(1 + \frac{\delta n}{fn} + 4K^2 \ell^2\right) \tag{49}$$

This expression yields essentially the same results that were obtained in Eq. (37). Thus we see that for a thin layer of free electrons (where ℓ is small but large enough so that the region can be considered homogeneous), the reflection coefficient is nearly identical to the value for an infinite layer. Reflections by a succession of such layers would be rather accumulative if the separation distance between the layers allowed the successive wave fronts to be in phase.

Thus under proper conditions a satellite would produce a slab-like region (or a series of rod-like regions if the wake has an oscillatory nature) of slightly higher density than its surroundings, which are assumed to have a density that is near the critical frequency. This region would be highly directional as a reflector of radio waves. The present treatment is still too general to obtain specific values of the cross section. Nevertheless, the values should be high.

7. Suggestions For Observational Techniques

These considerations at once suggest some useful modifications of the current experimental systems. The region from which radio reflections of satellite wake phenomena are to be expected is limited to the region for which the ambient density of electrons almost reaches the critical value. This region should be mapped out during the experiment by means of radio soundings. The experiment should be conducted only when this region is limited in extent and, furthermore, when known objects will be passing through the region. The early morning hours should be best for this purpose since observation would be made from a region of low density toward a nearby region of high density.

Since the orientation of the reflecting surface is determined by the satellite trajectory and the magnetic field, one can choose the optimum geometry for the radar transmitter and the several receivers.

A satellite in an orbit chosen so as to have it travel parallel to the magnetic field of the earth over a considerable part of its orbit and equipped for regulating its own charge would be useful for the studies.

References

1. S. F. Singer and E. H. Walker, "Plasma Compression Effects Produced by Spave Vehicles in a Magneto Ionic Medium", (Included as part of this report; see table of Contents).

2. W. K. H. Panofsky and M. Phillips, Classical Electricity and Magnetism, Addison-Wesley, Cambridge, Massachusetts, (1955).

3. L. Spitzer, Physics of Fully Ionized Gases, Interscience Publishers, New York, 1956.

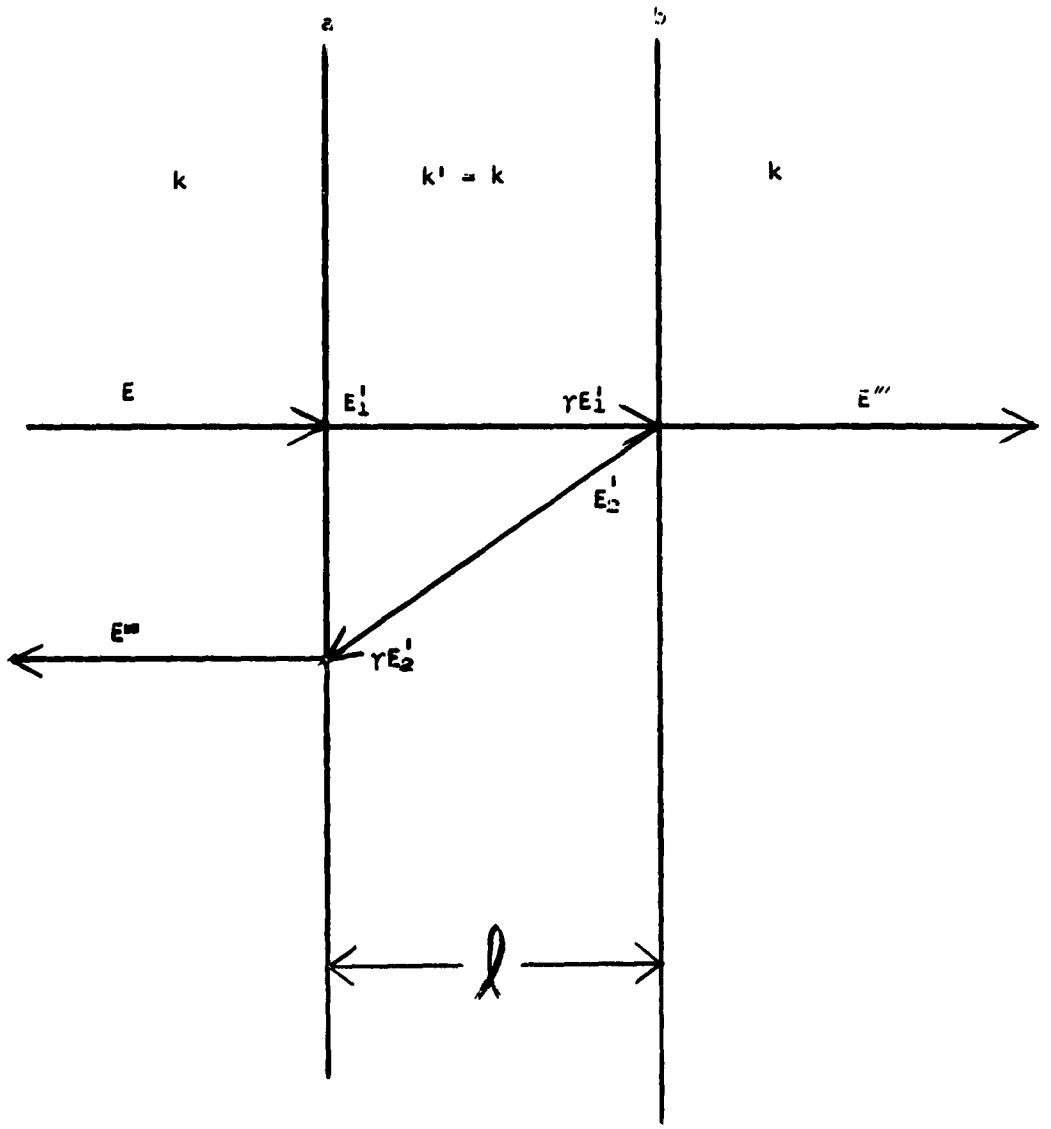

Fig. 1. Diagram to show the important quantities involved in the calculation of the reflection coefficient for an electromagnetic wave incident on a layer of thickness ℓ.

Interaction of West Ford Needles with the Earth's Magnetosphere

Prof. S. F. Singer

Abstract

The proposed West Ford experiment envisages the creation of a belt of orbiting dipoles for communication purposes. Because of the large area-to-mass ratio of the needles the perturbing effects of radiation pressure are of great importance. It is argued here that the needles will acquire an electric charge, and that perturbations due to Coulomb drag and Lorentz force cannot be neglected. Coulomb drag will lead to a much more rapid shrinkage of the orbit than ordinary drag; their effects are tabulated. Finally, a modification of the West Ford experiment is suggested which could separate the perturbing effects; this would lead to a direct experimental determination of the parameters which enter into the theory of the interaction of small particles with the magnetosphere (the region, from the ionosphere out to about 10 earth radii, where the geomagnetic field is a controlling factor).

Introduction

W. E. Morrow[1] of the Lincoln Laboratory of MIT has suggested the use of a new method for intercontinental communication. It is based on the use of belts of orbiting dipoles which act as a scattering medium for microwaves. This technique is claimed to have significant advantages over other satellite communication techniques. However, it has been pointed out by others, particularly observational astronomers, that this operational project labeled West Ford would have some undesirable side effects on optical astronomy[2] and on radio astronomy.[3] Our present paper is not concerned with these effects nor with communications and related topics.[4] Instead we shall examine in some detail certain aspects of the interaction of the West Ford medium with the exosphere, in particular, the interaction of the electric charge, which the needles are certain to carry, with the ionized portion of the exosphere. We want to point out the possibility of making unique observations which can help establish the important parameters of this interaction. Therefore, as far as possible, this paper will give numerical predictions of orbit changes. In addition, a useful modification of the experiment is suggested.

Forces acting on small particles in near space

The unique properties of the orbiting dipoles arise from the fact that they are so small. They have, in fact, close to the largest area-to-mass ratio (50 cm^2/gm) of any artificial satellite, and approach an area-to-mass ratio of small ($\sim$100 micron) interplanetary dust particles. Hence we can apply to the West Ford medium a similar analysis used for interplanetary dust in the vicinity of the earth.[5]

The motion of a particle is determined by the forces which act on

it. Within the region of the earth's exosphere (taken to extend out to about 10 earth radii) the gravitational force of the earth predominates and will be orders of magnitude greater than other forces for small particles. However, there are three other forces which need to be taken into account, particularly for orbiting particles: 1. radiation pressure; 2. the Lorentz force produced by the earth's magnetic field; and 3. Coulomb force produced by the interaction with the ionized exospheric gas.

1. The radiation pressure force is chiefly due to the solar radiation and, to a smaller extent, to the radiation scattered from and emitted by the earth. The dynamic effects of the radiation pressure force have been investigated by Jones and Shapiro.[6] The effects predicted for the West Ford medium are given in the paper by Morrow and MacLellan[4] and would indicate that the medium would disperse at a certain rate; also that the change in eccentricity produced by a resonant phenomenon would be particularly strong for polar orbits at altitudes of 3700 km.*

* These predictions concerning the behavior of the dipoles must be accepted with some caution since they are based on a certain value of area-to-mass ratio, i.e. 50 cm^2/gm and the implicit assumption that this ratio remains constant. Now in fact there will be powerful torques acting on these particles due to the interaction of their charge and possible magnetic moment with the plasma as well as with the earth's magnetic field. This may give rise to a variable area-to-mass ratio which may be related to position within the orbit. Thus it is conceivable that when viewed from the sun this will lead to other resonances, and it is not immediately obvious whether they will reinforce or cancel and overcome the resonances calculated for a spherical particle.

2. The Lorentz force acts perpendicular to the particle's velocity vector. It will be most pronounced in the polar regions where the

magnetic field is strong and always perpendicular to the particle's velocity vector. Only one general statement may be made about the effects of the Lorentz force: it cannot change the total energy of the particle. In other words, the semi-major axis of the orbit will remain constant but the other parameters of the orbit may vary.

3. The Coulomb (electrostatic) drag force has been shown to be one of the most important forces for particles moving in interplanetary space.[7] This electrostatic drag force acts generally between any charged body moving through a plasma and has therefore been also considered for the case of earth satellites by various authors who however arrive at varying conclusions.[8,9,10,11,12,13] Our view agrees most closely with that of Lehnert[8] who first showed that the Coulomb drag would not be particularly effective for earth satellites of nominal dimensions.

The importance of the Coulomb force then hinges on two points: 1. the small size of the body, and; 2. the question of its charge. In general we may say that if the body is very much smaller than the Debye screening distance, then the question of the Coulomb drag should be investigated in detail. The dynamics of the charging situation was investigated by the writer, who also discussed the competition between photoelectric emission and accretion of charge by ambipolar diffusion from the surrounding plasma. It was concluded that in interplanetary space dust particles would most likely be positively charged.[7] Whipple[14] has

pointed out explicitly that the charge becomes less positive as one approaches the earth, and becomes negative in the ionosphere.

Since the Coulomb drag produces a dissipation effect akin to friction, it will decrease the semi-major axis of the orbit continuously and eventually cause the particle to enter the dense atmosphere of the earth. We will therefore be particularly interested in investigating the effect of Coulomb drag on the particle's lifetime.

Analysis of the Coulomb drag force. For the purposes of our discussion we will adopt a treatment introduced by Chandrasekhar and Spitzer in which the orbiting particle will be referred to as the "test particle" and the ions and electrons of the exosphere as the "field particles". The drag deceleration is given by[15]

$$a_C = - A_D \left(\frac{m_1}{2kT_1}\right) \left(1 + \frac{m}{m_1}\right) \quad G(x) \qquad (1)$$

where the subscript 1 always refers to the field particles;

$$x = (1.5)^{1.5} \; w/C_1$$

where $C_1 = (3kT_1/m_1)^{\frac{1}{2}}$ is the RMS velocity

w = test particle velocity ($\sim$5 km/sec)

$$G(x) = \frac{\phi(x) - x\,\phi'(x)}{2x^2}$$

$$\phi(x) = 2\pi^{-\frac{1}{2}} \int_0^x \exp(-y^2)\, dy$$

$$A_D = 8\pi e^4 n_1 Z_1^2 Z^2 \ln \Lambda/m^2$$

$$\Lambda = 3(2Z Z_1 e^3)^{-1} (k^3 T_1^3/\pi n_1)^{\frac{1}{2}}$$

where n and Z denote particle concentration and charge, respectively; for the exosphere $Z_1 = 1$.

With an exospheric temperature T_1 of 1500° K; we obtain: C_1 = 6.1 km/sec

for protons; C_1 = 260 km/sec for electrons. Under these conditions $\ln\Lambda \sim 20$; $G(x) \sim 0.2$ for the field protons and less than 0.015 for field electrons. Since the particle mass $m >> m_1$, Eq. (1) reduces to

$$a_c = 1.23 \times 10^{-23} Z^2 n_1/m \qquad (2)$$

In the derivation of Eq. (2) some approximations have been made; e.g. the particle's velocity w was assumed constant and appropriate to a circular orbit at an altitude of 9500 km. No greater refinement appears necessary in view of the gross approximations which must be made in the calculation of the charge Z.

Calculation of electric charge

The electric charge of the particle is given by its electric capacity multiplied by the potential of its surface. For a conducting sphere of radius a cm

$$Z = 6.95 \times 10^6 \text{ aV} \qquad (3)$$

where V is measured in volts. For a body of different shape the capacity must be calculated; in the absence of detailed data we will adopt a system of two spheres each with "effective" radius of 1.5×10^{-3} cm. Thus for the West Ford needles we take

$$Z \sim 2 \times 10^4 \text{ V} \qquad (4)$$

The calculation of the potential V also presents special problems since it depends on the position of the particle, and therefore in turn on the characteristics of the particle's orbit. It also depends on the work function W and photoelectric yield δ of the particle material, its shape and its attitude towards the sun. As explained earlier, we calculate V in an analysis involving competition between the photoelectric effect and ambipolar diffusion.[7] The ambient electron density above $\sim 1.5\ R_E$ (earth

radii) is given by Helliwell as

$$n_1 \sim 10^4 r^{-3} \tag{5}$$

where r is measured in terms of earth radii.

The photo emission is determined by the ultraviolet spectrum of the sun; i.e. by N_ν the photon flux per cm^2/sec with energy $h\nu \geq eV + W$. We assumed the relation $N_\nu = f V^{-\delta}$; where $f = 10^{19}$ and $\delta = 4$. On the basis of Hinteregger's measurements[16] a better set of values is

$$N_\nu = 2.2 \times 10^{13} \; V^{-1.844} \quad [cm^2 \; sec]^{-1} \tag{6}$$

The equilibrium potential is given by[10]

$$V_+ \sim + (\gamma f / n_e c_e)^{1/\delta} \tag{7}$$

when the particle has a large positive potential and the ion current can be neglected. In the earth's shadow, where photo emission is negligible, the equilibrium potential is given by

$$V_- = - (kT_e/2e) \; \ell n \; (m_i T_e / m_e T_i) \tag{8}$$

In view of the uncertainties in γ, W, attitude and orbit orientation we have decided to make some drastic approximations and represent the potential by

$$V = 7.5(r - 2) \tag{9}$$

As can be seen, V varies from -7.5 volt in the F-layer to +60 volt at 10 R_E. Note that V = 0 at 2 R_E; the implication will be discussed below.

It should perhaps be pointed out explicitly that another powerful charging process exists, namely the high flux of fast electrons in the outer radiation belt; it is however quite localized and confined mainly to the vicinity of the lines of force which extend to 3-5 R_E in the plane of the magnetic equator. Its effect is to produce (or enhance) the

negative charge (by accretion and secondary electron emission); this effect must be considered for orbits which intersect the outer radiation belt.

By combining Eqs. (2), (4), (5) and (9) we obtain for the Coulomb drag deceleration

$$a_C = \sim 3 \times 10^{-9} \, (r-2)^2 \, r^{-3}/m$$

With the needle mass given[4] as 10^{-4} gm

$$a_C \sim 3 \times 10^{-5} \, (r-2)^2 \, r^{-3} \quad [\mathrm{cm/sec^2}] \tag{10}$$

This acceleration may be compared with the accelerations due to

(I) Radiation pressure

$$a_{RP} \sim \left(\frac{1.4 \times 10^6 \mathrm{erg/cm^2/sec}}{3 \times 10^{10} \mathrm{\ cm/sec}}\right)\left(\frac{50 \mathrm{\ cm^2}}{g}\right) = 2.5 \times 10^{-3} \mathrm{\ cm/sec^2} \tag{11}$$

(II) Gravity

$$a_G = 980 \, r^{-2} \tag{12}$$

(III) Magnetic

With the circular velocity $w \sim 8 \times 10^5 \, r^{-\frac{1}{2}}$ cm/sec, and with the magnetic field $B \sim 0.5 \, r^{-3}$ gauss, we obtain

$$a_M = Ze \, w \, B/m$$

$$= 10^{-5} \, (r-2) \, r^{-3.5} \ \mathrm{cm/sec^2} \tag{13}$$

Effects of Coulomb Drag

The orbit changes and lifetime of a satellite in the presence of a dissipative drag force F_D can be treated most simply by energy considerations.[17]

The energy loss per orbit in a circular orbit is $\Delta E = 2\pi r F_D$ and this will reflect itself in a lowering of the orbit by an amount Δr in a time which is simply the orbital period

$$T = 2\pi \ (GM_E)^{-1/2} \ r^{3/2} \tag{14}$$

Since the total (kinetic + potential) energy is given by $E = \frac{1}{2} GM_E m/r$, we obtain by differentiation

$$\Delta r = (-\Delta E) \ \frac{2 r^2}{GM m} \tag{15}$$

We can therefore obtain an expression for the rate of shrinkage of a circular orbit as follows

$$\Delta r/_{\Delta t} = 2\pi r F_D \cdot \frac{2 r^2}{GM m} \ \frac{(GM)^{1/2}}{2\pi r^{3/2}} = \frac{2}{(GM)^{1/2}} \frac{F_D}{m} \cdot r^{3/2} \tag{16}$$

$$= \frac{1}{\pi} \ T \ \frac{F_D}{m}$$

which is $(1/\pi)$ times the orbital period times drag deceleration.

We can also express $(\Delta r/\Delta t)$ as a function of r using our Eq. (10) for Coulomb drag and using $T = 5080 \ r^{3/2}$ for orbital period:

$$(\Delta r/\Delta t)_C = \sim 5 \times 10^{-2} \ (r-2)^2 \ r^{-3/2} \ \left[\text{cm/sec}\right] \tag{17}$$

This expression may now be compared to the neutral drag acceleration evaluated from

$$F_N/m = \tfrac{1}{2} C_D A\rho \ w^2/m = \tfrac{1}{2} C_D A(n_H m_H + n_O m_O) \ w^2/m \tag{18}$$

Using $w^2 = (7.9 \times 10^5)^2/r$; $m = 10^{-4}$ gm; $A = 5 \times 10^{-3}$ cm^2; $C \sim 2$; we obtain

$$F_N/m = 5 \times 10^{-3} \times 1.66 \times 10^{-24} (n_H + 16 \ n_O)(6.25 \times 10^{11}) \ 10^4/r$$

$$= 5.2 \times 10^{-11} (n_H + 16 \ n_O)/r \ \left[\text{cm/sec}^2\right] \tag{18'}$$

In the case of a particle belt it is more relevant to calculate $(\Delta r/\Delta t)$, rather than the change in orbital period.

$$(\Delta r/\Delta t)_N = 1/\pi \ (5080 \ r^{3/2}) \ 5.2 \times 10^{-11} (n_H + 16 \ n_O)/r$$

$$= 8.4 \times 10^{-8} (n_H + 16 \ n_O) \ r^{1/2} \qquad \left[\text{cm/sec}\right] \tag{19}$$

It is of considerable interest to establish the relative importance of the two drag forces. In order to do this we must adopt a model for the structure of the magnetosphere.

Observational information is limited to rather low altitudes. The distribution of mass density below 800 km is known from analysis of satellite drag[18]. The integrated thickness of the neutral hydrogen cloud around the earth is known from analysis of the profile of solar hydrogen Lyman-α[19]. Electron densities up to 1500 km are known from rocket measurements[20]. The electron density to several earth radii is inferred (with some uncertainty) from whistler observations[21,22].

On the other hand the relative distributions of the neutral constituents can be deduced from a theory of the exosphere[23]. The neutral components describe ballistic orbits without collisions above the base of the exosphere (530 km) and the distribution of concentration with altitude is calculable in a fairly straightforward manner. The ionized components (having much larger cross section because of Coulomb interaction) are distributed according to the barometric formula[24]. In each case the slope (or scale height) is determined by the temperature at the base of the exosphere. Using the data referred to above for normalization, it is possible to construct a model of the exosphere[25]. This model is shown in Table I.

TABLE 1

Concentration of major constituents in the terrestrial exosphere (cm^{-3})

r/R	O	O^+	H	H^+
1.100	1.2×10^7	5×10^5	10×10^3	---
1.200	2.7×10^4	2.5×10^4	6.6×10^3	9×10^3
1.300	1.7×10^2	1.7×10^3	4.4×10^3	6.6×10^3
1.400	1	1.3×10^2	3.1×10^3	5×10^3
1.500	---	11	2.3×10^3	3.7×10^3
1.75		<.1	1.25×10^3	2.1×10^3
2.00			8×10^2	1.3×10^3
3.00			2×10^2	3.5×10^2
4.00			82	1.5×10^2
5.00			43	85
6.00			25	51
7.00			16	33
8.00			12	23
9.00			9.1	17
10			6.5	11

TABLE 2

Drag Deceleration and Orbit Shrinkage

r/R	a_N (cm/sec^2)	$(\Delta r/\Delta t)_N$ (cm/sec)	a_c (cm/sec^2)	$(\Delta r/\Delta t)_c$ (cm/sec)
1.1	9×10^{-3}	1.7×10	1.8×10^{-5}	3.5×10^{-2}
1.2	3.6×10^{-5}	7.6×10^{-2}	1.1×10^{-5}	2.4×10^{-2}
1.3	1.5×10^{-6}	3.6×10^{-3}	6.9×10^{-6}	1.7×10^{-2}
1.4	3.7×10^{-7}	1×10^{-3}	4.0×10^{-6}	1.1×10^{-2}
1.5	2.1×10^{-7}	6.1×10^{-4}	2.2×10^{-6}	6.8×10^{-3}
1.75	9.8×10^{-8}	3.7×10^{-4}	3.6×10^{-7}	1.4×10^{-3}
2.0	5.5×10^{-8}	2.5×10^{-4}	(0)	(0)
3.0	9.5×10^{-9}	7.9×10^{-5}	1.1×10^{-6}	9.6×10^{-3}
4.0	3×10^{-9}	3.9×10^{-5}	1.9×10^{-6}	2.5×10^{-2}
5.0	1.4×10^{-9}	2.4×10^{-5}	2.1×10^{-6}	4.0×10^{-2}

Both neutral and Coulomb drag decelerations are shown in Table 2, as well as the resulting values of $(\Delta r/\Delta t)$. It must be cautioned however that the Coulomb drag depends on many detailed factors, (some of which were discussed earlier), involving the particular properties of the particle, of the exosphere, and of the sun; as well as the particulars of the orbit.

The zero value of Coulomb drag at $2R_E$ should not be taken literally; it merely indicates that somewhere in this altitude range there may be a minimum. As discussed elsewhere, small fluctuations of charge will produce a drag (since it depends on the square of Z and not on the sign); in particular, the day-night effect sets a lower limit to the Coulomb drag[5]. This minimum may give rise to a high concentration of interplanetary smoke (particles $\gtrsim$ 1 micron) near 2 earth radii <u>if they exist</u>.

Discussion

It would be of interest to calculate the lifetimes of the West Ford particles. Since the details of the orbit have not been revealed and, in particular, since the altitude and orbit inclination is not known, it does not seem worthwhile to attempt any refined calculations. There are in any case uncertainties about the electric charge of the particle, about its attitude with respect to magnetic field and with respect to the sun, and also about the actual values of air density.

With initial orbit details available, the subsequent history of the West Ford particles can only be obtained by numerical methods. It is clear, by referring to Table 2, when the neutral drag may be neglected. It is clear also, by referring to Eqns. (10), (11), and (13), that probably none of the forces can be neglected, except for very special orbits.*

In a numerical computation, particular attention must be paid to the day-night effect, not only on radiation pressure, but also on the particle charge. In fact, because of fluctuations in radiation belt intensity, solar flares, and similar factors, the charge will fluctuate unpredictably. This effect will contribute to a spreading of the belt which is in addition to the dispersion calculated by the Lincoln Laboratory[4].

* It is interesting to note the importance of the radiation pressure in relation to the Coulomb drag. This is due to the geometric shape of the needles.

It should be noted that for a spherical interplanetary dust particle the radiation pressure acceleration is $\sim 5 \times 10^{-5}\ \pi a^2/m$ and is, relatively, 100 - 1000 times smaller when compared to the Coulomb drag[5,7].

Nevertheless, the shrinkage of an initially circular orbit produced by energy loss due to drag is a gross effect which should be observable, and which gives some information on air density, as well as about the importance of Coulomb drag.

A Proposed Experiment

However, a much more refined experiment is possible which illuminates the interaction of small particles with the magnetosphere. It is based on a separation of the perturbing forces.

Consider, for example, an initially circular orbit at $\sim$ 3200 km altitude ($r = 1.5\ R_E$), nearly polar and perpendicular to the earth-sun line. In this special orbit the radiation pressure does not produce any appreciable perturbation (at least initially), and the Lorentz force perturbation can be determined quite simply, although it is again negligibly small. Since the particle's velocity vector is more or less in the plane of the magnetic meridian, the chief perturbation will be orthogonal and cause a rotation of the orbital plane. The sense of the rotation establishes the sign of the electric charge on the particle. Using the analysis leading up to Eq. (13) we estimate the rate of rotation of the orbital plane as about 10^{-11} rad/sec.

Next consider a modification of the photoelectric properties of the copper needles. Specifically, one-third could be left with their present copper surface, one-third would be coated with a material of high work function W and low photoelectric yield γ (e.g. platinum), and the remainder with a material of opposite characteristics (possibly a cesium alloy). For our particular orbit, the Cu particles would be negative, the Pt particles even more negative, while the Cs particles would have a nearly zero potential, or perhaps even positive.

Because of Coulomb drag the three belts will shrink at a different rate. Using the analysis leading up to Eq. (17) we estimate a differential rate of shrinkage of orbit radius amounting to nearly 1 km per day.

Thus the separation of this West Ford belt into three layers might be resolvable with the available radar methods, provided the dispersion of particles at injection can be held very small.[20]

References

1. W. E. Morrow, Jr. "Orbit Scatter Communication " XIIIth URSI Assembly, London, September, 1960.
2. Wm. Liller, Astron. J. 66, 114 (1961).
3. A. E. Lilley, Astron. J. 66, 116 (1961).
4. W. E. Morrow, Jr., and D. C. MacLellan, Astron. J. 66, 107 (1961).
5. S. F. Singer, "Distribution of Dust in Cislunar Space - Possible Existence of a Terrestrial Dust Belt", in Am. Astronaut. Soc. Lunar Flight Symp. (Dec. 1960), MacMillan Co., New York, 1961.
6. H. M. Jones and I. I. Shapiro, Science 131, 920 (1960).
7. S. F. Singer, "Measurement of Interplanetary Dust" in Scientific Uses of Earth Satellites, Univ. of Michigan Press, Ann Arbor, 1956.
8. B. Lehnert, Tellus 8, 408 (1956).
9. R. Jastrow and C. A. Pearse, J. Geophys. Res. 62, 413 (1957).
10. K. P. Chopra and S. F. Singer, "Drag of a Sphere Moving in a Conducting Fluid in the presence of a Magnetic Field" in 1958 Heat Transfer and Mechanics Institute, Stanford Univ. Press. Palo Alto, 1958 .
11. L. Krauss and K. M. Watson, Phys. Fluids 1, 480 (1960).
12. D. B. Beard and F. S. Johnson, J. Geophys. Res. 65, 1 (1960).
13. K. P. Chopra, Rev. Mod. Phys. 33, 153 (1961).
14. F. L. Whipple, "Meteoric Material in Space" in Physics and Medicine of the Atmosphere and Space, Wiley, New York, 1960.
15. L. Spitzer, Jr., "Physics of Fully Ionized Gases" Interscience, New York, 1956.
16. H. E. Hinteregger, J. Geophys. Res. 66, 2367 (1961).
17. S. F. Singer, Am. Rocket Soc. (1954); Astronaut. Acta 2, 125 (1956).
18. D. G. King-Hele, Nature 184, 1267 (1959).
19. J. D. Purcell and R. Tousey, J. Geophys. Res. 65, 370 (1960).
20. W. W. Berning, J. Geophys. Res. 65, 2589 (1960).
21. R. L. Smith and R. A. Helliwell, J. Geophys. Res. 65, 2583 (1960).
22. G. McK. Allcock, J. Atm. Terr. Phys. 14, 185 (1959).
23. E. J. Opik and S. F. Singer, Phys. Fluids 4, 221 (1961).
24. F. S. Johnson, J. Geophys. Res. 65, 577 (1960).
25. S. F. Singer, J. Geophys. Res. 65, 2577 (1960).
26. I. I. Shapiro and H. M. Jones, Science 134, 973, (1961).

Further on the Interaction of West Ford Needles with the Earth's Magnetosphere.

S. F. Singer, Physics Department
University of Maryland
College Park, Maryland*

The purpose of the present paper is to amend and expand my earlier discussion of the "Coulomb drag"[1]. Originally the interest lay in calculating the drag force acting on a charged spherical dust particle moving through an ionized gas[2]; the treatment can be extended to the case of the orbiting dipole needles, used in Project West Ford[3]. Now that much of the underlying theory has been published and the orbit has been detailed[4], it becomes possible to discuss the influence of Coulomb drag on the lifetime of the needles.

Details of West Ford Experiment[4]

The copper needles have a length ℓ of 1.77 cm, and a diameter d of 2.8×10^{-3} cm. The mass M is 10^{-4} gm. They are supposed to rotate in propeller-like fashion at about 2 rev. per second; their (projected area)/mass ratio A/M will vary

* Present address: Jet Propulsion Laboratory, California Institute of Technology, Pasadena, California

between a maximum value of 50 cm^2/gm and a minimum value of 35 cm^2/gm.

The initial orbit is supposed to be a nearly circular polar orbit (i.e. with inclination $i = 90^\circ$ and eccentricity $e \sim 0$) at an altitude of about 3800 km above sealevel, or with semimajor axis $a \sim$ 1.6 R (earth radii) from the earth's center. The orbital plane is supposed to make a small angle initially with the sun-earth line.

Radiation Pressure Resonance Effect

For special orbits, and for a certain band of orbital parameters near these orbits, there exists an effect produced by solar radiation pressure which can limit the lifetime of a satellite. For a resonant orbit the eccentricity e will increase, with no appreciable change in a; essentially the orbit is displaced within its plane until the perigee

reaches the denser atmosphere and the orbit shrinks and decays. This is the picture as presented by Shapiro and Jones.[4] They show that the lifetime of the West Ford needles will be about 7 years for the initial orbit chosen. The range of the resonance is rather narrow; for A/M = 50 cm^2/gm, the altitude range is ± 150 km, the range of inclination is ± 1^o. For A/M = 35, the resonance region is considerably narrower but not quoted; the lifetime is increased in inverse proportion to A/M, i.e. to about 10 years.

Without detailed numerical orbit calculations it seems difficult to establish, e.g., the lifetimes near the edge of the resonance region, or its width. However we can quite easily establish the dependence of a for the resonant orbit on i. The rate of change of the argument of a nearly circular orbit

perigee is given by (see e.g. Ref 5)

$$\dot{\omega} \sim 5\,(a/R)^{-3.5}\,(5\cos^2 i - 1) \qquad (1)$$

The regression of the node of the orbit is given by

$$\dot{\Omega} \sim 10\,(a/R)^{-3.5}\cos i \qquad (2)$$

and must be added to $\dot{\beta}$, the rate of rotation of the sun with respect to the initial orbital plane. Of course, $\dot{\beta} \sim 1$. (All angular rates are given in degrees per day). The resonance condition demands

$$\dot{\beta} + \dot{\Omega} = \dot{\omega}, \qquad (3)$$

For i near 90°, and for $a \sim 1.6$ R it follows that

$$da/di \sim 100 \text{ km per degree} \qquad (4)$$

Assuming that the needles are launched into a perfect resonant orbit, we must investigate if there exist any perturbations which can spoil the resonance. For example, a drag force which decreases a by about 50 km per year would be sufficient, in a matter of only 3 years to pull the orbit

out of resonance, provided the inclination is changed at the same time by a lesser amount than given by Eq. (4).

Neutral drag is clearly too small, leading to a rate of change $\left(\Delta r/\Delta t\right)_N = \dot{a} \sim$ - 0.1 km per year[1]. The Coulomb force appears to be the only one of importance. It will be examined quantitatively later; let it be denoted by F. We must note that no matter how its magnitude may fluctuate, it will always be directed opposite to the relative velocity vector between the needle and the plasma. We consider the latter to be corotating with the earth's angular velocity, ω_E, at least as far up as auroral latitudes, say $\lambda \sim 65^\circ$. Hence the needle, assumed to be in a polar orbit, will experience a cross component of force $F \sin\theta \cos\lambda$

where $\tan\theta = \omega_E r / V_c \approx \omega_E \left(G M_E\right)^{-1/2} r^{3/2}$

For $r = 1.6R$, $V_c \sim 6.3$ km/sec, $\tan\theta \sim \sin\theta \sim 0.12$.

We now calculate the shrinkage of the orbit, given by

$$(\Delta r/\Delta t) = -(T/\pi)(F/M) = -(2r/V)(F/M) \quad (5)$$

where T is the orbital period $5080\,(r/R)^{3/2}$ seconds

During an interval Δt the increment in cross velocity is

$$\Delta V_\perp = \Delta t/T \int_0^T (F/M) \sin\theta \cos\lambda \, dt$$

$$= (2/\pi)(F/M) \sin\theta \, \Delta t \quad (6)$$

Therefore the change in inclination will be given by

$$\Delta i = (\Delta V_\perp / V) \quad (7)$$

We can now calculate the resultant

$$\Delta a/\Delta i = (\pi r/\sin\theta)(\pi/180)$$

in km per degree. (8)

Note that this ratio is independent of F. For r ~ 1.6 R

$$\Delta a/\Delta i \sim 4.8 \times 10^3 \quad \text{km per degree.} \quad (9)$$

This result is about 50 times greater than the slope of the "line of resonance", given by Eq. (4).

We conclude therefore that a drag force yielding $|\dot{a}| > 20$ km per year will indeed pull the orbit out of resonance. We therefore arrive at the paradoxical result that an increased drag could lead to a much longer lifetime. However, if the drag is very much greater, say $|\dot{a}| >$ 500 km per year, then the lifetime could be even shorter than the value of 7 years deduced from resonance considerations.

Calculation of Coulomb Drag for a Needle

The calculation of the drag force consists of three steps: (i) the electrical capacity C ; (ii) the electrical potential V , and finally (iii) the drag force F.

(i) Capacity. In spite of the admonition[1] that "for a body of different shape [from a sphere] the capacity must be calculated", I omitted to do this and adopted an incorrect value which turns out to be appropriate to a sphere of diameter $\sqrt{2} \times 3 \times 10^{-3}$ cm but not to a needle. If we approximate the dipole by a prolate spheroid (as suggested to me by Professor Leverett Davis), its capacity is given (in MKS units)[6]

$$C_{ps} = 4\pi \in (a^2 - b^2)^{1/2} \left[\tanh^{-1}(1 - b^2/a^2)^{1/2}\right]^{-1} \qquad (10)$$

while a sphere of radius a has a capacity

$$C_s = 4\pi \in a = 1.1128 \times 10^{-10}\, a \qquad (11)$$

A lower limit to C, the actual capacity of the needle, is obtained by taking $a = l/2 = 8.9 \times 10^{-3}$ m and $b = d/2 = 1.4 \times 10^{-5}$ m.

Since $b \ll a$, we can approximate

$$C_{ps} \sim 4\pi\epsilon a \left[\tfrac{1}{2} \ln(1+\chi) - \tfrac{1}{2} \ln(1-\chi)\right]^{-1} \quad (12)$$

$$\sim 4\pi\epsilon a \left[6.45\right]^{-1}$$

where $\chi = (1 - b^2/a^2)^{1/2} \sim 1 - \tfrac{1}{2} b^2/a^2$

An upper limit to C is obtained from the capacity of the spheroid which circumscribes the needle, assumed to be cylindrical; $C'_{ps} = \sqrt{2}\, C_{ps}$

I therefore adopt a mean value

$$C \sim 1.2\, C_{ps} = 0.186\, C_s \sim 20a \ [\mu\mu fd] \quad (13)$$

It is interesting to note that the sphere which circumscribes the cylinder has a capacity ~ 5.5 times that of the needle.

For the case of the West Ford needle,

$$C \sim 0.18 \ \mu\mu fd \ (\pm 20\%) \quad (14)$$

The quoted inaccuracy stems partly from our insufficient knowledge of the detailed shape of the needles (straight or bent? ends flattened? smoothed?). It should be noted that C is about 58 times greater than my previously adopted value in Ref. 1; hence the needle charge Z should be increased by the same factor, and the drag by $(58)^2$.

(ii) Electrical Potential. As stated before,[1] the potential V, and therefore the number of electronic charges Z, are the most uncertain quantities in the calculation of the drag. Depending on the position of the body in space, three processes are of importance: (a) accretion of ions and electrons from the magnetospheric plasma; (b) ejection of photoelectrons by solar ultraviolet radiation; (c) absorption of high velocity electrons (and protons) trapped in the earth's magnetic field. Charging Processes: Before attempting any numerical estimates for the West Ford orbit, it is of interest to make some general remarks on the calculation of charging rates for the three processes. Both (a) and (b) depend on the body's potential V, while (c) is reasonably independent of V; as a result (b), and more particularly (a), are "compensating" processes which adjust their rates in such a way as to minimize V; (process (a) can even change its sign). The basic reason for this is that (c) involves energies much greater than V, while (a) and (b) do not.

Next, it should be noted that for process (c) the omni directionally averaged area is relevant (assuming that the trapped particles are isotropically incident). For (b) the unidirectionally (i.e. along the sun line) averaged projected area matters, while for process (a) the area depends on V in a complicated way, as well as on the shape of the body, orientation of the magnetic field, and temperature of the plasma. (This problem is being investigated in a fundamental way by Mr. E. H. Walker at the University of Maryland as part of his Ph.D. dissertation.)

Superimposed on these fundamental problems are more detailed ones arising from uncertainties of the physical parameters:

(a) Of crucial importance is the velocity distribution of the plasma electrons, particularly the existence of a high energy tail. The ions make good thermal contact with the neutral atoms below the exosphere base; hence they are reasonably certain to have a Maxwellian distribution appropriate to a temperature of about 1500°K, i.e. kinetic energy $\sim$ 0.195ev. The electrons however are ejected with energies higher by 1 or 2 orders of magnitude and must thermalize through collisions. It is quite likely that a goodly fraction of the high energy tail escapes upward into the magnetosphere (particularly at higher latitudes where the lines of force are more nearly vertical) for two reasons: the path length is shorter; and the Coulomb scattering cross section decreases as $(1/\text{energy})^2$.

Consider the situation in the earth's shadow and assume only process (a) effective. The equilibrium potential would be given by

$$V = - (kT_e/2e) \ln (m_i T_e / m_e T_i) \qquad (15)$$

If we adopt for an electron "temperature" T_e appropriate to their non-Maxwellian distribution,

$$T_e = (2/3k) (\overline{\tfrac{1}{2} m v_e^2}) = f T_i \qquad (16)$$

then V~0.75f volts for an O^+ plasma, and $\sim$25% less for an H^+ plasma. With f between 1 and perhaps 10, we may adopt a provisional value for V of - 3.6 volts.

At an altitude of 3800 km we adopt a density of 3×10^3 H^+ ions per cm^3. Under these conditions the accretion rate of positive ions is $\sim 10^8$ per sec, very roughly.

(b) For the flux of solar photons with energy greater than $h\nu$ we had adopted[1]

$$N_\nu = f\,\nu^{-\gamma} = 2.2 \times 10^{13}\ \nu^{-1.844}\ \ [\mathrm{cm^2\ sec}]^{-1}. \qquad (17)$$

However the expression Eq. (7) for the equilibrium potential V_+ quoted earlier[1] applies only when the body has a large positive potential, and is therefore inappropriate for the West Ford orbit. Major uncertainties in process (b) involve the photoelectric quantum yield γ and the work function W. With some crude estimates, $\gamma \sim 0.1$, $W \sim 10$ volts we derive a photoelectric charging flux of $(3 \times 10^{10}\ \mathrm{cm^{-2}\ sec^{-1}}) \times (5 \times 10^{-3}\ \mathrm{cm^2}) \sim 1.5 \times 10^{8}$ per sec, comparable to the flux of positive ions.

(c) Since maximum high energy proton fluxes in the inner radiation belt only amount to $\sim 10^4$ per $\mathrm{cm^2}$-sec, we need to consider only the effects of high energy trapped electrons. Mainly because of instrumental considerations we can divide them into three energy categories: (i) $>$ 100 kev with a peak flux of $\sim 10^9$ per $\mathrm{cm^2}$ - sec, located between 3 - 4 R in the equatorial plane, hence at magnetic latitude 50° near the earth (Explorer VI data of Winckler et al; Fan, Meyer, Simpson; Farley and Rosen; Lunik data of Vernov et al) (ii) "Auroral" electrons of rather lower energies (10 - 50 kev) with flux of $\sim 10^{10}$ per $\mathrm{cm^2}$-sec (Sputnik 3 data of Krassovsky; rocket data of McIlwain)

(iii) A rather hypothetical electron component, assumed to be responsible for the magnetic storm ring current (rather than the conventionally assumed 20 kev protons). An average magnetic storm demands an energy density of ~ 50 kev per $\mathrm{cm^3}$; thus if the mean energy of these electrons is 300 ev their flux will be 2 x 10" per $\mathrm{cm^2}$ - sec. (Singer).

The omnidirectionally averaged area of a needle is $(\pi/4)\,\ell d$ $\sim 4 \times 10^{-3}$ cm^2. A mean thickness is $\sim 2 \times 10^{-2}$ gm - cm^{-2}; hence a good fraction, say $\frac{1}{2}$ of component (i) will be absorbed (if we include the effects of scattering). As we go to lower energies the effects of secondary electron emission as well as back scattering become of increasing importance.[7] Thus we estimate a charge accretion of $\frac{1}{2}$ for component (ii), and only 1/10 for component (iii).

Thus we would estimate that for particular portions of the orbit, constituting perhaps 20% of it, we have an electron accretion of $\sim 10^8$ per second, with a variability of $\pm$ 1 - 2 orders of magnitude.

For the West Ford orbit (polar, at altitude 3800 km), it would appear from the preceeding discussion that the charge is always negative, being largest on the nightside in the auroral zone, and smallest on the dayside at low latitudes.

Adopted Values: For the purpose of further calculation we adopt a potential V of - 3.6 volt, and estimate a high probability that it stays within a factor of 2, ie, between -1.8 volt to -7.2 volt.

It should be pointed out specifically however that one cannot really average the potential over an orbit, or over a period of time. Since the drag depends on V^2, it should be pointed out explicitly also that for a small particle the drag is independent of the sign of the potential; for a large body a negative potential leads to a lower drag than the same value of positive potential. Averaging could lead to a serious underestimate of the effects of possible peaks in the fluctuation of the particle's potential. To gauge these peaks we calculate the time constant involved in the charging process; with a nominal charge of

$CV/e = 4 \times 10^6$ electrons, this time turns out to be $\sim$0.04 seconds. I am not aware of any processes which have a shorter time constant and would therefore be effective in producing peaks; but their existence cannot be ruled out in advance.

(iii) The Drag Force: A massive body carrying a charge Ze moves with velocity w through a plasma with ions of mass m_1, charge Z_1, and of density n_1. The drag force may be deduced from expressions given by Spitzer[8]:

$$F = \left(\frac{4\pi e^4 Z_1^2 \ln \Lambda}{kT_1}\right) n_1 Z^2 G(x) = -6.8 \times 10^{-23} n_1 Z^2 G(x) \quad (18)$$

Table I shows G (x) for various conditions; $x = 1.5^{1.5} (w/C_1)$ where C_1 is the RMS velocity of the field particles, corresponding to a temperature T_1 of 1500°K. It can be seen that below 2000 km, O^+ is about 5 - 10% as effective as H^+, while the electrons are about $\frac{1}{2}$ as effective as H^+. Above 2000 km only H^+ needs to be considered. Beyond 10-15 R we must consider interplanetary plasma velocities and temperatures.

For a range of orbits near the West Ford resonant orbit we may take

$$F = 1.0 \times 10^{-23} n_1 Z^2 \quad (19)$$

Table I Selected Values of G(x)

Region:	H^+ Ionosphere		O^+	electrons
	1000-6000 km	2-10R	500-2000 km	
w (circular)	0.12	0.2	0.007	.018
w (escape)	0.06	0.15	0.003	.026

It is useful also to indicate the sensitivity of G to small charges in w.

For H^+ between 1000-6000 km $dG/dw \sim$ - 0.03 per km/sec;

For O^+ between 500-2000 km - 0.003 per km/sec

For electrons + 0.003 per km/sec

With a nominal charge Z of 4×10^6 electrons and with $n_e = 3 \times 10^3$ cm^{-3} we obtain $F = 4.8 \times 10^{-7}$ dynes.

Before this value can be accepted, it is necessary to prove that the size and shape of the body is of minor importance and that the drag depends only on Z^2. I have been able to show that the "effective area" of a needle is closely the same as that of a point charge. The potential ϕ in the vicinity of very thin straight wire segment of length ℓ is given by[9]

$$\phi = (2Ze/\ell) \tanh^{-1} (\ell/r_1+r_2) \qquad (20)$$

where r_1 and r_2 are the distances from the ends of the needle to point P; the equipotential lines are clearly ellipses.

The potential on the equatorial plane of the inscribed ellipsoid can be found by making use of the expressions

$$\tanh^{-1}x = \sinh^{-1}u = \ln 2u + \tfrac{1}{2}\frac{1}{2u^2} - \tfrac{3}{8}\frac{1}{4u^2} \cdots$$

where $x = u\,(u^2 + 1)^{-\frac{1}{2}}$.

In our case $x = 1 - \frac{1}{2} b^2/a^2 = 1 - (2\times10^{-6})$; $u \sim 500$; and $\tanh^{-1}x \sim \ln 2u = 6.9$.

We now wish to find the ellipse where the potential is about 1/10 of the surface value. This figure is chosen to be roughly equal to the ion kinetic energy and therefore defines approximately the line where the deflection of the ion is 90°. Hence, setting $\tanh^{-1}x = 6.9/10$, we obtain (from Tables) $(\ell/r_1 + r_2) = 0.5$ or $r_1 + r_2 = 2.0\ell$. This ellipse turns out to have semimajor axis $A = \ell$, semiminor axis $B = \ell\sqrt{3/4}$ and area

$$A_{90^\circ} = \pi\sqrt{3/4}\,\ell^2 = 0.87\,\ell^2 \qquad (21)$$

This area is to be compared to the case where the needle charge obtained from Eq. (14)

$$Q_N = 0.186\,(4\pi\epsilon a V) \tag{22}$$

is concentrated at a point. The distance r_0 at which the potential is $\frac{1}{10}$ V is given by

$$1/10\ V = Q_N (4\pi\epsilon r_0)^{-1}\ ;\ \text{i.e.}\ r_0 = 1.86\,a$$

The area enclosed by this circle is $\pi\,(1.86\,\ell/2)^2$ (23)

which is closely equal to the value of Eq. (21).

Note that a calculation for the two areas corresponding to the full potential V gives the values ℓd for the needle and $1/100 \times 0.87\pi\ell^2$ for the point charge; they are in the ratio of 1:17.2. However since the contribution to the drag comes predominently, i.e. by a factor $\ell n\ \Lambda \sim 20$, from small deflections produced by distant collisions, we are justified in stating that the total charge only, independent of body shape, determines the Coulomb drag force to a close approximation.

This statement evidently breaks down where the body's dimension becomes larger than either the Debye length $h = 6.9\sqrt{T_e/n_e} \sim 5\,cm$, or the distance r_0.

Effect of Coulomb Drag on Orbit

Lifetime: The major effect of Coulomb drag is a transfer of energy to the plasma in the magnetosphere. This leads to a decrease in the total energy of the body and to irreversible shrinkage of the orbit. For a near circular orbit at distance r from the earth's center the rate of shrinkage is given by Eq. (5).

For the West Ford case, with $M = 10^{-4}$ gm and a plasma density at 1.6R of $\sim 3 \times 10^{3}$ cm^{-3} we obtain the following result:
$dr/dt \sim 16$ cm/sec, or 5000 km per year, or 14 km per day.
This result refers to our nominal "average" potential of -3.6 volt; for 1.8 volt $dr/dt \sim 1250$ km per year; for -7.2 volt $dr/dt \sim 20000$ km per year, about 55 km per day.

It can be seen that the Coulomb drag provides an upper limit to the lifetime of a few weeks to a few years, rather less than the lifetime obtained from the radiation pressure resonance effect.

A further interesting (and seemingly paradoxical) point exists. Under the extreme assumption of a potential as low as 0.36 volts the rate of shrinkage is only 50 km per year; it would pull the orbit out of resonance in about 3 years and thereby increase the lifetime. But I estimate the probability for such a small potential as less than 10%.

Dispersion: The dispersion of the orbiting dipoles is likely to be dominated by the Coulomb drag. Fluctuations in the charging rate are produced by the day-night effect, and less predictably by solar flares, magnetic storms etc. The resultant dispersion might amount to a few

percent of the shrinkage rate, i.e. to a spread of about 1 km per day.

As discussed in the earlier paper,[1] by coating the copper needles in a suitable way the work function can be altered and the photoelectric charging rate can be modified. One can conceive of an experiment in which three groups of needles with different work functions are ejected; they would decay at an average rate of 14 km per day but with a difference amounting to a few km per day.

Rotation of Orbital Plane: For a nearly polar orbit the Lorentz force $Ze\ (v \times B)$ produces an orthogonal perturbation which is easily estimated by a simple geometric perturbation approach. It leads to a torque which precesses the orbit plane at a rate of about 5×10^{-10} radians per sec, or 1.5×10^{-2} rad per year; it can be considered as negligible.

Conclusions

The importance of the Coulomb drag on the orbits and lifetime of the West Ford needles is established beyond doubt. The upper limit to the lifetime ranges from a few weeks to a few years; the chief uncertainty is the electric potential acquired by the orbiting dipoles. Corresponding to a "minimum" potential of -1.8 volts we calculate a shrinkage rate of the orbit of ~ 4 km per day; for a "maximum" potential of -7.2 volts the rate is ~ 55 km per day.

Clearly, therefore, the observation of the orbit decay due to Coulomb drag gives direct information on the average potential of the orbiting particle, and - less sensitively - on the density of plasma in the earth's magnetosphere.

References

1. S. F. Singer, Nature, October 28, 1961.

2. S. F. Singer, "Measurement of Interplanetary Dust" in Scientific Uses of Earth Satellites (J. A. Van Allen, editor), University of Michigan Press, 1956, pp 301-316.

3. W. E. Morrow and D. C. McLellan, Astronomical Journal 66, 107 (1961)

4. I. I. Shapiro and H. M. Jones, Science 134, 973 (1961)

5. D. G. King - Hele, "Properties of the Atmosphere Revealed by Satellite Orbits", in Progress in Astronaut. Sciences Vol. 1 (S. F. Singer, editor) North Holland Publishing Company, Amsterdam 1961.

6. American Institute of Physics Handbook, p. 5-12, McGraw Hill, New York, 1957.

7. H. Bruining, Secondary Electron Emission, Pergamon Press, London, 1954.

8. L. Spitzer, Physics of Fully Ionized Gases, Interscience, New York, 1956.

9. O. D. Kellogg, Foundations of Potential Theory, p. 56, F. Ungar Publishing Company, New York, 1929.

The Generation of Electromagnetic Waves in the Wake of a Satellite.

E. H. Walker

November 1961

As a satellite presumed to be neutral moves through the upper atmosphere, it sweeps out the ions along its path; the electrons which have a higher thermal velocity move into this evacuated region before the ions do, thus producing a polarized layer. Siegel et al. have proposed a mechanism that may give rise to the production of electromagnetic radiation of about 100 megacycles as a result of oscillations of this polarized layer.

The purpose of this note is to consider such processes and the magnitude of the electromagnetic radiation to be expected from a satellite wake. The treatment to be used here is approximate, but it should be satisfactory to indicate the value of this mechanism for detecting satellites by the radio signals that their wakes generate.

We will assume for this problem that a satellite moving 7 km/sec having a diameter that will be chosen to one quarter wave length ($\lambda/4$, about 2 m.) passes through a region with an ambient density of 10^{11} m.$^{-3}$. We will assume, also, that the satellite can be approximated as a flat disk, oriented at a right angle to the direction of motion, that simply sweeps out the ions along its path, thereby producing an expanding (in length) cylinder in which the ions have been removed. The electrons, because of their much higher velocity, will rapidly move into this region, thereby, forming a polarized layer. This layer persists, possibly with some oscillation, for some time thereafter; we will consider the damping of these oscillations later. We assume that as this layer of electrons is formed, the electrons are collectively subjected to accelerations and that these accelerations of the charge gives rise to coherent radiation. The steady polarized layer, however, will not give rise to coherent radiation and therefore will be rather insignificant.

At a temperature of 1500^{o}K the velocity v_e of the electrons is about 2.61×10^5 m/sec. The electrons form a layer one Debye length in thickness,

$\lambda_D = 69\sqrt{T/N_o}$ in meters or about 8.45×10^{-3} m for the present case; thus their acceleration a is

$$a = v_e^2/2\lambda_D = 4.01 \times 10^{12} \text{ m sec}^{-2}$$

The time required for the electrons to move a distance λ_D is:

$$\tau = 2\lambda_D/v_e$$

This time corresponds to 1/4 cycle of the radio emission. The frequency f and the wavelength λ are therefore:

$$f = v_e\sqrt{N_o/T}\ 552 = 3.84 \text{ Mc}$$

$$\lambda = 78 \text{ m}$$

The total charge participating in this motion at any instant is given by the amount of charge lying in a ring about the satellite of radius R, thickness λ_D which is the thickness of the polarized layer, and length ℓ. The radius R has been chosen to be $\lambda/8$ since it will allow the opposite sides to emit radiation that will be in phase. The length of the ring is approximately given by the distance traveled by the satellite in a time τ.

$$\ell = 2\lambda_D\, v_s/v_e$$

where v_s is the satellite velocity. Thus, including an extra factor of 1/2 to take care of the results which would be obtained by an integration of the contributions to the amplitude of the electromagnetic wave from the various portions of the ring, we get for the total number of electrons N:

$$N = \frac{\pi}{4} N_o\lambda\, \lambda_D^2\, \frac{v_s}{v_e}$$

The total power is given by

$$P = \frac{N^2 e^2 a^2}{6\pi\ \epsilon_o\ c^3} = \frac{\pi e^2}{384\ \epsilon_o\ c^3}\ N_o^2\lambda^2\lambda_D^2\ v_s^2\ v_e^2$$

where e is the electronic charge and c is the velocity of light. If we substitute into this expression the values for λ and λ_D as they depend on

T and N_o we have

$$P = \frac{\pi e^2 T^2 v_s^2}{6 \epsilon_o c} \quad (69)^4$$

in MKS units. This is independent of both the frequency of the radiation and of the ambient density of the plasma. For our case this yeilds

$$P = 1.26 \times 10^{-14} \text{ watts}$$

The amount of power that falls on the receiving antenna is reduced by the factor $r^2/4d^2$ where r is the antenna radius and d is the distance to the satellite. Thus, the power falling on a 60 foot antenna, p_a, when the satellite is 100 miles away will be reduced by a factor of 8.1×10^{-10}. Thus, p_a will be 1.02×10^{-23} watts.

Apparently, the smallest amount of power on the antenna which can be detected by the 60 foot radio telescope is about 1.5×10^{-22} Δf (watts where Δf is the bandwidth. If Δf is taken to be 1% of the frequency of radiation, i.e. 36 Kc, then the minimum detectable total power would be about 5.4×10^{-18} watts. The galactic noise level is about 10^{-15} watts/m^2 at 3.8 Mc which is about six orders of magnitude greater than the power from the wake. Thus it would be possible to detect such radiations only from the satellite itself.

If we now return to the question of the damping of these oscillations, we can obtain an idea about the total electromagnetic radiation that is produced in the entire wake. We merely need to note that the Landau damping formula shows that for plasma wave oscillations with a wave length shorter then λ_D, the wave is damped out rapidly while for those oscillations with a wavelength much greater than λ_D, the oscillation will be damped out only very slowly. Since the wavelength for the plasma oscillation, λ_p is about $\lambda_D/10$ for the case considered here, the oscillation will be damped out immediately, thus agreeing with the treatment given. In any case, however, we could not

expect a situation to arise where the oscillations would continue for something like $10^6 \lambda/\lambda_p$ oscillations as would be necessary to make the signal observable with the 60 foot radio telescope.

There is also in this approximate treatment some degree of error produced by the artificial removal of the satellite from the problem. In the actual case, the satellite is still very much in the neighborhood when the electrons become subject to accelerations by the electric field. It is possible that the entire front surface of the satellite contributes to the production of radiation. Nevertheless, because of the low velocity of the satellite compared to that of the electrons, it does not seem that this would significantly change the results.

Although the detection of such radiation appears to be out of reach for the radio telescope at the present time, it seems that this radiation could be easily detected from the satellite itself. The author proposes, therefore, that an experiment be performed on an artificial earth satellite to try to observe the electromagnetic radiation over a wavelength of frequency that may be produced in the satellite's own wake.